AALTO UNIVERSITY

School of Engineering

Department of Applied Mechanics

Andres Rene Kurmiste

Analysis of Structural Safety of Ice-going Vessels in the Arctic and Antarctic

Master's Thesis

Espoo, 30.05.2016

Supervisor: Pentti Kujala, D.Sc. (Aalto University)

Instructors: Mikko Suominen, M.Sc. (Aalto University)

Author Andres Rene Kurmiste

Title of thesis Analysis of Structural Safety of Ice-Going Vessels in the Arctic and Antarctic

Degree programme Mechanical Engineering

Major/minor Marine Technology **Code** Kul-24

Thesis supervisor Pentti Kujala, D.Sc.

Thesis advisor(s) Mikko Suominen, M.Sc.

Date 30.05.2016 **Number of pages** 72+23 **Language** English

Abstract

Maritime operations in the Arctic and Antarctic are driven by different causes. In the Arctic the gradual decrease of the ice cover opens up possibilities for new routes for shipping mainly the Northern Sea Route. In addition, Arctic operations are increasing due to the natural resources found in the region. The operations in Antarctic waters are mainly related to ocean research and supplying research bases with goods in the Antarctica.

Both regions have severe ice conditions compared to other regions where ice may occur. This is due to these regions having multiyear ice in addition to first year ice. Therefore, to ensure the safety of the ships operating in those regions knowledge is require on loads occurring on the ship. There have been studies on the ice-induced loads based on full-scale measurements in Arctic and Antarctic waters. Though, no research has been made on how the different ice conditions affect the safety of the ships in those regions. The effects of ice conditions on the ice-induced loads have been studied before only in The Baltic Sea. However, only the effects of ice thickness on the loads were studied. Therefore, there are gaps in the knowledge on ice-induced loads and especially on the effects that ice conditions have on the ice-induced loads in polar waters.

The thesis aims to analyze the effects of different ice conditions on the structural safety of ice-going vessels operating in polar waters. The ice conditions are categorized based on ice thickness and ice concentration. The structural safety is analyzed for local structures in ice strengthened areas of the hull.

The results based on full-scale measurements onboard S.A. Agulhas II in the Antarctic were more reliable than the results measured onboard M/T Uikku in the Arctic. Since, S.A. Agulhas had 6 times more data on ice-induced loads, due to more time spent in ice. Nevertheless, the results were interesting, as generally for the bow both ships showed a decrease in safety indices with the increase of the ice thickness and ice concentration. However, for the stern an increase in safety indices was observed with increasing ice thickness and ice concentration.

Keywords Arctic and Antarctic, reliability analysis, ice-induced loads , ice conditions

Acknowledgments

The thesis was carried out in Aalto University under the supervision of Professor Pentti Kujala. I greatly appreciate the valuable advice and guidance he gave me during the whole thesis. I am also thankful that he motivated me to finish this thesis finally.

I would like to thank my advisor M.Sc. Mikko Suominen who provided me with information on the present topic. I am also grateful that he was very helpful when help was needed.

Finally, I would like to thank anyone who was in anyway helping me get towards the goal of finishing this thesis.

Andres Rene Kurmiste

Espoo, May 30, 2016

Table of Contents

List of Figures

List of Tables

Abbreviations

FSICR	Finnish-Swedish Ice Class Rules
IACS	International Association of Classification Societies
POLARIS	Polar Operational Limit Assessment Risk Indexing System
AIRSS	Arctic Ice Regime Shipping System
PC	Polar Class
RV	Risk Index Value

1. Introduction

In this chapter the background drivers for this thesis are given. In addition, the aim and scope of the thesis is defined and a literature review is conducted on the state of the art in full-scale measurements and reliability analysis in different ice conditions.

1.1. Background

Maritime operations in the Arctic and Antarctic are driven by different causes. In the Arctic the gradual decrease of the ice cover opens up possibilities for new routes for shipping mainly the Northern Sea Route. In addition, Arctic operations are increasing due to the natural resources found in the region. The operations in Antarctica are mainly related to ocean research and supplying research bases with goods in the Antarctica.

Both regions have severe ice conditions compared to other regions where ice may occur. This is due to these regions having multiyear ice in addition to first year ice. Therefore, to ensure the safety of the ships operating in those regions knowledge is require on loads occurring on the ship. There have been studies on the ice-induced loads based on full-scale measurements in Arctic and Antarctic waters. However, no research has been made on how the different ice conditions affect the safety of the ships. The effect of ice conditions on the ice-induced loads have been studied before only in The Baltic Sea [1]. However, only the effects of ice thickness on the loads were studied. Therefore, there are gaps in the knowledge of ice-induced loads and especially on the effects that ice conditions have on the loads in polar waters.

There is a need for studies where other factors than ice thickness are considered in the analysis of the loads, as it is well known that many different parameters have an effect on the ice-induced loads. Thus, small steps in researching ice-induced loads have to be taken to get forward and find out which parameters have an effect on the ice loads and which don't. Therefore, in this thesis in addition to ice thickness the effects of ice concentration on the ice-induced loads are studied.

1.2. Aim of the thesis

The aim of this thesis is to analyze the effects of different ice conditions on the structural safety of ice-going vessels operating in polar waters. The ice conditions are categorized

based on ice thickness and ice concentration. The structural safety is analyzed for local structures in ice strengthened areas of the hull. In other words, only framing and plating members are investigated. Thus, global strength is not studied.

Two ice-going vessels are investigated – S.A. Agulhas II and M/T Uikku. The former being a Polar Supply and Research Vessel and the latter a motor tanker. Full-scale measurements had been conducted onboard both ships in order to gather data on ice-induced loads. S.A. Agulhas II gathered data in Antarctic waters and M/T Uikku in Arctic waters. These gathered loads are divided into different ice condition categories based on the prevailing ice conditions during the measuring period. The prevailing ice conditions are based on visual observations gathered during a voyage.

Firstly, the safety of the local structures is analyzed with ice loading data, which is not categorized into different ice conditions. The local structure analyzed for safety are framing and plating members.

Secondly, different ice conditions are used to analyze the structural safety of local structures. Here, we only analyze the safety of the framing. Thus, plating is not separately analyzed in terms of safety. Nevertheless, plating is implicitly included in the safety calculations of the framing members as an attached plate flange.

During the safety analysis of the structures a sensitivity analysis is also included. The effect of ice load height on the safety of the plating is studied. Three different load heights are studied, which are later also relevant in calculating the risk-based structures for the ships.

Finally, a comparison is done between the safety indices calculated in this thesis and Risk Index Values (RVs) given in POLARIS. The RVs in POLARIS are based on level ice conditions. Thus, safety indices calculated for ice condition categories with the appropriate ice concentration value can be compared to the RVs.

1.3. State of the art

In order to analyze the safety of ice-going vessels, knowledge is required on ice-induced loads. Full-scale measurements of ice-induced loads have clearly indicated at the stochastic nature of the loads. This is primarily due to variations in ice conditions and in ice-breaking processes [2]. Nevertheless, studies have shown that the loads are representable by statistical distributions. The first to apply a statistical distribution to

measured ice-induced loads were Russian scientist Kheisin and Popov [3]. They found the peak load amplitudes at a bow frame to follow an exponential distribution. Kujala and Vuorio also adopted the peak load amplitude distribution to study the statistical characteristics of short-term ice-induced loads measured onboard I.B. Sisu [4] [5]. The statistical distributions they studied were: Rayleigh, Weibull, Log-Normal and Exponential. Similarly to Kheisin and Popov they found the exponential distribution to fit the measured data best. In addition, they found the Weibull distribution to fit the data fairly good as well. In a later study by Suominen and Kujala [6] it was concluded that short-term ice load peak amplitudes measured onboard MS Kemira are most suitably described by the Weibull distribution, if the Weibull shape parameter equals 0.75. Since the exponential distribution and the Weibull distribution have an exponentially decaying tail, the distribution of their extremes values will converge to the Type I asymptotic form [7], i.e. Gumbel I distribution. As the peak load amplitude distribution is essentially an initial distribution of the ice-induced loads, the statistical characteristics of the loads can be studied based on extreme values statistics. In other words, the study is based on the distribution of maximum values measured during a constant time period. The advantage of studying ice-induced loads with extreme values is that the scatter decreases when the period and number of loads increases [8]. This is beneficial when estimating the lifetime loads encountered by a ship. In addition, the estimated lifetime loads based on peak load amplitude distributions are more sensitive to the potential errors in the estimation of the initial distribution than extreme value distributions.

Gumbel I distribution has been used to estimate the lifetime ice-induced loads based on full-scale measurements of maximum loads for some time. However, in early studies (e.g. [4], [5] and [9]) the statistical parameters of the distribution were not related to the prevailing ice conditions. Therefore, the results of the study could not be related to similar ships sailing in the same area. Moreover, the results were specific to the operational profile of the ship studied. Kujala was the first to explicitly study the effects of ice conditions on the lifetime ice-induced loads. He assumed that the measured 12 hour maximum values of ice-induced loads in different areas of the Baltic Sea during one winter can be related to the winter's maximum equivalent ice thickness in those areas of the sea [10] [1]. In his method the mean value and the coefficient of variation of the measured 12 hour maximum loads were functions based on the equivalent ice thicknesses in different areas of the Baltic Sea (Bothnian Bay, Bothnian Sea, Gulf of Finland and

Baltic Proper). Thus, the mean value and the coefficient of variation could be related to the Gumbel parameters in different areas of the Baltic Sea with different ice conditions. However, there is a lack of studies where other parameters of the prevailing ice conditions besides ice thickness are related to the lifetime loads. For instance, in a recent study by Suominen et al. [11] a clear relation was shown between ice-induced loads and ice concentration, due to the measured 10-minute maximum ice-induced loads increasing as a function of ice concentration. The study was based on full-scale measurements conducted onboard S.A. Agulhas II in Antarctic waters. Moreover, there are no studies based on data gathered from Polar Regions that compare the prevailing ice conditions with the lifetime ice-induced loads in those regions.

The safety of ice-going vessels has been studied in previous studies [12] [13] [14] based on level 2 reliability analysis, i.e. with a second-moment formulation method [15]. However, different ice condition effects on the safety of the ship were explicitly considered only in [13]. In that study Kujala calculated the safety of the frames of the ship in the bow, mid and aft area. He used a less refined version of the method presented in his dissertation to estimate the lifetime ice loads in different areas of the Baltic Sea. These different areas of the Baltic Sea reflected the different ice conditions based on maximum winter ice thicknesses in those areas. In the later study [12] he implicitly included the ice conditions by fitting the Gumbel I distribution straight to the measured data, although with the data divided into Gulf of Finland and Bay of Bothnia measurements. In addition, besides the frames he calculated the safety of the plating in relation to the allowed permanent deflection. However, the study considered only the bow of the ship.

2. Safety analysis of structures

In this chapter the theory is elaborated behind the analysis of safety of ice-going vessels based on reliability analysis. The first sub-chapter introduces the principles of reliability analysis. The following sub-chapter presents limit state equations for plating, i.e. serviceability limit state equations. And the final sub-chapter presents the frame limit state equations, i.e. ultimate limit state equations.

2.1. Basic principles of reliability analysis

There are three levels of reliability analysis as described in [16]. Level 1 reliability analysis refers to the traditional safety index approach where a single value is defined for each variable. Level 2 reliability analysis, also called the safety index approach or second-moment approach, is most commonly used to assess the safety of structures. The level 2 analysis uses the first and second moments, i.e. the mean values and variances, of the random variables to measure the reliability of structures. Level 3 reliability analysis means the full use of statistical properties in the calculation of the reliability, such as a joint distribution of the design variables. However, since the joint distribution is usually unknown level 3 analyses are rare.

With the second-moment approach the reliability may be assessed with a function of the first and second moments of the design variables – namely the safety index β. It must be pointed out that the second-moment approach is also consistent with the equivalent normal representation of non-normal distributions (e.g. Gumbel I distribution). [15]

2.1.1. Basic principles of level 2 reliability analysis

Assessing the reliability of a structure requires knowledge on the loads acting on the structure and the capacity of the structure to withstand loads. The basic definitions of reliability analysis presented in this sub-chapter are from [16]. The starting point for reliability analysis can be defined as follows:

$$\begin{aligned} P(R-S\le 0) &= P_f = 1-L \\ P(g(X)\le 0) &= P_f = 1-L \end{aligned} \tag{2.1}$$

Where P_f is the probability of failure, $L=1-P_f$ is the reliability of the structure not being damaged, R is the capacity of the structure to withstand loads, S is the load acting on the

structure, *g(X)* is the limit state of the structure and *X* is a vector including all of the statistical variables affecting the limit state – load, material properties, dimensions of the structure etc.

The joint distribution F_{RS} of the capacity *R* and load *S* is:

$$F_{RS}(r,s) = P(R \le r \cap S \le s) = \int_{-\infty}^{r}\int_{-\infty}^{s} f_{RS}(r,s)drds \tag{2.2}$$

The failure probability based on the joint distribution is then:

$$P_f = P(R - S \le 0) = \iint_{\{r,s|r-s\le 0\}} f_{RS}(r,s)drds \tag{2.3}$$

A graphical representation of the failure probability based on Equation (2.3) is shown in Figure 2.1. The failure probability in this case is the volume of the *R* and *S* joint distribution where $r<s$.

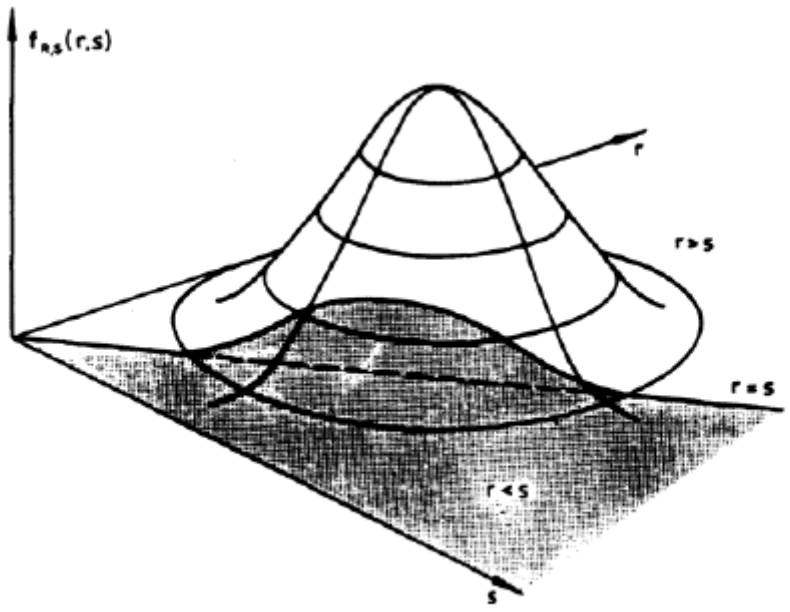

Figure 2.1 Joint probability distribution of capacity R and load S [17]

If the capacity *R* and load *S* are assumed to be statistically independent and their statistical distributions are known the joint distribution can be presented as follows:

$$f_{RS}(r,s) = f_R(r)f_S(s) \tag{2.4}$$

Where $f_R(r)$ and $f_S(s)$ are the probability density functions of capacity R and load S.

The probability of failure is now:

$$P_f = P(R - S \le 0) = \iint_{\{r,s|r-s\le 0\}} f_R(r) f_S(s) dr ds = \int_{r=-\infty}^{\infty} \int_{s=r}^{\infty} f_R(r) f_S(s) dr ds = \\ = \int_{-\infty}^{\infty} f_R(r)[1 - F_S(r)] dr = 1 - \int_{-\infty}^{\infty} f_R(r) F_S(r) dr \tag{2.5}$$

Equation (2.5) is graphically represented in Figure 2.2. The probability of failure increases with the overlap of distributions of capacity *R* and load *S*.

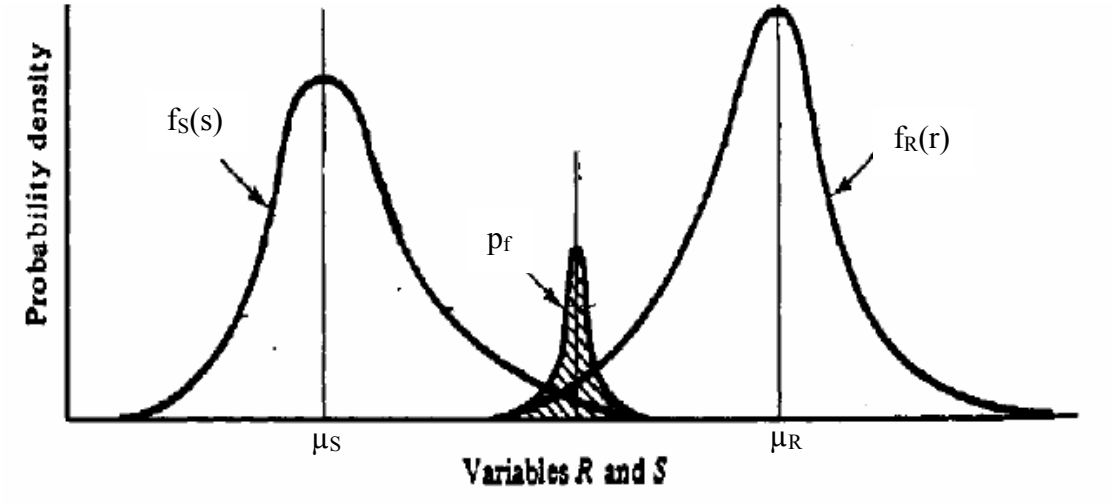

Figure 2.2 Probability of failure when capacity R and load S are statistically independent [17]

By assuming that capacity *R* and load *S* are described with normal distributions the Equation (2.5) can be simplified. Furthermore, the mean and standard deviation of capacity *R* and load *S* are known and indicated by μ_R, μ_S for the mean and σ_R, σ_S for the standard deviation. Therefore, the safety margin $Z=R-S$ is also normally distributed and its mean and standard deviation are as follows:

$$\mu_Z = \mu_R - \mu_S \\ \sigma_Z = \sqrt{\sigma_R^2 + \sigma_S^2} \tag{2.6}$$

The cumulative distribution function of the safety margin *Z* can now be presented as a standard normal distribution as follows:

$$F_Z(z) = \Phi\left(\frac{z-\mu_Z}{\sigma_Z}\right) \tag{2.7}$$

Where Φ is the cumulative distribution function of the standard normal distribution. The failure probability $P_f=P(Z\leq 0)$ can now be determined in a simplified form as follows:

$$P_f = F_Z(0) = \Phi\left(\frac{0-\mu_Z}{\sigma_Z}\right) = \Phi\left(-\frac{\mu_R-\mu_S}{\sqrt{\sigma_R^2+\sigma_S^2}}\right) \tag{2.8}$$

The failure probabilities can be now determined using the cumulative distribution of the standard normal distribution. Equation (2.8) can also be represented in the following form:

$$\begin{aligned} P_f &= \Phi(-\beta) = 1-\Phi(\beta) \\ \beta &= \frac{\mu_Z}{\sigma_Z} = \frac{\mu_R-\mu_S}{\sqrt{\sigma_R^2+\sigma_S^2}} \end{aligned} \tag{2.9}$$

Where β is the so called safety index. The meaning of Equation (2.9) is shown in graphical form on Figure 2.3. The safety index β depicts the distance of the safety margin's mean value from the origin. The distance is given in relation to the standard deviation. Typical values of safety index β vary between 2 to 3 [12].

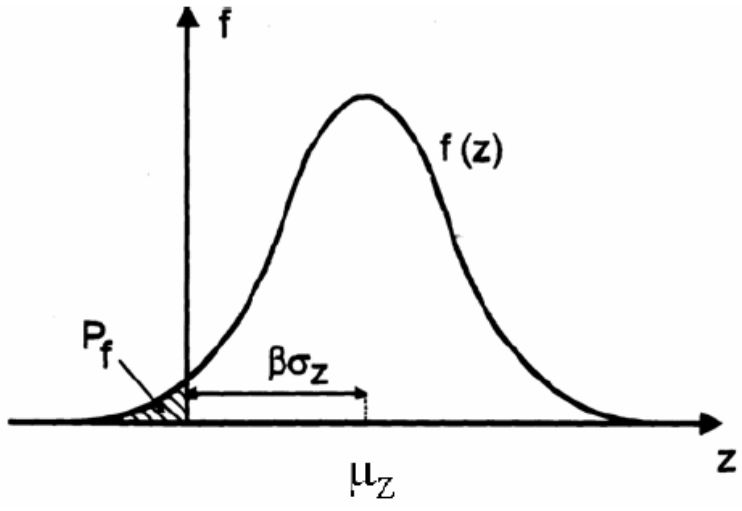

Figure 2.3 Safety margin Z distribution f(z) and probability of failure P_f [17]

On Figure 2.4 an iterative algorithm used in this thesis for the calculation of the safety index β is shown. This was developed by Kujala in [10]. The algorithm uses the generalized formulation of the second moment approach. In addition, the reduced variates

of capacity *R* and load *S* are used. The generalized formulation with reduced variates is explained in detail by Ang and Tang in [15].

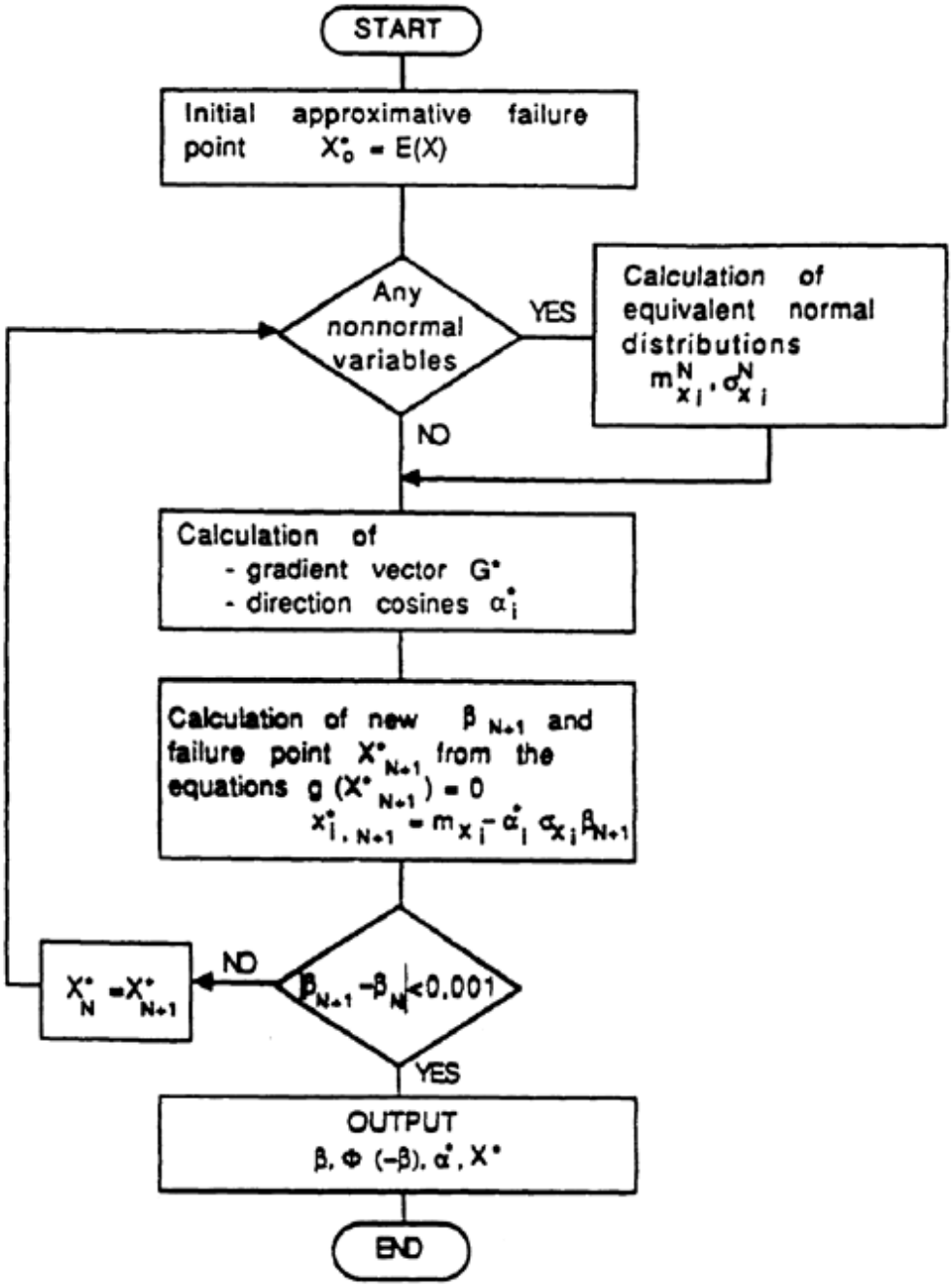

Figure 2.4 Iterative algorithm for safety index β calculation [10]

2.2. Serviceability limit state equations

The serviceability limit state equation used in this thesis is developed by Hayward [18]. The approach he developed estimates the load at which permanent deflection are caused

to the side plating. It is based on extensive finite element calculations to find out a correction factor f_D, which considers the effects of load height on the permanent deflections. He compared the finite element analysis results to the results obtained with yield line theory for uniform pressure on plating, which was formulated by Jones [19]. This was the foundation for the analytical expression of Hayward's approach. The correction factor f_D equation and following equations are only presented for transversally framed plating, as both ships considered in this thesis are transversally framed. The average correction factor for transversally framed plating f_{DT} has the following form [18]:

$$f_{DT} = -0{,}1330x_T^2 + 0{,}6071x_T \tag{2.10}$$

Where x_T is calculated as follows:

$$x_T = \frac{h_c}{s}\left(\frac{s}{t}\right)^{0,2} \tag{2.11}$$

Where h_c is the load height, s is the frame spacing and t is the plate thickness.

Based on the yield line theory for uniform pressure by Jones [19] the Hayward approach [18] for the required line load q at which permanent deflections are caused when $w_p/t \leq 1$ is as follows:

$$q = \frac{p_c h_c}{f_{DT}}\left[1 + \frac{w_p^2}{3t^2}\left(\frac{\zeta_0 + (3 - 2\zeta_0)^2}{3 - \zeta_0}\right)\right] \tag{2.12}$$

And when $w/p > 1$:

$$q = \frac{2p_c h_c w_p}{tf_{DT}}\left[1 + \frac{\zeta_0(2 - \zeta_0)}{3 - \zeta_0}\left(\frac{t^2}{3w_p^2} - 1\right)\right] \tag{2.13}$$

Where t is the plate thickness, w_p is the permanent deflection, ζ_0 is the shape parameter and p_c is the threshold pressure causing double Y-shape yield line. The permanent deflection w_p for the limit state of the plating is taken as 1/12 of the frame spacing s. This is defined in DNV instructions for surveyors [20] as the allowable deflection for plating. The threshold pressure p_c is calculated as follows [19]:

$$p_c = \frac{48M_p}{s^2\left(\sqrt{3+\left(\frac{s}{l}\right)^2}-\frac{s}{l}\right)^2} \tag{2.14}$$

Where l is the frame span and M_p is the plastic moment of the plating. The shape parameter ζ_0 is in the following form:

$$\zeta_0 = \frac{s}{l}\left(\sqrt{3+\frac{s^2}{l^2}}-\frac{s}{l}\right) \tag{2.15}$$

The plastic moment M_p is calculated as follows:

$$M_P = \sigma_y \frac{t^2}{4} \tag{2.16}$$

Where σ_y is the yield stress of the material.

2.3. Ultimate limit state equations

For reliability analysis a simplified version of the equations presented by Varsta et al. [21] are used. This is due to the original equations describing the load on the frame, at which the limit state of the frame occurs, requiring the load to be solved with an iterative process, complicating the reliability analysis significantly. The simplified approach was presented by Kujala [10]. The load on the frame causing the limit state of the three plastic hinge mechanism presented by Varsta et al. [21] is as follows:

$$F = 4\frac{M_p + M_{ps}}{l} \tag{2.17}$$

Where M_p is the plastic moment, without the effect of shear, required to cause the plastic hinge at the mid span of the frame. M_{ps} is the plastic moment, including the effect of shear, required to cause the plating hinge at the ends of the frame. The simplified approach by Kujala [10] assumes that the plastic section modulus including shear Z_{ps} is equal to the plastic section modulus without shear Z_p:

$$Z_{ps} = Z_p \tag{2.18}$$

The plastic moment M_p is calculated as follows:

$$M_p = \sigma_y Z_p \tag{2.19}$$

Thus based on Equations (2.18) and (2.19) the Equation (2.17), which estimate the load on the frame causing the limit state in the frame, is in the simplified form as follows:

$$F = 8\frac{M_p}{l} \tag{2.20}$$

3. Statistical analysis of the measured ice loads

In this chapter the ice-induced loads gathered during full-scale measurements onboard S.A. Agulhas and M/T Uikku are analyzed. First a short description of the gathered ice-induced loads on both ships is given. Secondly the basic theory behind Gumbel I distribution is given and the long term loads are presented as function of the return period.

3.1. Short description of the measured ice-induced loads

3.1.1. Full-scale measurements onboard S.A. Agulhas

The measured ice-induced loads for S.A. Agulhas are from two separate voyages in the Antarctic waters. The first of those voyages was conducted from December 2013 to February 2014, which was followed by a second voyage from December 2014 to February 2015. The loads were measured continuously during the voyages. The 10-minute maximum loads for bow and stern are studied in this thesis. The maximum values for the bow are taken as the maximum of frame #134+400 and #134. For the stern the maximum values are taken as the maximum of frame #41, #40+400, #40 and #39+400. A 10 kN threshold is set for the data to get rid of any noise or open-water measurements. During the voyages visual observations were also gathered on the ice conditions with 10-minute intervals. The ice-induced loads are synchronized with the visual observations. As a result, the continuously measured data was shrunk from 30 000 data points to about 3000 data points. In addition, based on the visual observation any data that was clearly measured in open-water conditions was left out for the analysis of the loads. Based on the 30 000 measured 10-minute loads gathered form two voyages, the average time spent in those ice conditions per year was calculate to be about 11 days.

3.1.2. Full-scale measurements onboard M/T Uikku

The measured ice loads onboard M/T Uikku are from one voyage to Ob-estuary in the Arctic waters, which was from April to May in 1998 [22]. During the voyage M/T Uikku was always either in convoy or lead by an ice-breaker. Thus, the voyage was assisted whereas S.A. Agulhas made non-assisted voyages. 20-minute maximum loads onboard M/T Uikku were measured in the bow, bow-shoulder and stern. A 10 kN threshold is set for the data to get rid of noise and open-water measurements. Also visual observations were done on the ice-conditions. However, for M/T Uikku the visual observations were

not conveniently measured in 20-minute periods as the loads. Thus, the visual observations were synchronized to the loads. An average of the measured visual observations during a 20-minute period was taken that were coherent with the 20-minute period where the maximum load was measured. Unfortunately as the voyage was quite short only about 500 measured 20-minute loads are available for the analysis. Based on the 500 measurements the time in those ice conditions per year was calculate to be about 7 days.

3.2. Gumbel I distribution and the return period of ice loads

The Gumbel I distribution is fitted to the measured ice loads as it has proven to give good fit to the data (see e.g. Kujala [1]) due to, the initial distributions of the ice loads having an exponentially decaying tail [7]. The cumulative distribution function of Gumbel I distribution is as follows [15]:

$$G(x) = e^{-e^{-\alpha_n (x-\mu_n)}} \tag{3.1}$$

Where α_n is the inverse measure of dispersion and u_n is the characteristic largest value. The Gumbel parameters α_n and u_n can be determined based on the mean μ and standard deviation σ of the measured loads as follows:

$$\begin{aligned} \alpha_n &= \frac{\pi}{\sigma\sqrt{6}} \\ u_n &= \mu - \frac{\gamma}{\alpha_n} \end{aligned} \tag{3.2}$$

Where $\gamma=0.577$ is the Euler constant.

As a threshold value of 10 kN is used, the load range is incomplete. Therefore, a truncated cumulative distribution function for Gumbel I distribution is required, which is derived as follows:

$$G_t(x) = \frac{G(x) - G(x_t)}{1 - G(x_t)}, x_t \le x \tag{3.3}$$

Where x_t is the threshold value. The long term extreme value distribution required for the calculation of the lifetime safety index of the ships after N events can be determined now as follows:

$$G_t(x) = \left[\frac{G(x) - G(x_t)}{1 - G(x_t)} \right]^N \tag{3.4}$$

The amount of load events *N* during a ships lifetime of 25 years can be estimated for both ships based on the amount of days per year in ice and the used time period for maximum loads. Thus, for S.A. Agulhas the amount of events per day is 144 and as the ship is assumed to be in ice per year for 11 days, the amount of 10-minute maximum loads during the lifetime is *N=39600*. And for M/T Uikku the amount of events per days is 72 and the assumed days per year in ice is 7, therefore the amount of 20-minute maximum loads during the lifetime is *N=12600*.

The long term loads are in general presented as a function of the return period, with which an estimation to the maximum lifetime load after a certain amount of days can be gained, the return period in our case can be formulated as follows:

$$T(x) = \frac{1}{C} \cdot \frac{1}{1 - G_t(x)} \tag{3.5}$$

Where *C* is a constant that defines the amount of measurement per day due to the used time period for maximum loads. For instance *C=2* if 12-hour measuring periods are used. S.A. Agulhas with its 10-minute period gives the constant a value of *C=144* and for M/T Uikku with its 20-minute periods *C=72*.

3.2.1. Long term return periods for S.A. Agulhas

The long term return periods for S.A. Agulhas bow and stern without the loads divided into different ice conditions are presented here. Thus, the whole data of the loads, which were synchronized with the visual observation are used. In Appendix 1 the long term return periods in different ice conditions for the bow and stern are given. The return periods for the bow and stern of the ship based on measurements and predictions by Gumbel I distribution are given on Figure 3.1 and Figure 3.2 respectively. In addition the parameters for Gumbel I distribution and measured loads are given in Table 3.1 for the bow and stern.

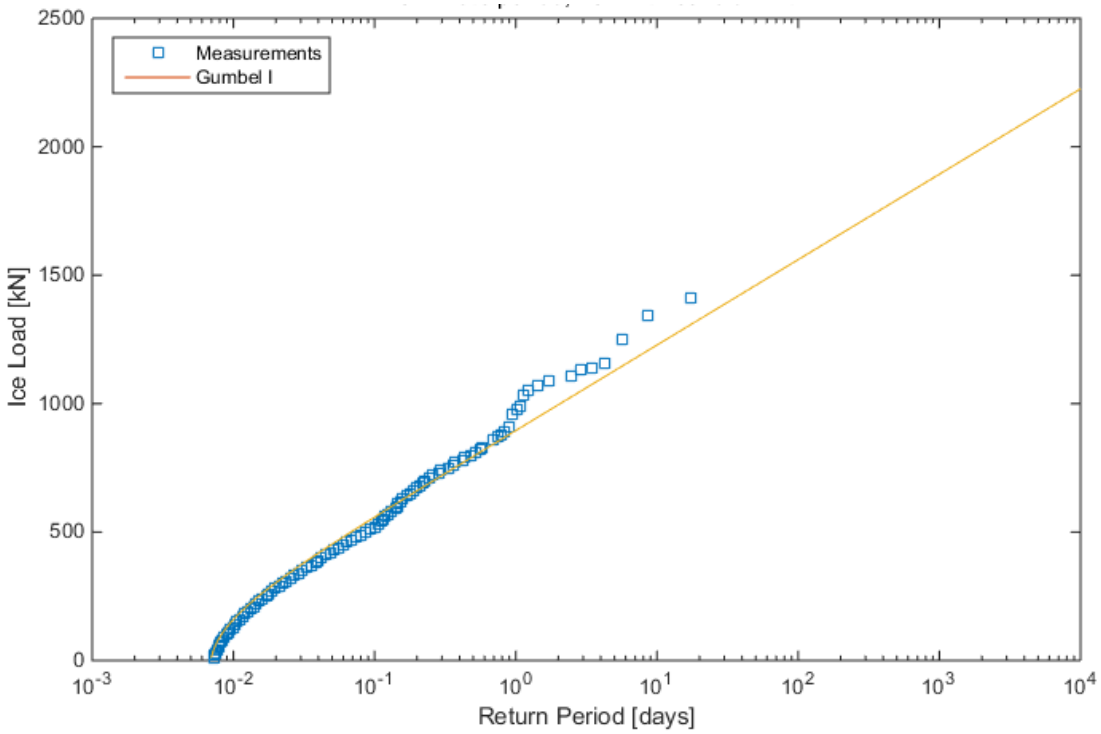

Figure 3.1 The return period of time for the measured and predicted ice loads (S.A. Agulhas bow)

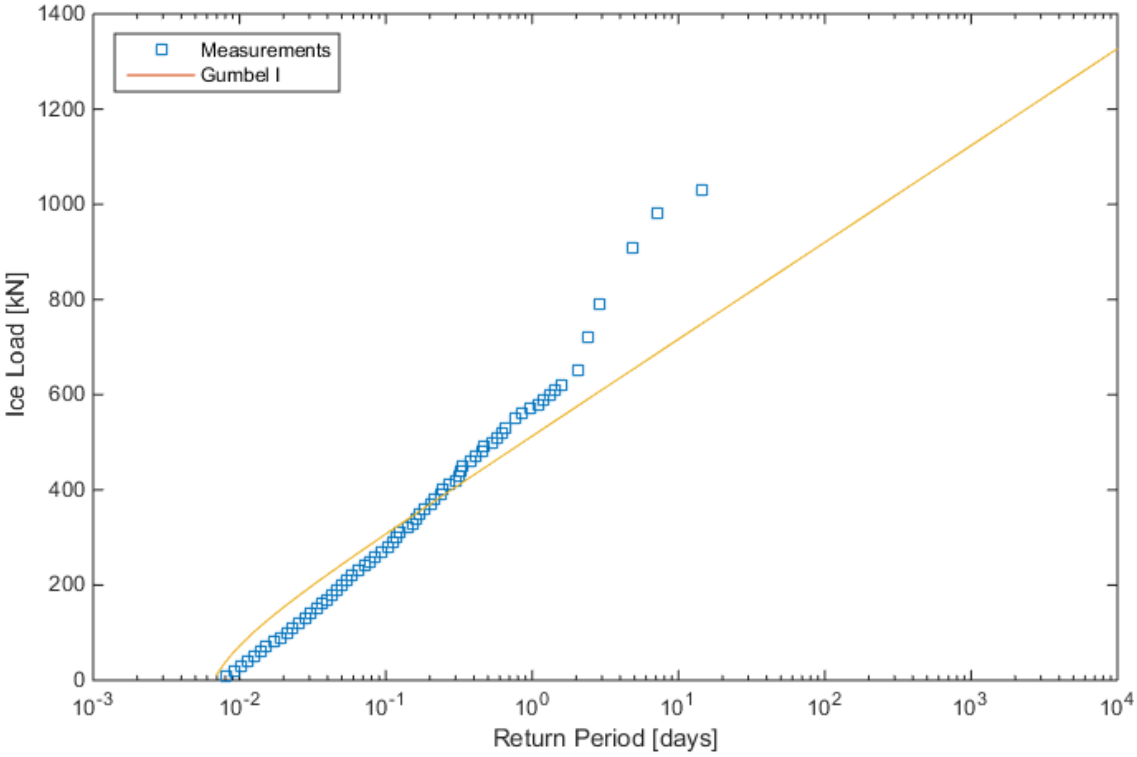

Figure 3.2 The return period of time for the measured and predicted ice loads (S.A. Agulhas stern)

Table 3.1 Statistical parameters of ice-induced loads (S.A. Agulhas II bow and stern)

	Bow	**Stern**
Mean value, μ [kN]	254,44	107,01
Standard deviation, σ [kN]	185,19	113,31
Gumbel parameter, α_n	0,0069	0,0113
Gumbel parameter, u_n	171,13	56,02

The measured data fits quite well to Gumbel I distribution at the bow. At the stern there is slight overestimation at low loads and after the return period of 20 days the Gumbel I predications start to be significantly lower than the measured loads.

Based on the assumed days per year in ice, which was 11 days, the lifetime expected maximum ice-induced loads can be estimated. During 25 years, which is the lifetime of the ship, the ship would be in ice for 275 days. Thus, the expected lifetime load for the bow is about 1710 kN and for the stern about 1010 kN.

3.2.2. Long term return periods for M/T Uikku

The long term return periods for M/T Uikku bow and stern without the loads divided into different ice conditions are presented here. In Appendix 2 the long term return periods in different ice conditions for the bow, bow-shoulder and stern are given. However, in Appendix 2 the small amount of measured ice-induced loads onboard M/T Uikku becomes apparent, as when the loads are divided into different ice conditions little data is left for each ice condition on which to analyze the ice loads statistically. Thus, poor fit to the predicted Gumbel I return periods is seen. In certain cases where more data above the threshold value is present the fit is quite good, but in many cases there are just two or three data points which were above the threshold value and thus there is high uncertainty in the predicted return period for loads.

The return periods for the bow, bow-shoulder and stern of the ship based on measurements and predictions by Gumbel I distribution are given on Figure 3.3, Figure 3.4 and Figure 3.5 respectively. In addition the parameters for Gumbel I distribution and measured loads are given in Table 3.2 for the bow, bow-shoulder and stern.

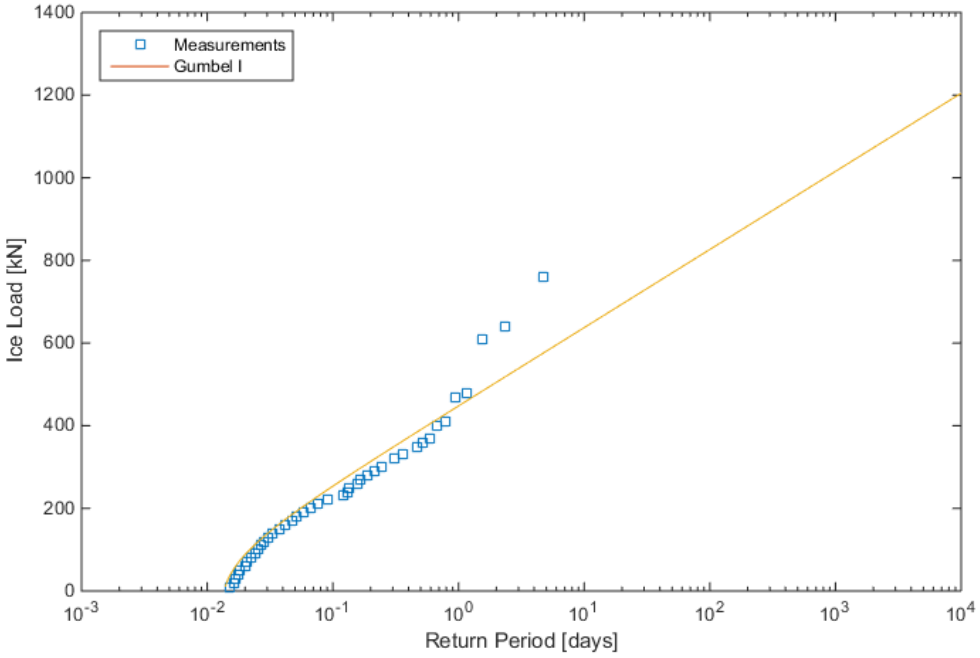

Figure 3.3 The return period of time for the measured and predicted ice loads (M/T Uikku bow)

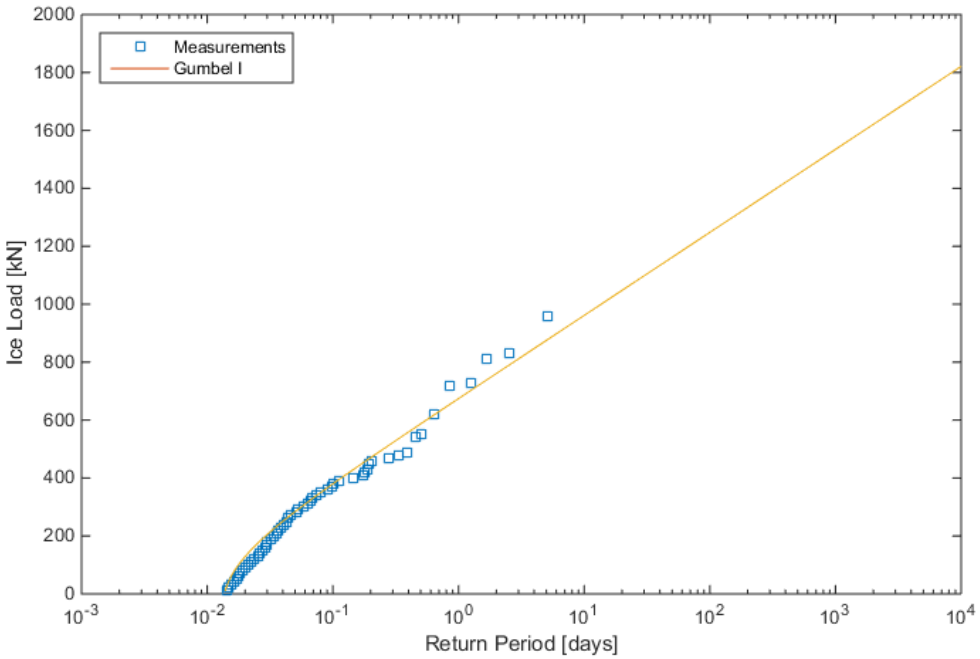

Figure 3.4 The return period of time for the measured and predicted ice loads (M/T Uikku bow-shoulder)

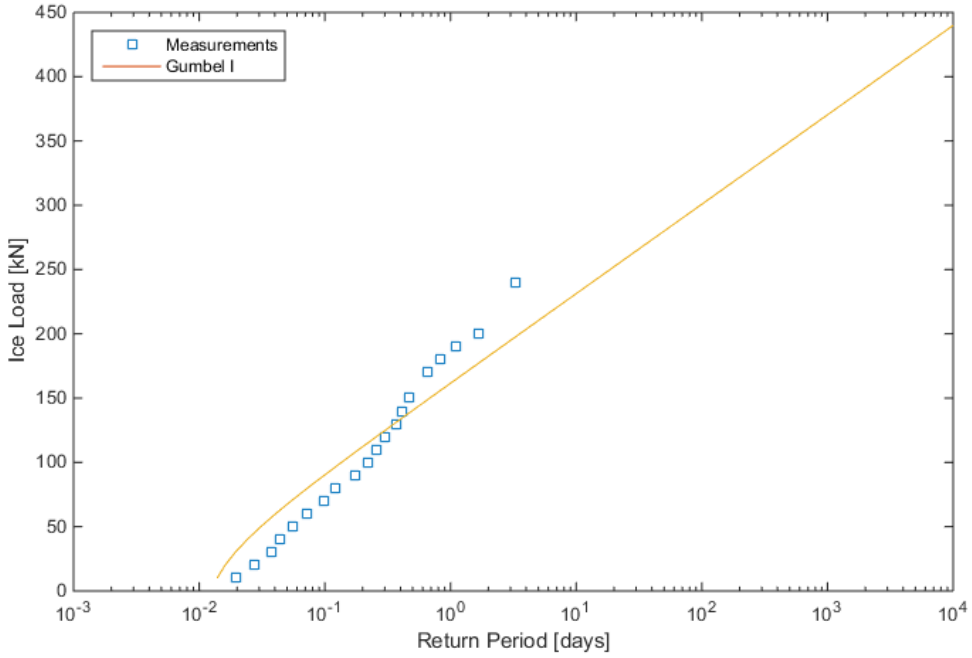

Figure 3.5 The return period of time for the measured and predicted ice loads (M/T Uikku stern)

Table 3.2 Statistical parameters of ice-induced loads (S.A. Agulhas II bow, bow-shoulder and stern)

	Bow	**Bow-shoulder**	**Stern**
Mean value, μ [kN]	138,92	205,91	44,22
Standard deviation, σ [kN]	105,30	159,62	38,74
Gumbel parameter, α_n	0,0122	0,0080	0,0331
Gumbel parameter, u_n	91,55	134,10	26,79

The measured data shows the same trend here as for S.A. Agulhas II, meaning that if higher loads are measured then the tail end of the data also fits better to the Gumbel I distribution. The bow-shoulder measured values fit the predictions best. However, the lack in stern data is evident, as there are few data points of measured loads above 10 kN. In addition, the stern return period distribution is over estimated at the beginning and the tail end is under estimated, but not as significantly as for S.A Agulhas II stern. The bow data starts to deviate from the predictions at the return period of 20 days as did the stern data for S.A. Agulhas II.

Based on the assumed days per year in ice, which was 7 days, the lifetime expected maximum ice-induced loads can be estimated. During 25 years, which is the lifetime of the ship, the ship would be in ice for 175 days. Thus, the expected lifetime load for the bow is about 880 kN, for the bow-shoulder about 1320 kN and for the stern about 320 kN.

4. Case study

This chapter presents the results of the structural safety analysis for S.A. Agulhas II and M/T Uikku. Furthermore, risk- and rule-based structures are compared and rule-based ice classes are evaluated on their suitability for the Arctic and Antarctic. The first sub-chapter contains the specifications of both ships. This is followed by a sub-chapter where reliability analysis is performed including the complete loading data. In the next sub-chapter the structural safety analysis is conducted with ice loading data, which is divided into different ice conditions. Finally the risk-based and rule-based structural designs are compared and the RVs from POLARIS are compared to the calculated safety indices.

4.1. Descriptions of the ships and their instrumentation

4.1.1. S.A. Agulhas II

The main particulars of S.A. Agulhas II are presented in Table 4.1. S.A. Agulhas II was built to be classified as Polar ice class PC5 and the hull was constructed in accordance with DNV ICE-10. Three areas of the starboard side of the hull were instrumented with strain gauges when she was under construction in 2011/2012. Ice-induced loads were determined by instrumenting the upper and lower parts of the frame with V-shaped strain gauges, which measured the shear strains occurring in the frame [23]. The instrumentation was applied to two adjacent frames at the bow, three adjacent frames at the bow-shoulder and four adjacent frames at the stern-shoulder, see Figure 4.1. [24]. The measured maximum loads at the bow were the maximum loads of frames #134 and #134+400. For the stern the maximum load was the maximum from frames #39 ½, #40, #40 ½ and #40.

Table 4.1 Main particulars of S.A. Agulhas.

Length, bpp.	121,8 m
Breath, mould.	21,7 m
Draught, design	7,65 m
Deadweight at design displacement	5000 t
Displacement	13632 t
Speed, service	14 kn
Propulsion power	9 MW

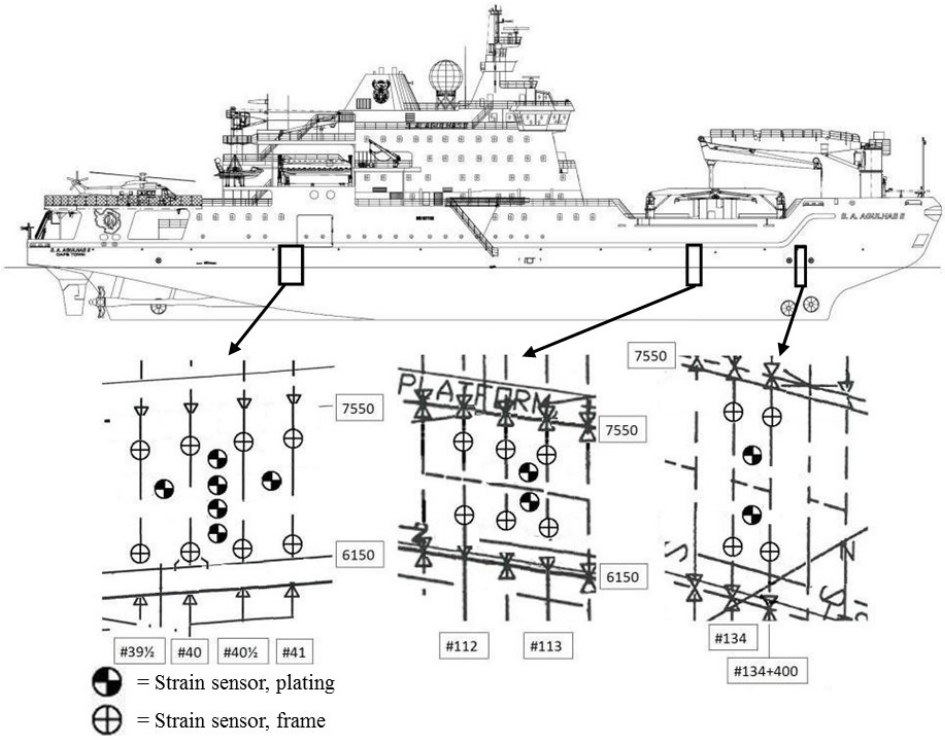

Figure 4.1 Instrumented areas of S.A. Agulhas II [24].

4.1.2. M/T Uikku

The main particulars of M/T Uikku are presented in Table 4.2. M/T Uikku is classified by DNV as class +1 A Tanker for Oil, FSICR classify it as ice class 1 A Super. She was built in 1976 and over-went an Azipod conversion in 1993. To measure ice-induced loads on the hull the frames of the ship were fitted with instrumentation in the bow, bow-shoulder, mid-ship and aft area. The ice loads were evaluated by measuring shear strains at roughly the neutral axis of the frame. The instrumented frames are show on Figure 4.2 [22]. The measured maximum loads at the bow were the maximum loads at frame #196.5. For the bow-shoulder the maximum load was the maximum from frame #175.5. The maximum load for stern was taken from frame #52.5.

Table 4.2 Main particulars of M/T Uikku.

Length, bpp.	150 m
Breath, mould.	22,2 m
Draught, design	9,5 m
Deadweight at design displacement	15 748 t
Displacement	22 654 t
Speed, service	17 kn
Propulsion power	11,4 MW

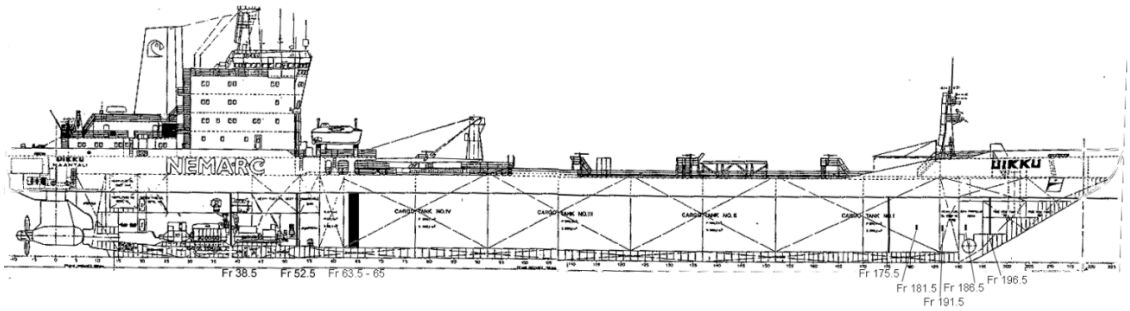

Figure 4.2 Instrumented frames of M/T Uikku [22].

4.2. Reliability analysis with entire ice loading data

First the safety indices for both ships were calculated with the entire data, meaning that the data was not divided into different ice conditions. For S.A. Agulhas the entire data consisted of about 3000 individual ice-load measurements. On the other hand, M/T Uikku has only about 500 ice load measurements. This is due to the full-scale measurements conducted onboard M/T Uikku in the Arctic region lasting only two weeks.

Long-term safety indices were calculated for both ships. The hulls of the ships were calculated according to rules by IACS [25] and FSICR [26]. For IACS the following classes were calculated: PC3, PC4, PC5 and PC6. For FSICR IA Super and IA ice classes were calculated. In addition, a risk-based structural design was calculated, which had requirement to have the safety index $\beta \geq 2$. The safety index according to [12] is between 2 and 3 generally. Thus, the lower limit for the safety index is taken as $\beta=2$. Furthermore, a sensitivity analysis was done for the plate calculations to see how load height affects the safety index of the plating.

4.2.1. S.A. Agulhas II

The hull of S.A. Agulhas II was assumed to be made out of S355 steel. The statistical characteristics of steel S355 were taken from [27] and are presented in Table 4.3. Structural scantlings for the bow are T-frames and for the stern I-frames. The frame span for the bow is 2.065 m and 1.4 m for the stern, the frame spacing is 0.4 m.

Table 4.3 Statistical characteristics of steel S355

Mean value [MPa]	Standard deviation [MPa]
395,68	25,126

By knowing the statistical distribution of the load and the structure, we can calculate the safety index based on the methods described in Chapter 2. First we shall look at the bow safety index. The safety index β for bow frames based on IACS and FSICR calculations are shown in Table 4.4. In addition the probability of failure P_f, the frame dimensions and the plastic section modulus Z_p of the frames are given in table. Graphical comparison of the safety index for the bow is shown in Figure 4.3.

Table 4.4 Safety indices of the bow frames (S.A. Agulhas II)

	PC3	**PC4**	**PC5**	**PC6**	**IA Super**	**IA**
β	2,01	0,22	-2,92	-7,01	-8,08	-10,74
P_f	0,02	0,41	1,00	1,00	1,00	1,00
Frame [mm]	T-340x16 / 80x20	T-320x14 / 70x20	T-300x12 / 60x18	T-280x10 / 60x16	T-240x12 / 50x15	T-220x12 / 50x15
Z_p [cm^3]	1512	1178	870,5	652,3	611,3	527,7

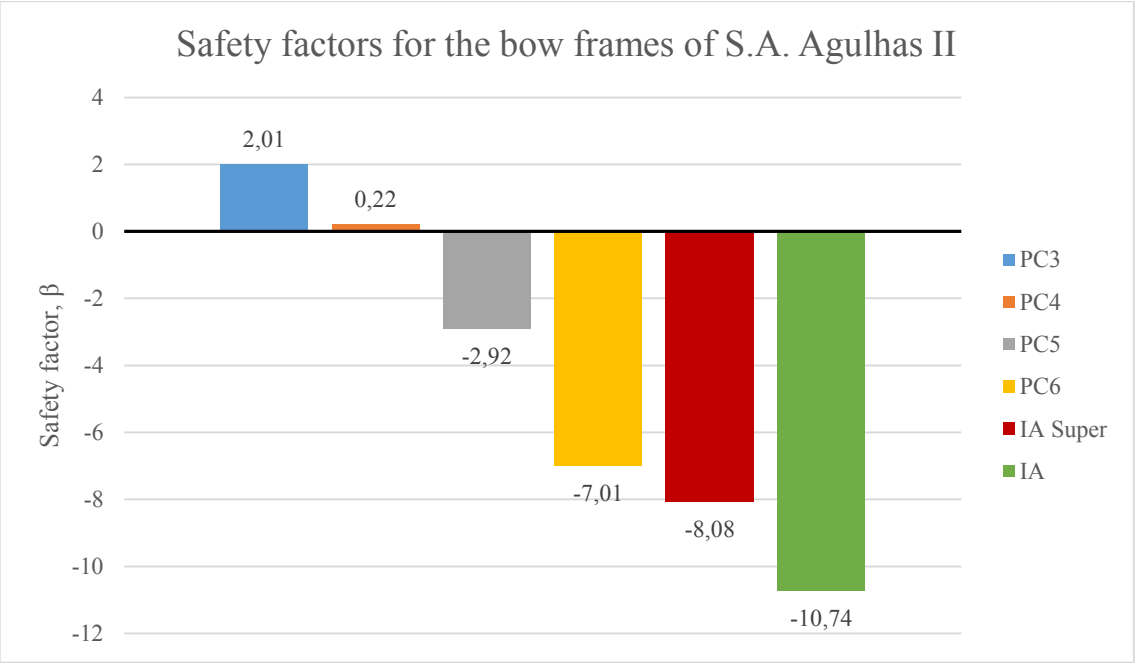

Figure 4.3 Safety indices of the bow frames (S.A. Agulhas II)

The safety indices for the bow frames show that IACS PC3 ice class is barely above the safety index of 2, which is taken to be the lower limit of risk based designs. A safety index of 2 gives a probability of failure of 0.02, meaning 2 out of 100 ship during their lifetime of 25 years will exceed the limit state.

The safety index for bow plating based on IACS and FSICR calculations are shown in Table 4.5 and Table 4.6 respectively. A sensitivity analysis is done with plate serviceability limit state to see how the load height h_c effects the safety index of the plating. The safety index for bow plating are shown in graphical form on Figure 4.4 and Figure 4.5.

Table 4.5 Safety indices of the bow plating (S.A. Agulhas II, IACS rules)

	PC3			**PC4**			**PC5**			**PC6**		
hc [mm]	100	300	500	100	300	500	100	300	500	100	300	500
β	3,88	4,86	6,06	2,68	3,76	5,05	1,74	2,98	4,36	-0,10	1,61	3,28
Plate [mm]	30			25			22			18		

Table 4.6 Safety indices of the bow plating (S.A. Agulhas II, FSICR rules)

	IA Super			**IA**		
hc [mm]	100	300	500	100	300	500
β	1,74	2,98	4,36	0,94	2,36	3,86
Plate [mm]	22			20		

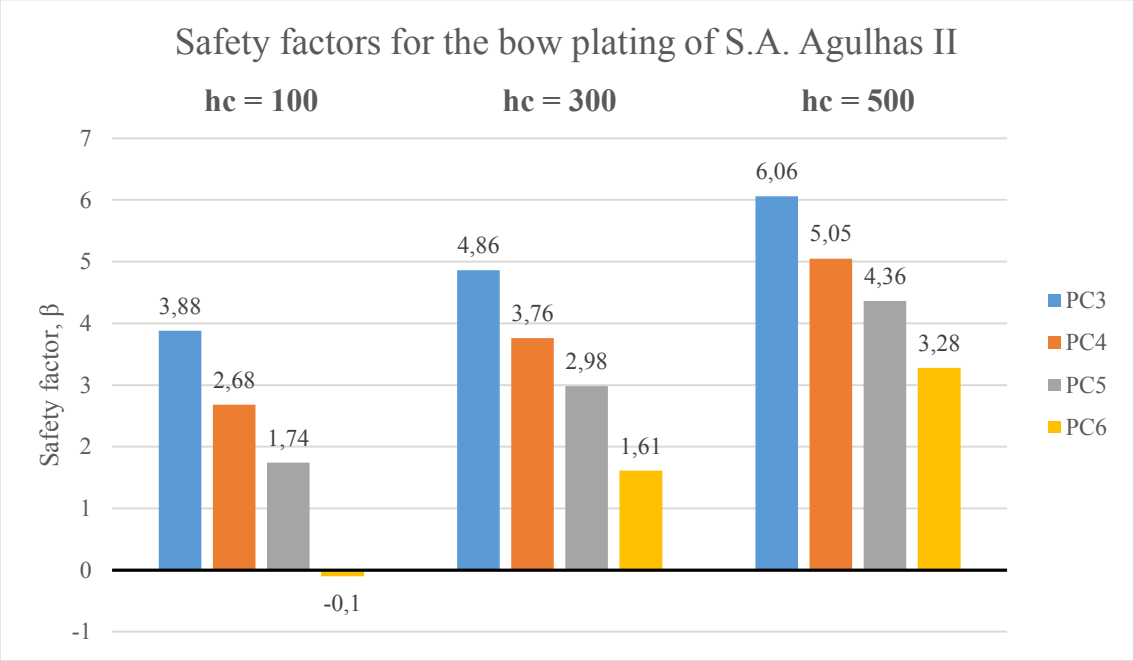

Figure 4.4 Safety indices of the bow plating (S.A. Agulhas II, IACS rules)

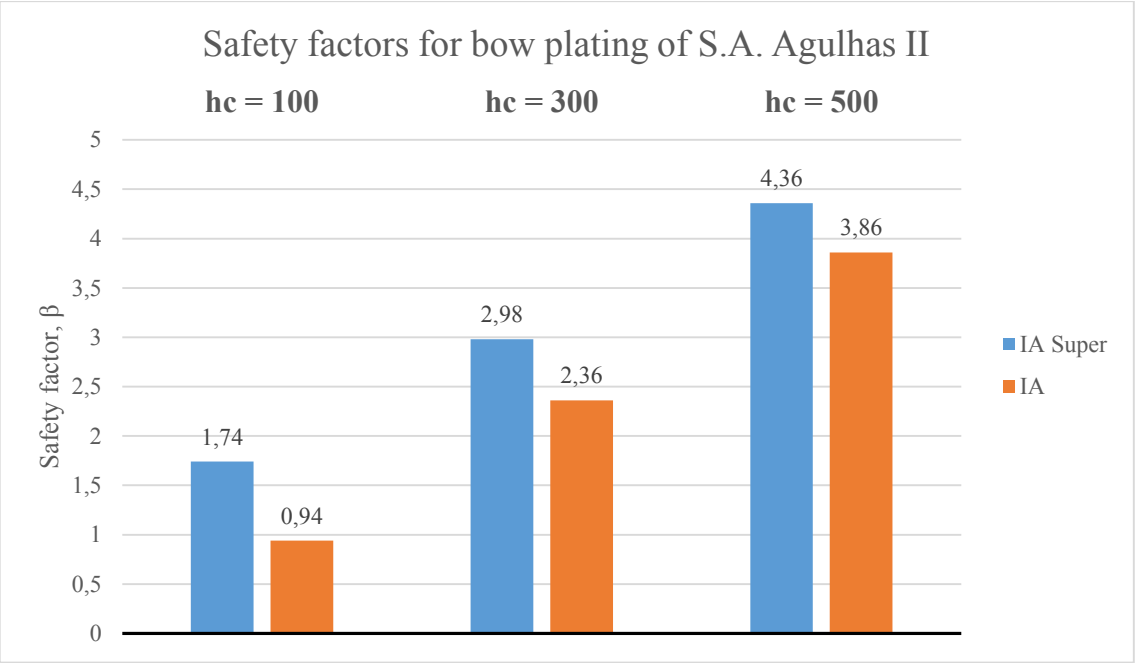

Figure 4.5 Safety indices of the bow plating (S.A. Agulhas II, FSICR rules)

As we can see from the figures the increase in load height significantly increases the safety indices of the plating, this is to be expected as a narrower load causes higher stresses. Nearly all of the combinations of load heights and plate thicknesses are above the safety index of 2, thus the plating thicknesses are estimated quite high for the rules.

Now we shall go over the safety indices of the stern framing and plating on S.A. Agulhas II. Safety indices for the stern frames based on IACS and FSICR rules are presented in Table 4.7. In graphical form the safety indices are shown on Figure 4.6.

Table 4.7 Safety indices of the stern frames (S.A. Agulhas II)

	PC3	**PC4**	**PC5**	**PC6**	**IA Super**	**IA**
β	3,17	1,22	-3,69	-11,92	-12,73	-18,33
P_f	0,00	0,11	1,00	1,00	1,00	1,00
Frame [mm]	I-250x22	I-220x20	I-180x18	I-150x15	I-150x14	I-140x12
Z_p [cm^3]	753,1	539,8	326,6	196,7	189,0	147,2

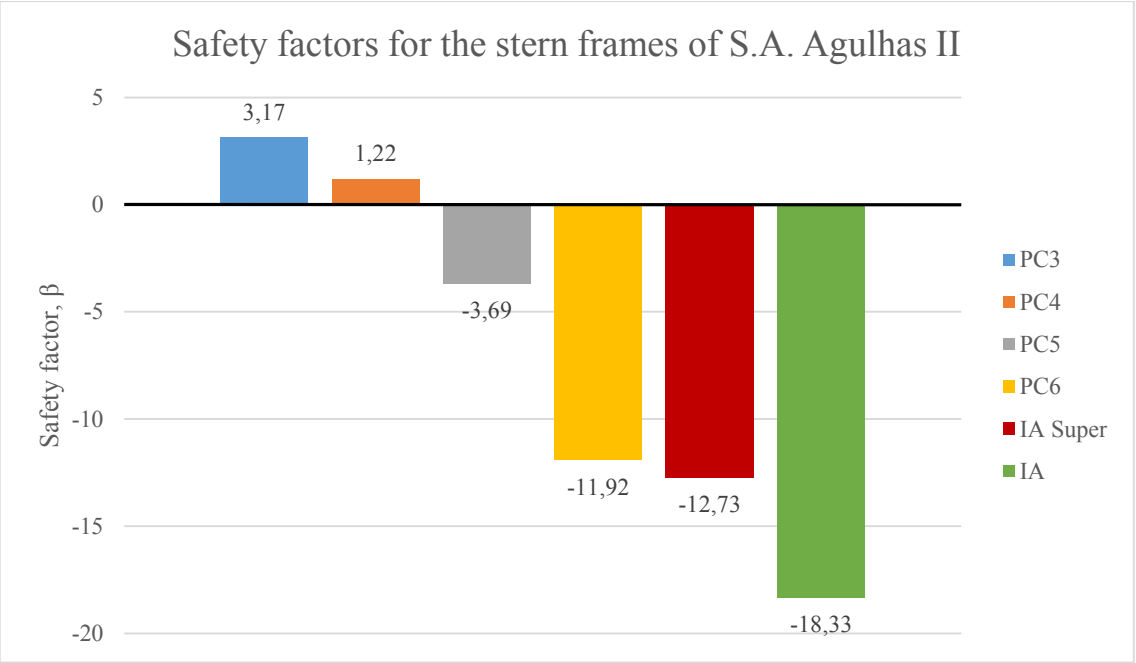

Figure 4.6 Safety indices of the stern frames (S.A. Agulhas II)

The stern of the ship is better equipped for the Antarctic at the better IACS ice classes, however as sharp drop off in safety is viewable at PC6, which continues onto the FSICR classes.

Stern plating thicknesses and the corresponding safety indices for IACS and FSICR are shown in Table 4.8 and Table 4.9 respectively. In graphical form the stern plating safety indices are shown in Figure 4.7 and Figure 4.8.

Table 4.8 Safety indices of the stern plating (S.A. Agulhas II, IACS rules)

	PC3			**PC4**			**PC5**			**PC6**		
hc [mm]	100	300	500	100	300	500	100	300	500	100	300	500
β	4,75	5,79	7,15	4,17	5,23	6,60	2,77	3,96	5,43	1,84	3,18	4,75
Plate [mm]	22			20			16			14		

Table 4.9 Safety indices of the stern plating (S.A. Agulhas II, FSICR rules)

	IA Super			**IA**		
hc [mm]	100	300	500	100	300	500
β	1,84	3,18	4,75	1,84	3,18	4,75
Plate [mm]	14			14		

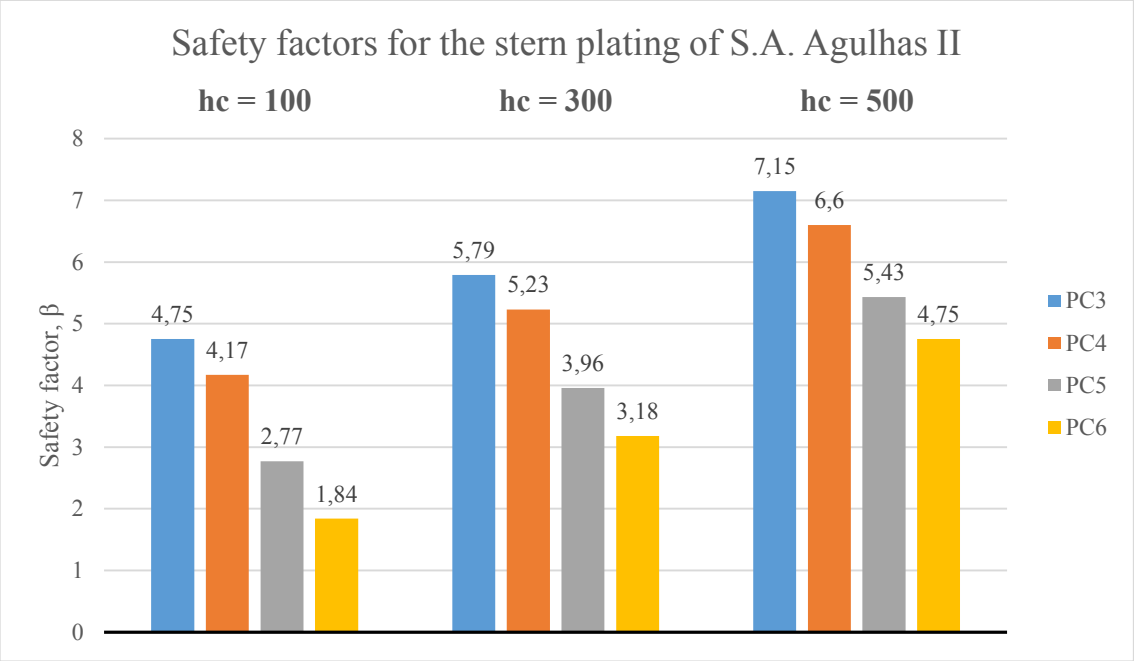

Figure 4.7 Safety indices of the stern plating (S.A. Agulhas II, IACS rules)

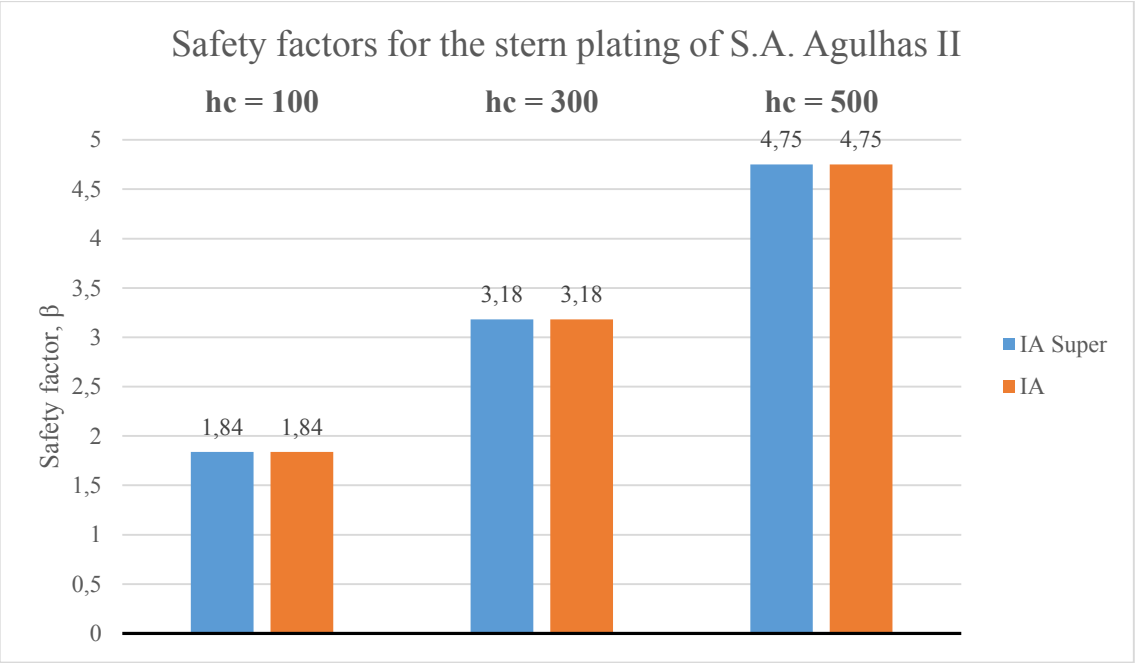

Figure 4.8 Safety indices of the stern plating (S.A. Agulhas II, FSICR rules)

The stern plating has quite similar safety indices as the bow plating had. The safety indices in the stern are slightly higher.

It is difficult to say which ice load height should be used for calculating the safety indices of the plating. Kaldasaun in his thesis [14] used a load height of 0.075 m, which was derived based on the work done in Valkonen's thesis [28]. However, load height according to IACS rules [25] is ~0.5 m and according to FSICR rules [26] it is about 0.3 m. This gave an incentive to undertake a sensitivity analysis to see how the safety index is affected by different ice load heights. It can be clearly seen that the load height has a significant effect on the safety indices.

4.2.2. M/T Uikku

The hull of M/T Uikku was also assumed to be made out of S355 steel. The statistical characteristics of steel S355 are shown in Chapter 4.2.1. Structural scantlings for the bow and stern of M/T Uikku were taken to be the same as for S.A. Agulhas II, T-frames and I-frames respectively. For the bow-shoulder of M/T Uikku T-frames were also used. The frame span for the bow is 2 m, 2.92 m for the bow-shoulder and 1.22 m for the stern, the frame spacing is 0.35 m.

Let's again first look at the bow frames and plating safety indices, then at the bow-shoulder safety indices and finally at stern safety indices. The reason why S.A. Agulhas

II did not have bow-shoulder safety indices calculated was, because the loads recorded by the sensors we deemed to be not reliable, which was probably due to a fault in the instrumentation. The bow frames safety indices for M/T Uikku are presented in Table 4.10. Graphically the safety indices are shown in Figure 4.9.

Table 4.10 Safety indices of the bow frames (M/T Uikku)

	PC3	**PC4**	**PC5**	**PC6**	**IA Super**	**IA**
β	6,86	5,47	3,97	2,75	-0,20	-1,41
P_f	0,00	0,00	0,00	0,00	0,58	0,92
Frame [mm]	T-410x18 / 90x18	T-380x16 / 80x16	T-340x14 / 70x16	T-320x12 / 70x14	T-230x12 / 50x15	T-210x12 / 50x15
Z_p [cm^3]	2088	1557	1130	879,6	556,8	487,8

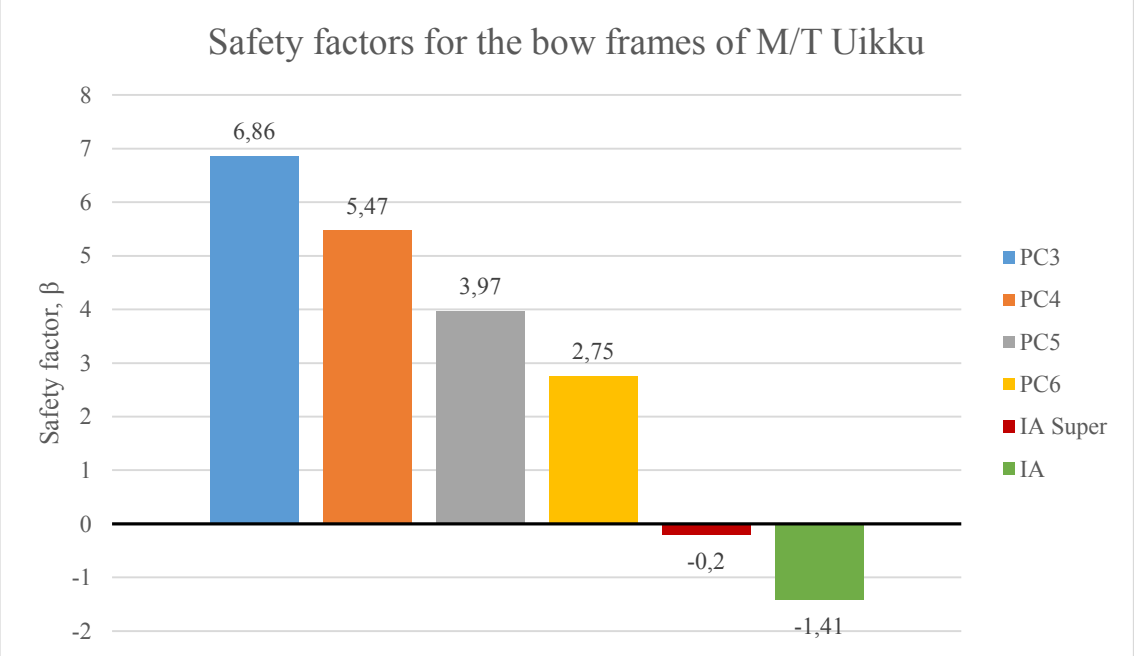

Figure 4.9 Safety indices of the bow frames (M/T Uikku)

Now we shall look at the safety indices of the bow plating on M/T Uikku, which are presented for IACS and FSICR in Table 4.11 and Table 4.12 respectively. A sensitivity analysis was also done for M/T Uikku's plating to see how the ice load height h_c effects the safety indices. The graphical form of the plating safety indices for the bow of M/T Uikku are shown in Figure 4.10 and Figure 4.11 respectively.

Table 4.11 Safety indices of the bow plating (M/T Uikku, IACS rules)

	PC3			PC4			PC5			PC6		
hc [mm]	100	300	500	100	300	500	100	300	500	100	300	500
β	6,39	7,50	N/A	5,28	6,41	8,04	4,53	5,68	7,25	3,98	5,15	6,75
Plate [mm]	30			25			22			20		

Table 4.12 Safety indices of the bow plating (M/T Uikku, FSICR rules)

	IA Super			IA		
hc [mm]	100	300	500	100	300	500
β	3,98	5,15	6,75	3,98	5,15	6,75
Plate [mm]	20			20		

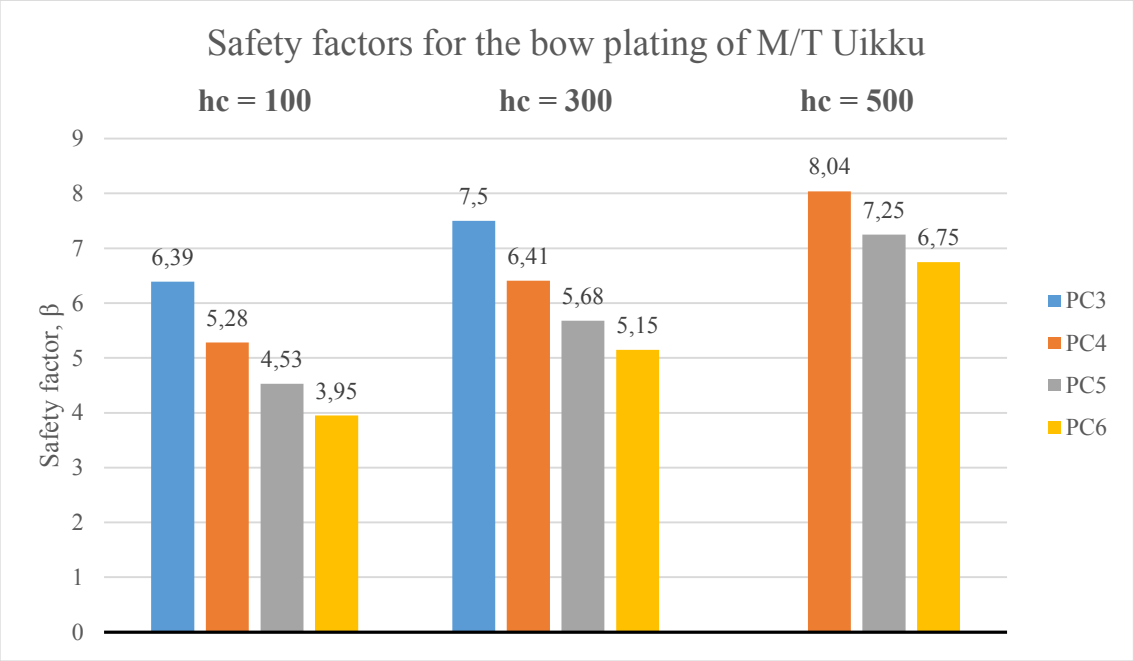

Figure 4.10 Safety indices of the bow plating (M/T Uikku, IACS rules)

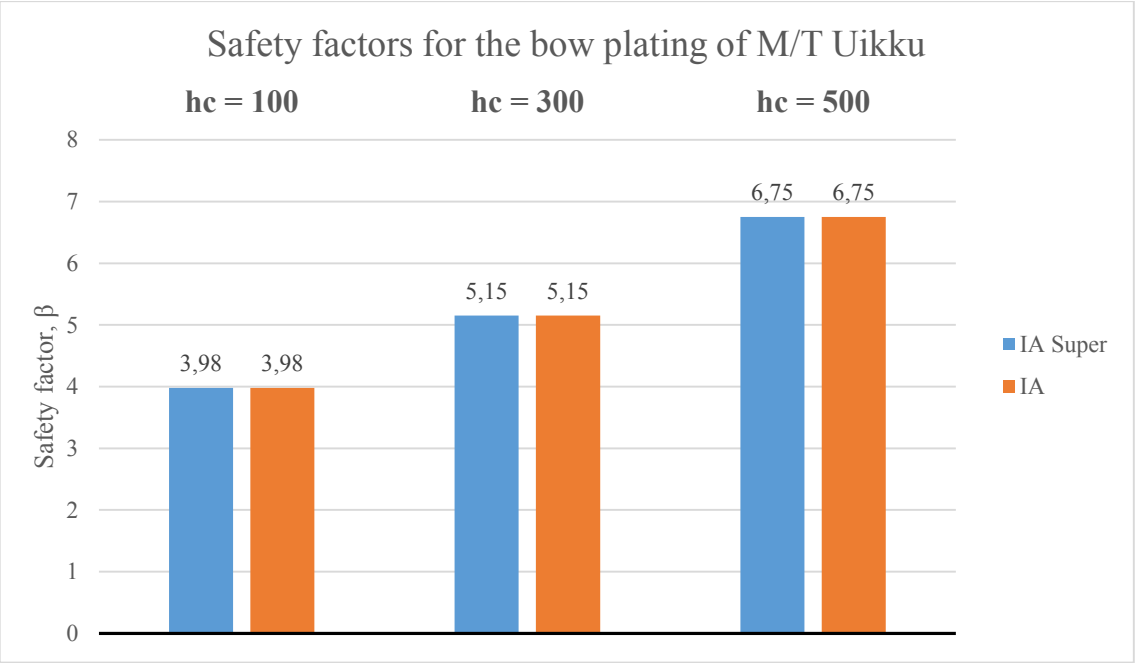

Figure 4.11 Safety indices of the bow plating (M/T Uikku, FSICR rules)

We can see that M/T Uikku's plating is for every ice class well over the safety index of 2, which we set for risk-based designs. On Figure 4.10 at load height $h_c = 500\ mm$ the PC3 ice class safety index could not be calculate. This was due to the algorithm not converging to a result, but with certainty we can say that the safety index of PC3 ice class for bow plating at that load height would be higher than the PC4 class safety index is.

The safety indices for the bow-shoulder frames of M/T Uikku were calculated and are presented in Table 4.13. Graphical representation of the safety indices of the bow-shoulder frames is given in Figure 4.12.

Table 4.13 Safety indices of the bow-shoulder frames (M/T Uikku)

	PC3	**PC4**	**PC5**	**PC6**	**IA Super**	**IA**
β	3,91	2,33	0,41	-2,47	-3,72	-5,52
P_f	0,00	0,01	0,34	0,99	1,00	1,00
Frame [mm]	T-420x18 / 90x22	T-380x16 / 80x20	T-360x14 / 70x16	T-340x12 / 60x14	T-280x14 / 60x15	T-260x14 / 60x14
Z_p [cm^3]	2460	1792	1325	972,1	874,2	762,9

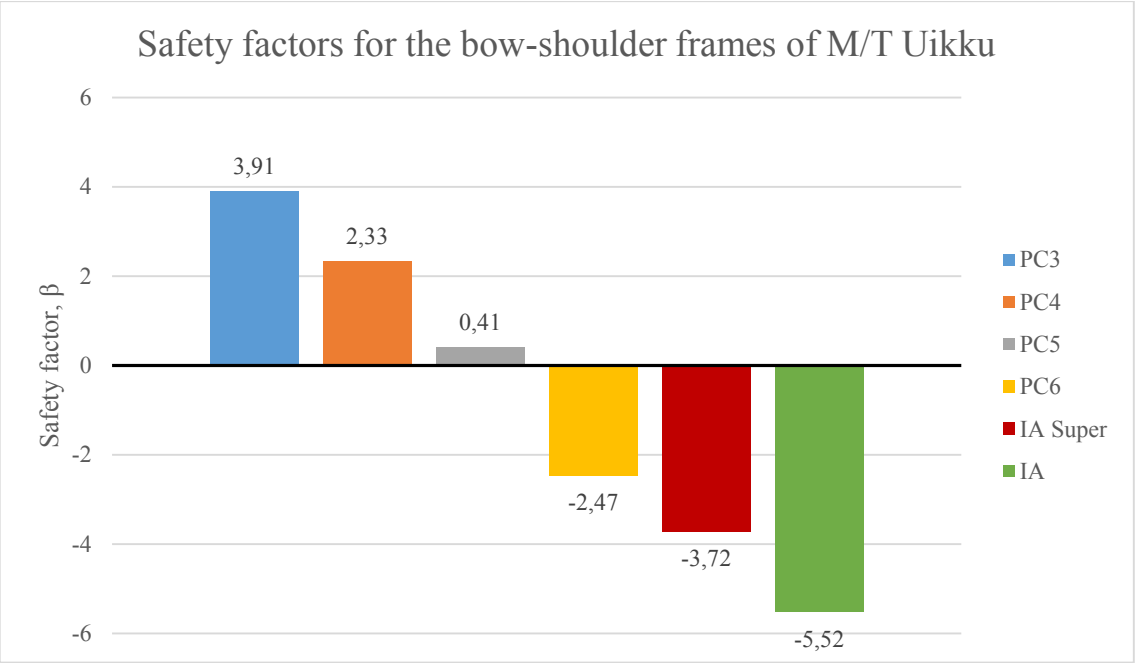

Figure 4.12 Safety indices of the bow-shoulder frames (M/T Uikku)

Figure 4.12 illustrates effectively how the safety indices of the bow-shoulder frames are lower than the bow frames shown in Figure 4.9. This is to be expected as the Uikku IACS bow life-time ice loads on the bow-shoulder were higher than on the bow.

The bow-shoulder plating safety indices are presented in Table 4.14 and Table 4.15 for IACS and FSICR respectively. A graphical representation of the safety indices of the bow-shoulder based on IACS and FSICR are shown on Figure 4.13 and Figure 4.14 respectively.

Table 4.14 Safety indices of the bow-shoulder plating (M/T Uikku, IACS rules)

	PC3			**PC4**			**PC5**			**PC6**		
hc [mm]	100	300	500	100	300	500	100	300	500	100	300	500
β	3,27	4,4	5,87	2,47	3,70	5,23	1,82	3,16	4,77	-0,04	1,80	3,70
Plate [mm]	25			22			20			16		

Table 4.15 Safety indices of the bow-shoulder plating (M/T Uikku, FSICR rules)

	IA Super			**IA**		
hc [mm]	100	300	500	100	300	500
β	1,82	3,16	4,77	1,82	3,16	4,77
Plate [mm]	20			20		

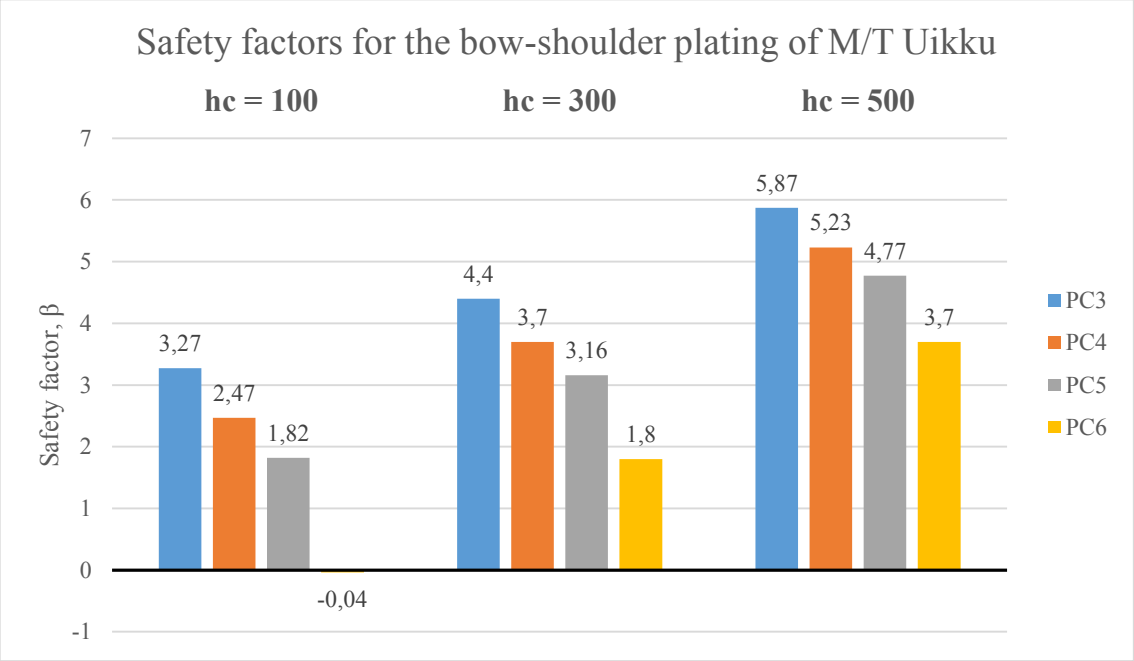

Figure 4.13 Safety indices of the bow-shoulder plating (M/T Uikku, IACS rules)

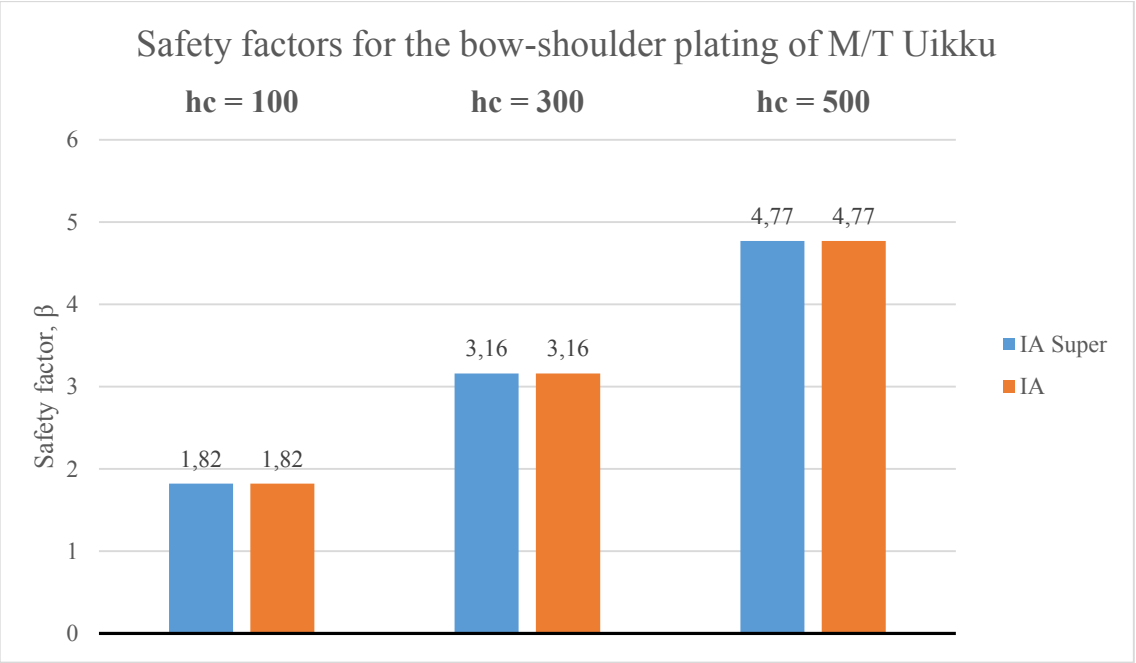

Figure 4.14 Safety indices of the bow-shoulder plating (M/T Uikku, FSICR rules)

By comparing the safety indices from Figure 4.10 and Figure 4.13 we can see that also for the plating the safety indices at the bow-shoulder are about two times smaller than at the bow, which shows again that the bow-shoulder is much more prone to failure than the bow.

Finally we shall look at the stern frames and plating safety indices. First let us have a look at the frames safety indices. The safety indices for the stern frames are given in Table 4.16. A graphical representation of the safety indices is shown on Figure 4.15.

Table 4.16 Safety indices of the stern frames (M/T Uikku)

	PC3	**PC4**	**PC5**	**PC6**	**IA Super**	**IA**
β	8,87	7,09	4,55	2,03	1,04	-0,35
P_f	0,00	0,00	0,00	0,02	0,15	0,64
Frame [mm]	I-200x25	I-210x20	I-170x18	I-140x15	I-130x14	I-120x14
Z_p [cm^3]	665,5	489	285	171,5	145,8	121,5

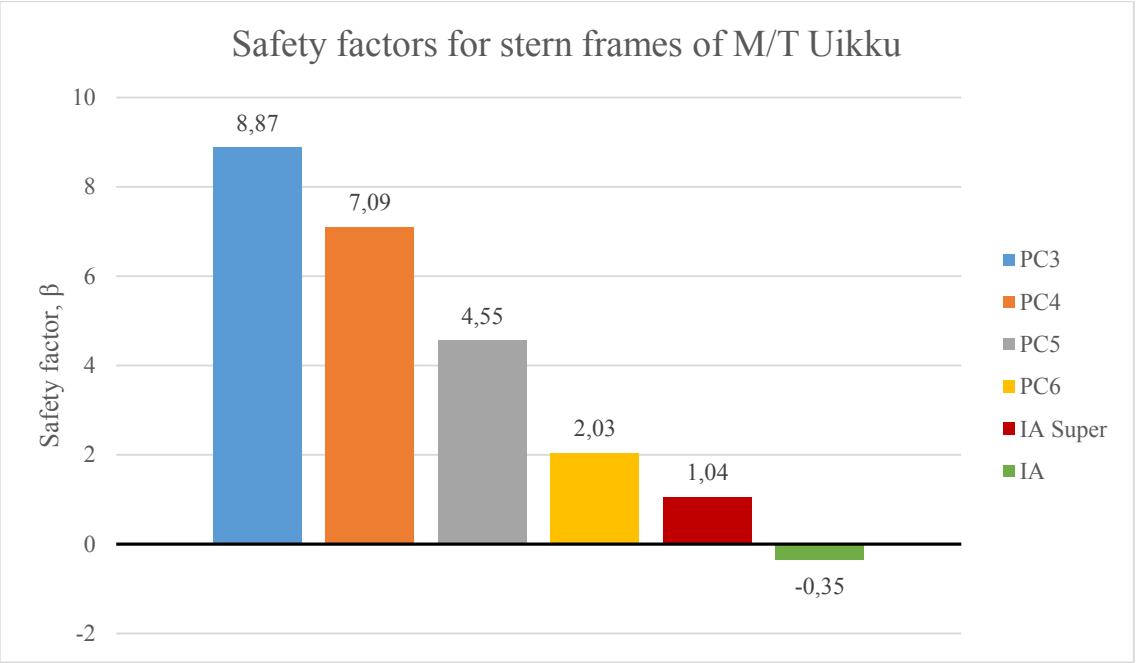

Figure 4.15 Safety indices of the stern frames (M/T Uikku)

As we can see ice class PC6 would be sufficient according to our predetermined threshold safety index of 2. However, we know that the ship was classified as IA Super, thus from Figure 4.15 we can observe that safety index is lower than we want it to be at 1.04, which equates to 15 ships out of 100 succumbing to frame failure during the ships life-time of 25 years.

The stern plating safety indices for plating calculated with IACS and FSICR are presented in Table 4.17 and Table 4.18 respectively. In graphical form the safety indices for the stern plating are shown on Figure 4.16 and Figure 4.17 for IACS and FSICR respectively.

Table 4.17 Safety indices of the stern plating (M/T Uikku, IACS rules)

	PC3			**PC4**			**PC5**			**PC6**		
hc [mm]	100	300	500	100	300	500	100	300	500	100	300	500
β	10,49	11,83	13,21	9,73	11,22	12,84	7,48	9,17	11,40	7,07	8,65	11,02
Plate [mm]	22			20			15			14		

Table 4.18 Safety indices of the stern plating (M/T Uikku, FSICR rules)

	IA Super			**IA**		
hc [mm]	100	300	500	100	300	500
β	7,07	8,65	11,02	6,18	7,57	10,11
Plate [mm]	14			12		

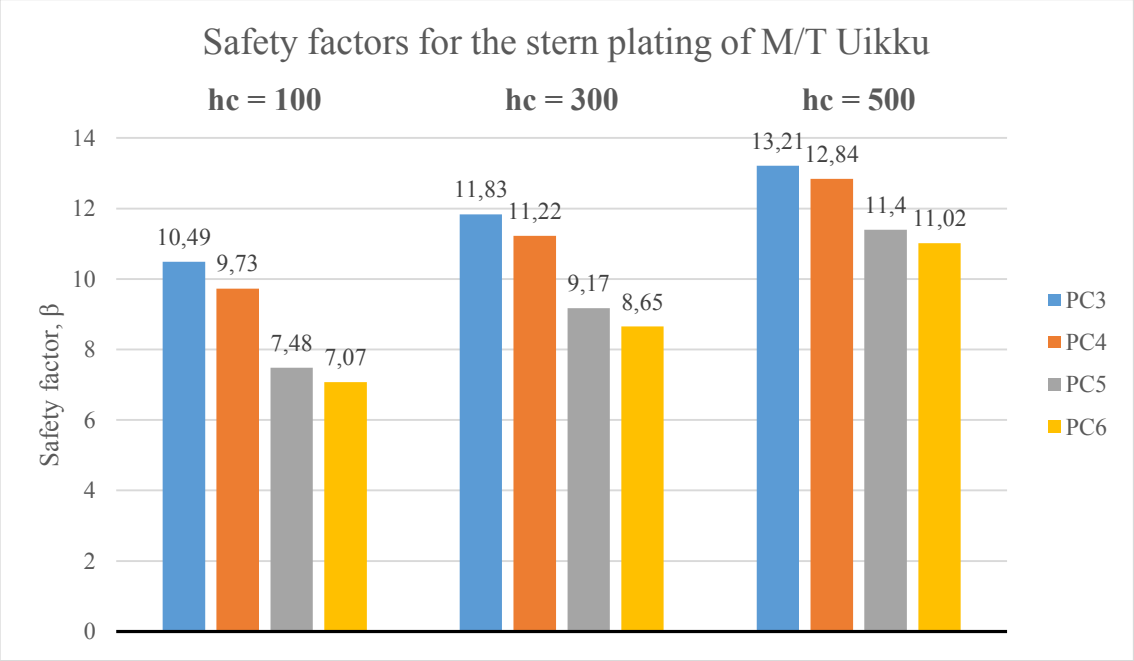

Figure 4.16 Safety indices of the stern plating (M/T Uikku, IACS rules)

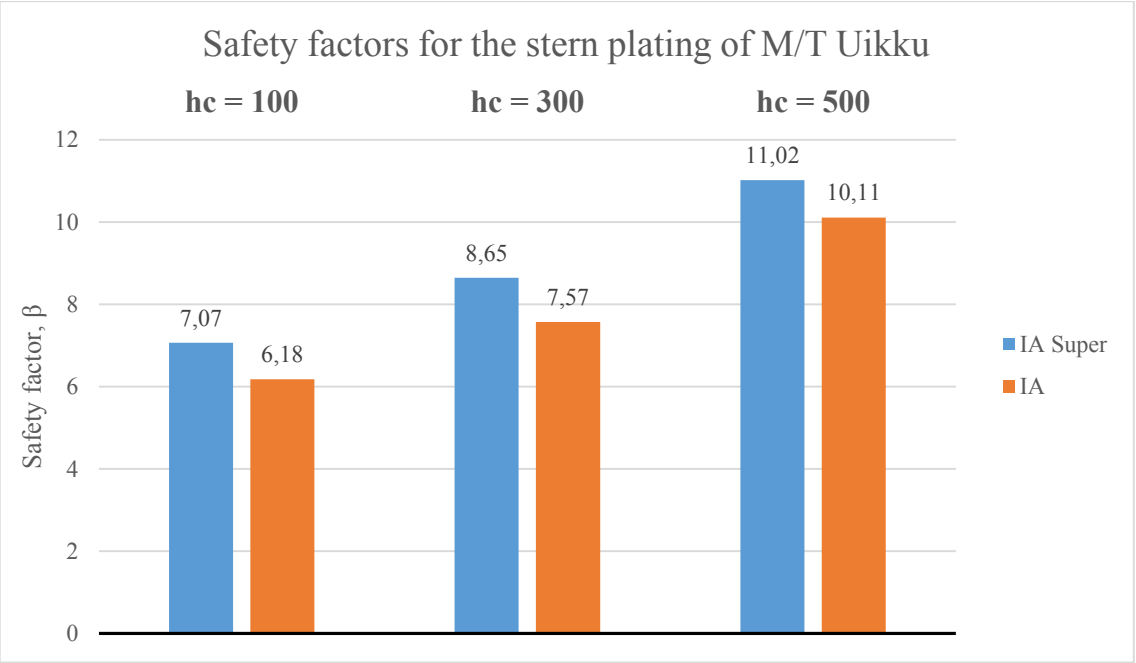

Figure 4.17 Safety indices of the stern plating (M/T Uikku, FSICR rules)

The stern plating safety indices are well above the plating that is calculated for risk-based plating. These high safety index values are due to low loads on the stern, which might be caused by the fact that the ship was being towed or assisted during the voyage in the Arctic. Thus, the ship was always in an ice channel and since the ice channel was probably wide enough that the stern of the ship during turning did not press against the level ice edge. Probably the loads at the stern were from larger pieces of rubble in the channel hitting the stern of the ship during turns. That would explain the high amount of sub 10 kN loads on the stern frames, which was also the threshold limit set for filtering out open water loads.

4.3. Reliability analysis in various ice conditions

The different ice conditions chosen are based on the definitions from the Polar Code [29], which takes it ice condition definitions from WMO Sea Ice Nomenclature [30]. Since as Kujala et al mentioned in [31] that it is not explicitly mentioned in polar code or WMO how ice thicker than 2 m is categorized, meaning is it second year ice or multiyear ice. Thus, a conservative approach was taken and ice thicker than 2 m was chosen to be classified as second year ice. Also a conservative approach was taken for ice that is thinner than 0.7 m and chosen to be classified as thin first year ice 1st stage.

In Table 4.19 the different ice conditions cases are presented for which the safety indices are calculated. The loads are divided based on the prevailing ice conditions in 10 minute intervals into the corresponding ice condition cases. The prevailing ice condition during a 10 minute period was based on the ice regime during that period. Ice regime is described by POLARIS [32] and AIRSS [33] as an area with relatively consistent distribution of any mix of ice types, including open water. Visual observations provided the ice regimes for each 10 minute period and 20 minute period for S.A. Agulhas and M/T Uikku respectively. The prevailing ice condition for each time period was chosen to be the maximum ice thickness and the average ice concentration during that period. Maximum ice thickness was chosen over average ice thickness as we are dealing with maximum loads, thus it seems sensible to assume that the maximum loads occurred during the time period in the thickest ice during that period. However, it must be said that for M/T Uikku's voyage there is no data in ice condition cases where ice thickness is above 2 m, because during the voyage ice thickness above 2 m was not seen in visual observations. In addition, some ice conditions had only two or less data points for the load, which unfortunately is not enough data to calculate the safety indices or analyze the ice loading data statistically. These ice condition cases will be mentioned explicitly further on.

Table 4.19 Different ice condition cases used in the study

		Ice thickness [m]			
		< 0,7	0,7 – 1,2	1,2 – 2,0	> 2,0
Ice concentration [%]	< 70	Case 1	Case 2	Case 3	Case 4
	70-90	Case 5	Case 6	Case 7	Case 8
	> 90	Case 9	Case 10	Case 11	Case 12

As mentioned above M/T Uikku has no data for ice thickness above 2 m, thus cases 4, 8 and 12 are not going to be presented in this study for M/T Uikku.

4.3.1. S.A. Agulhas II

Fortunately S.A. Agulhas II has gathered enough data during 2 voyages in the Antarctic. Thus, quite an in depth view can be seen on how the different ice conditions effect the

safety index of the ship. The frames and plating of the ship used in these calculations are the same as can be seen in the previous Chapter 4.2. For ease of understanding the framing and plating of S.A. Agulhas II for the bow and stern for different ice classes is shown in Table 4.20.

Table 4.20 Bow and stern framing and plating (S.A. Agulhas II)

	PC3	**PC4**	**PC5**	**PC6**	**IA Super**	**IA**
	Bow					
Frame [mm]	T-340x16 / 80x20	T-320x14 / 70x20	T-300x12 / 60x18	T-280x10 / 60x16	T-240x12 / 50x15	T-220x12 / 50x15
Plate [mm]	30	25	22	18	22	20
	Stern					
Frame [mm]	I-250x22	I-220x20	I-180x18	I-150x15	I-150x14	I-140x12
Plate [mm]	22	20	16	14	14	14

The safety indices for the bow of the ship in different ice conditions is gone over now. Ice conditions cases 1-4 and the safety indices for different ice classes are shown in Figure 4.18. Safety indices for ice condition cases 5-8 are shown in Figure 4.19. Safety indices for ice condition cases 9-12 are shown in Figure 4.20. It must be said that for ice condition cases 5 and 9, which correspond to ice thickness < 0.7 m and ice concentrations of 70-90 % and > 90 % respectively, there were significantly fewer loads than for the other conditions. Thus the results for case 5 and 9 might not give an actual overview of the safety indices that really should be in those conditions. Therefore the results in these cases might be biased. Especially biased seems to be the data in case 5, however in case 9 the bias is not that visible. The amount of data in cases 5 and 9 is about 10 times less than the average amount of data in each case. In point of view of amount of data the third lowest case had about 5 time more data than cases 5 and 9.

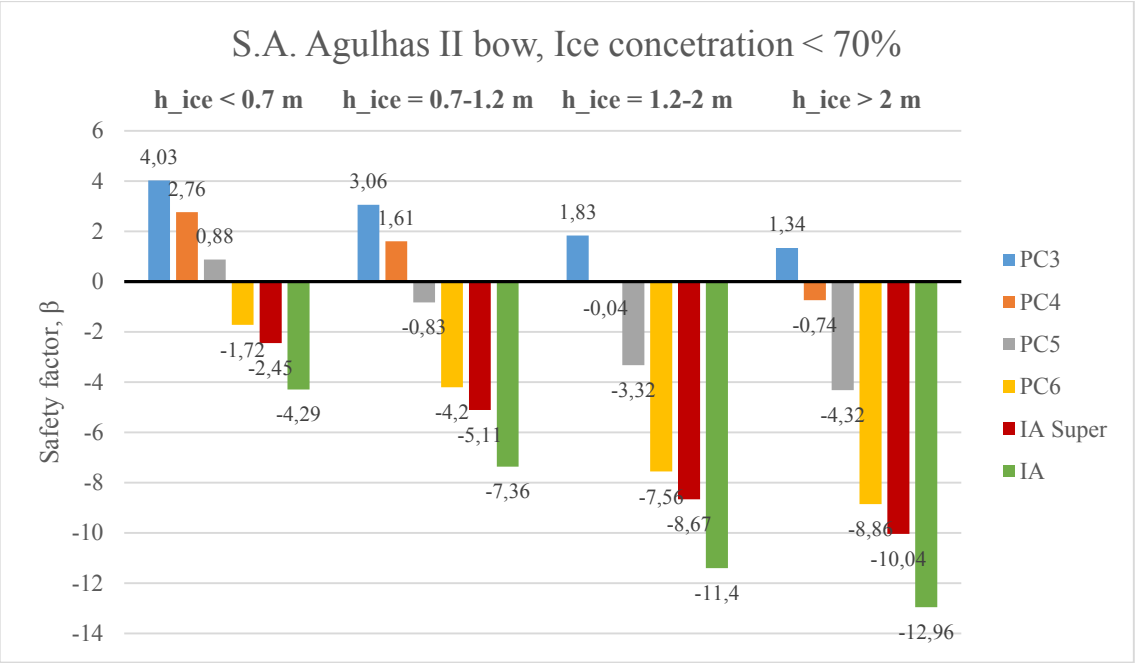

Figure 4.18 Safety indices of bow framing in ice condition cases 1-4 (S.A. Agulhas II)

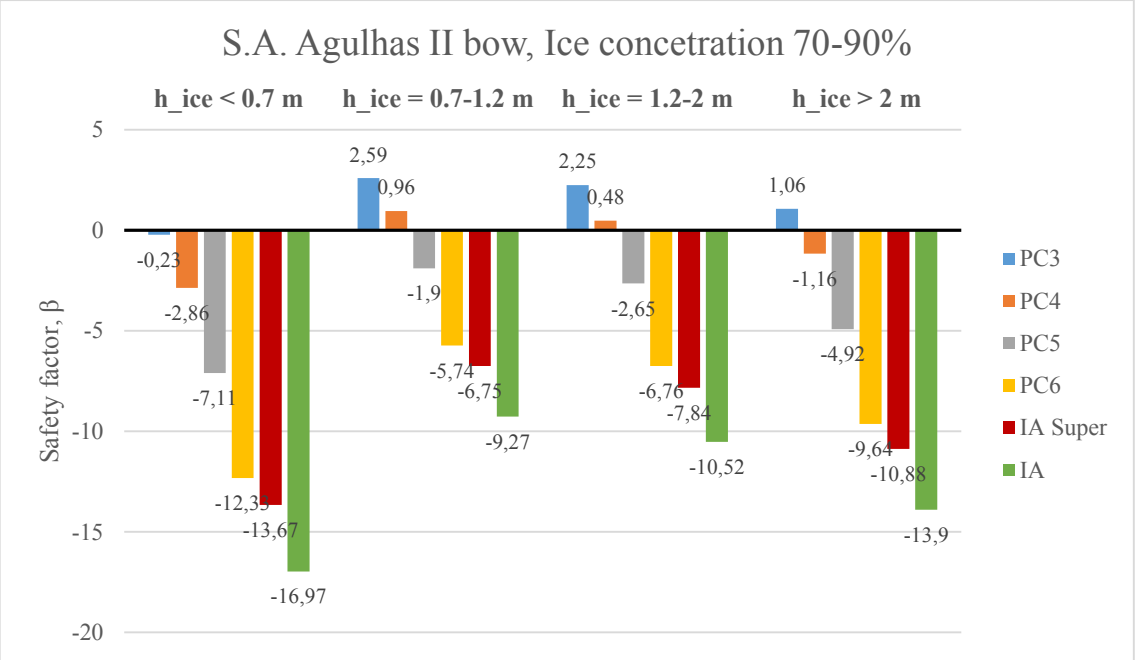

Figure 4.19 Safety indices of bow framing in ice condition cases 5-8 (S.A. Agulhas II)

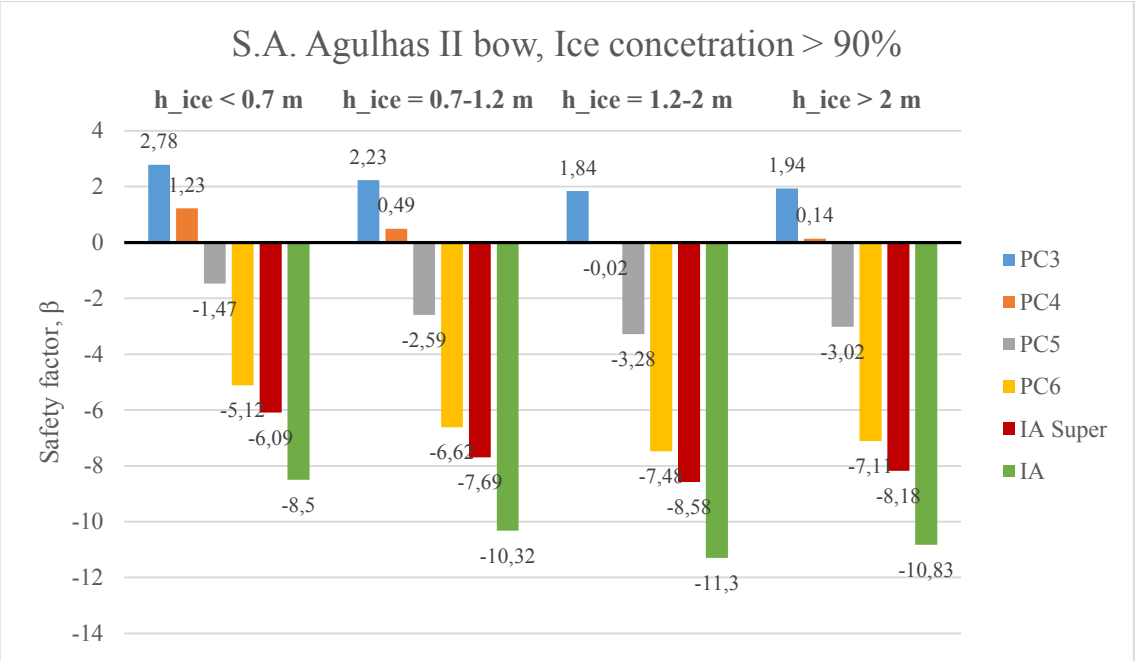

Figure 4.20 Safety indices of bow framing in ice condition cases 9-12 (S.A. Agulhas II)

In general these figures show that increasing ice thickness in any ice concentration causes a decrease in safety indices. In the ice conditions where ice concentration was < 70% and 70-90% this statement holds up well. However, for ice conditions where ice concentration is > 90% it seems that the increase in ice thickness has some effect on the safety indices, but not for cases where ice thickness is above 1.2m. Thus, an interesting question arises, why at lower ice concentrations the ice thickness has a visible effect on the safety indices, whereas at an ice concentration >90% and ice thickness >1.2m the effects of ice thickness on the safety indices disappear. It might be due to a slower sailing speed at level ice conditions and higher speeds at lower ice concentrations, which could lead to high loads on the hull when the ships hits thick ice. Additionally, we can see that the most dangerous ice condition is case 8, when not taking into account case 5 due to its probable bias.

Now the stern framing safety indices at different ice conditions are analyzed. As the stern has the exact same data division into ice conditions as the bow, case 5 and 9 are probably biased in the results on the safety indices. Safety indices for the stern of the ship in ice condition cases 1-4 are shown in Figure 4.21. Safety indices for ice condition cases 5-8 are shown in Figure 4.22. Safety indices for ice condition cases 9-12 are shown in Figure 4.23.

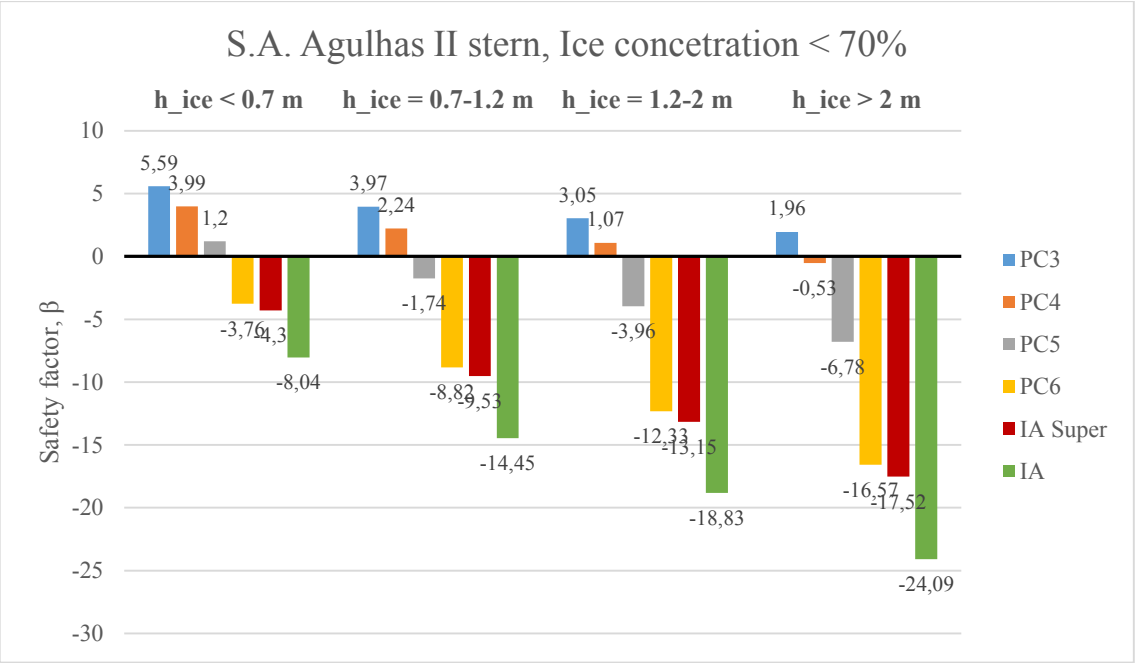

Figure 4.21 Safety indices of stern framing in ice condition cases 1-4 (S.A. Agulhas II)

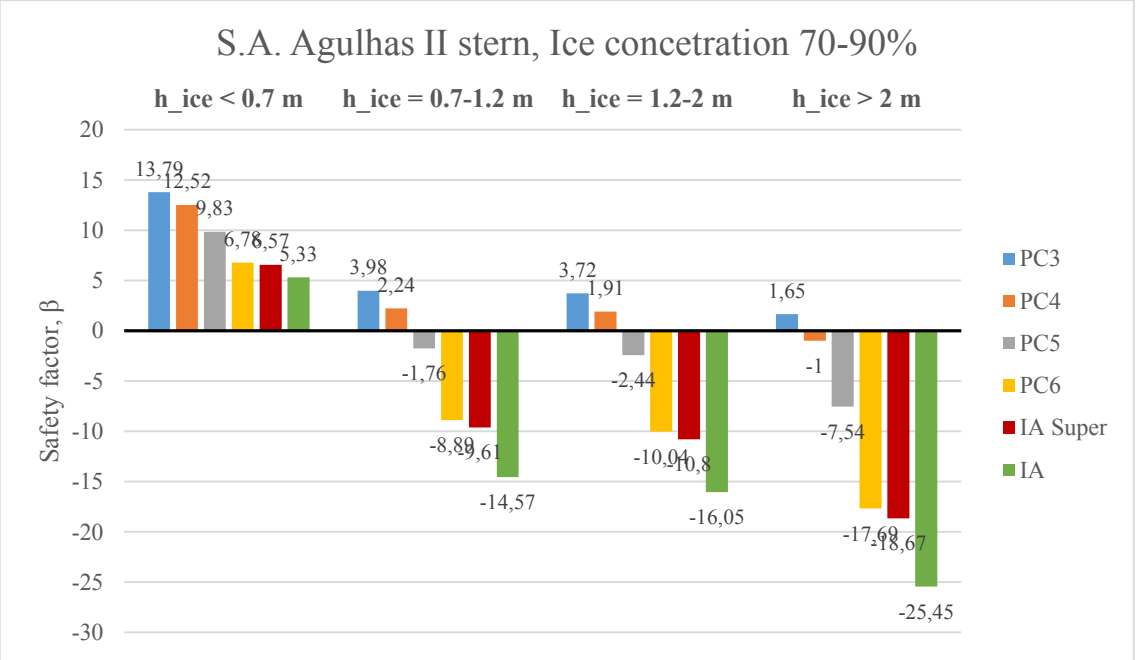

Figure 4.22 Safety indices of stern framing in ice condition cases 5-8 (S.A. Agulhas II)

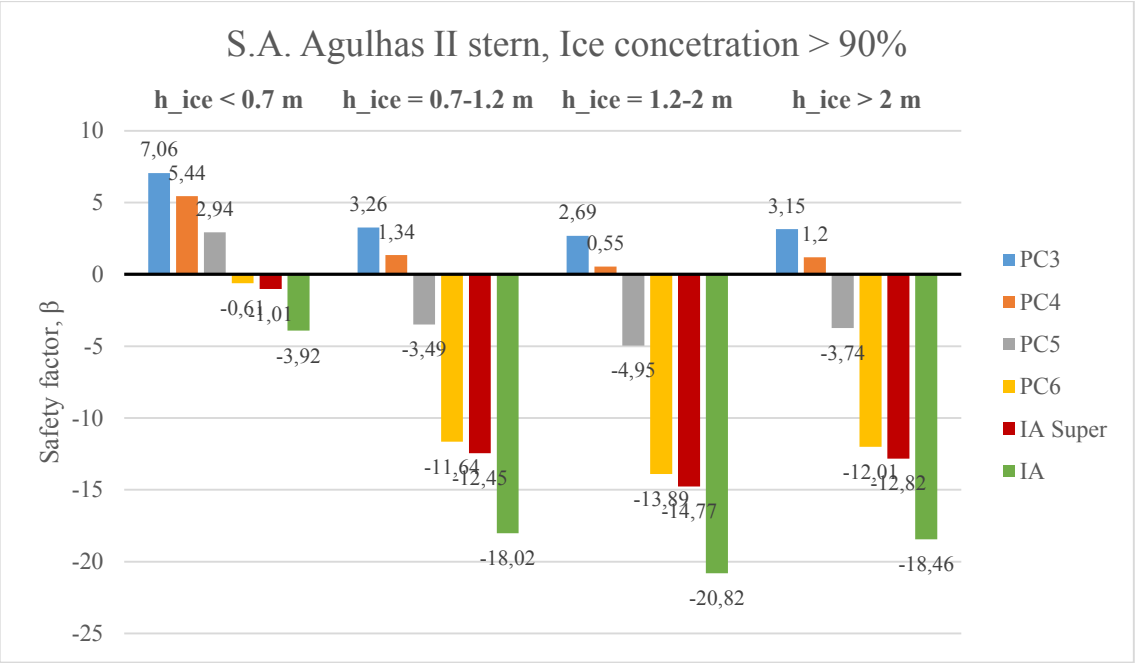

Figure 4.23 Safety indices of stern framing in ice condition cases 9-12 (S.A. Agulhas II)

It's clearly seen again in cases 1-4 where ice concentration is <70% that increase in ice thickness causes a decrease in safety indices. In cases 5-8 where ice concentration is 70-90% the same conclusion is evident. However, again case 5 where ice thickness is <0.7m the safety indices are clearly biased due to lack of data in that ice condition case. In the stern case 9-12 exhibits also a clearer biased outcome on case 9. Stern cases 10-12 are very similar in to their bow counterparts where there is not a clear drop in safety indices with the increase of ice thickness. Although both the stern and bow cases 10-12 have similarly the lowest safety indices in the 1.2-2m ice thickness range, which is interesting. Probably the same reason as mentioned in the bow section are drivers for the drop in safety indices when ice thickness increases. Also as for the cases where ice concentration is above 90%.

4.3.2. M/T Uikku

Gathered ice loading data for M/T Uikku is scarce due to the voyage being only 2 weeks long. In addition, the loading data was gathered in 20 minute intervals, meaning there is two times less data if it would have been done in 10 minute intervals. Due to this cases 2, 5 and 6 did not have enough data to conduct a statistical analysis on the ice loads. As mentioned also before cases 4, 8 and 12 have no data at all, since visual observations did not show any ice above thickness of 2 m. It must also be said that probably due to lack of ice loads in cases 1, 3, 5 and 7 the safety indices might be biased. Fortunately the ice

conditions where ice concentration was above 90% there is plentiful of data and as can be seen later the results seem nicely fit the expectations.

Now let's take a look at the bow safety indices in different ice conditions. The safety indices for cases 1 and 3 are shown on Figure 4.24. For ice conditions 5-8 the safety indices are shown on Figure 4.25.

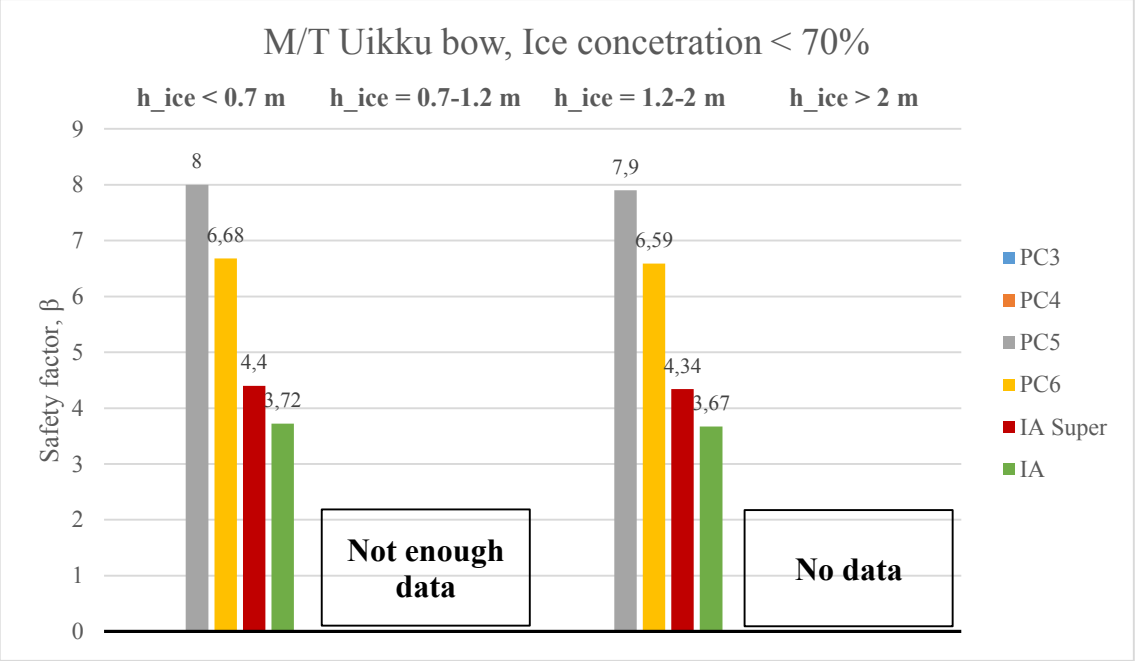

Figure 4.24 Safety indices of bow framing in ice condition cases 1-4 (M/T Uikku)

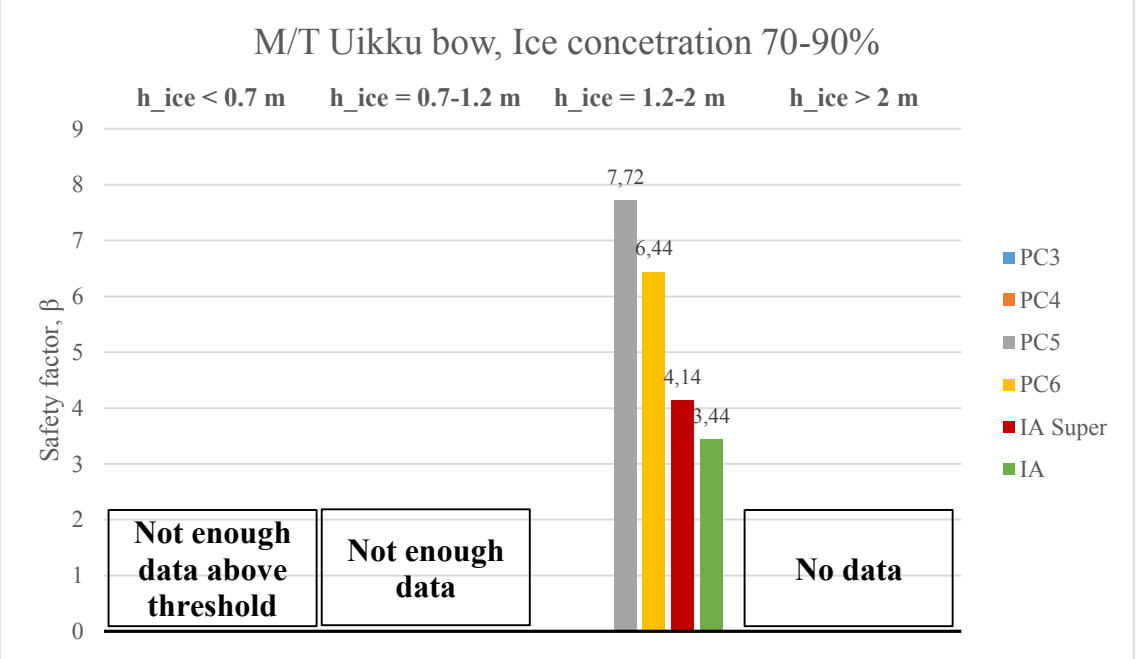

Figure 4.25 Safety indices of bow framing in ice condition cases 5-8 (M/T Uikku)

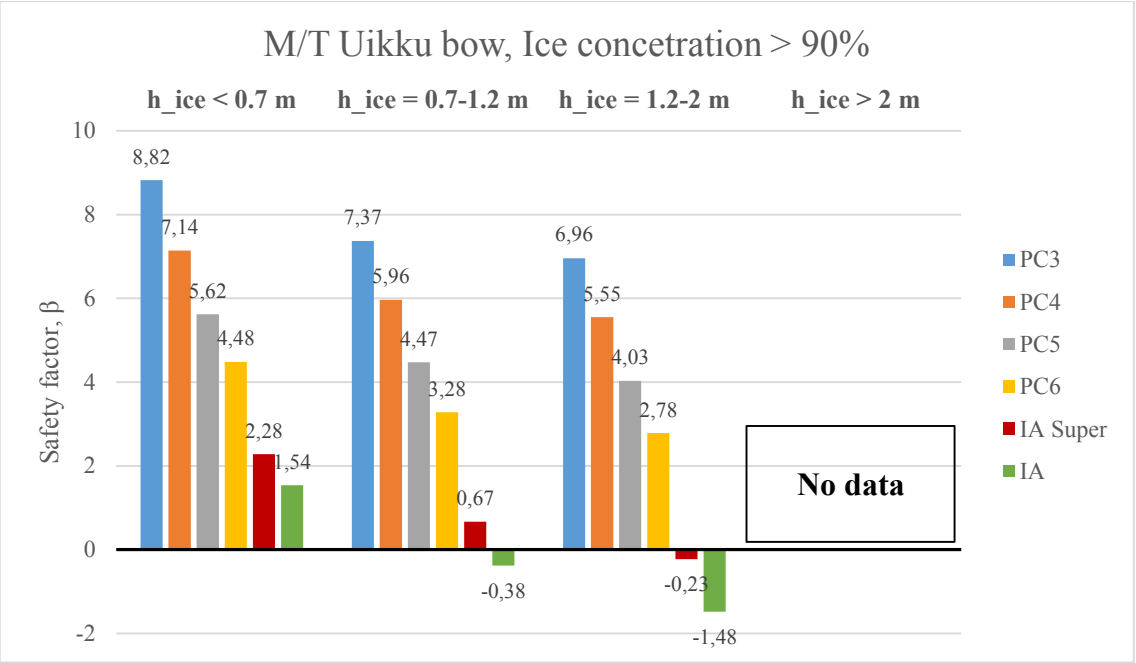

Figure 4.26 Safety indices of bow framing in ice condition cases 9-12 (M/T Uikku)

Unfortunately the safety indices in cases where ice concentration is not above 90% are quite close to each other, thus no interesting signs for conclusion. It might be due to due to the lack of data in these cases. In addition, in all of those cases PC3 and PC4 ice class safety indices are missing due to the safety index calculation algorithm not being able to converge to a result. However, for cases where ice concentration is above 90% the safety indices show a decrease in safety as the ice thickness increases. This is interesting as for S.A. Agulhas there was no such conclusion evident. Reasons why M/T Uikku shows this kind of behavior in safety indices might be due to the fact that throughout the voyage the ship was convoyed behind an icebreaker, thus even when the ice concentration is high the ship is still sailing in a channel and might be operated as S.A. Agulhas II was in lower ice concentrations. This assumption has to do with human actions, which cannot be confirmed in this study, but should be further investigated.

The safety indices for the bow-shoulder in different ice conditions are elaborate next. Ice condition cases 1-4 and their safety indices are shown on Figure 4.27. For ice condition cases 5-8 the safety indices are shown in Figure 4.28. Cases 9-12 are shown in Figure 4.29.

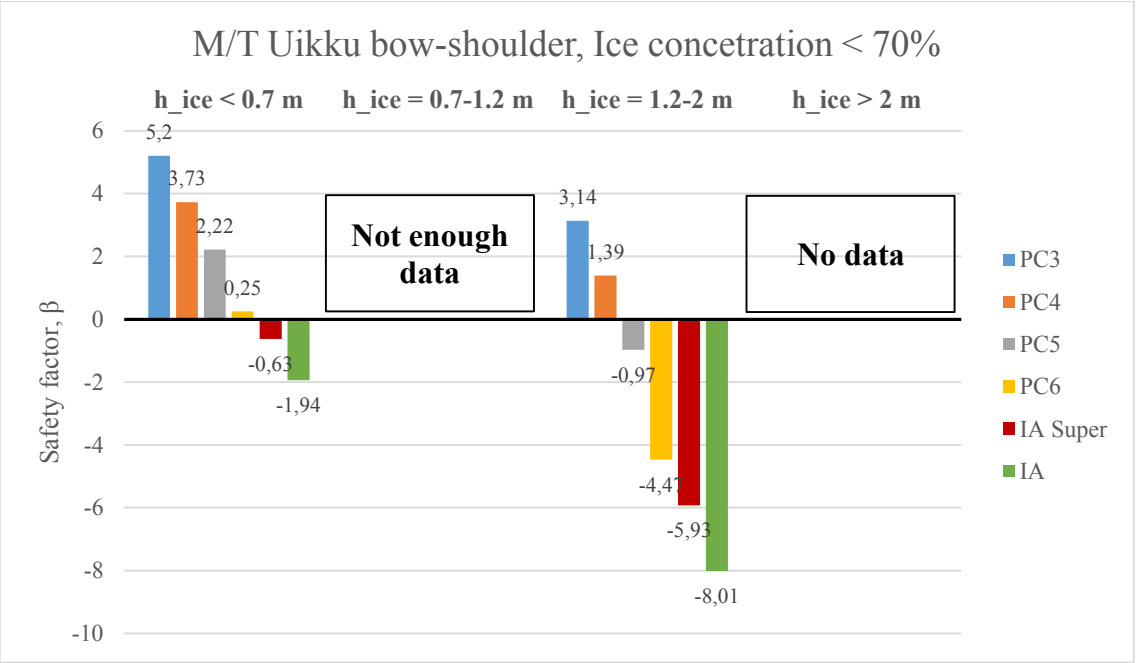

Figure 4.27 Safety indices of bow-shoulder framing in ice condition cases 1-4 (M/T Uikku)

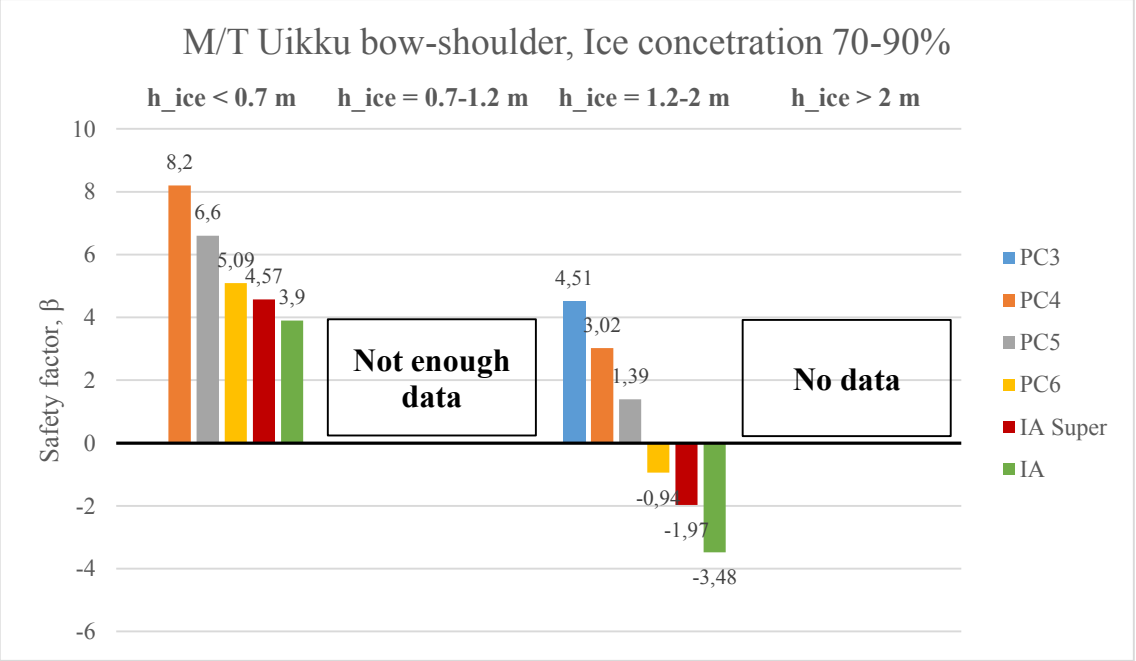

Figure 4.28 Safety indices of bow-shoulder framing in ice condition cases 5-8 (M/T Uikku)

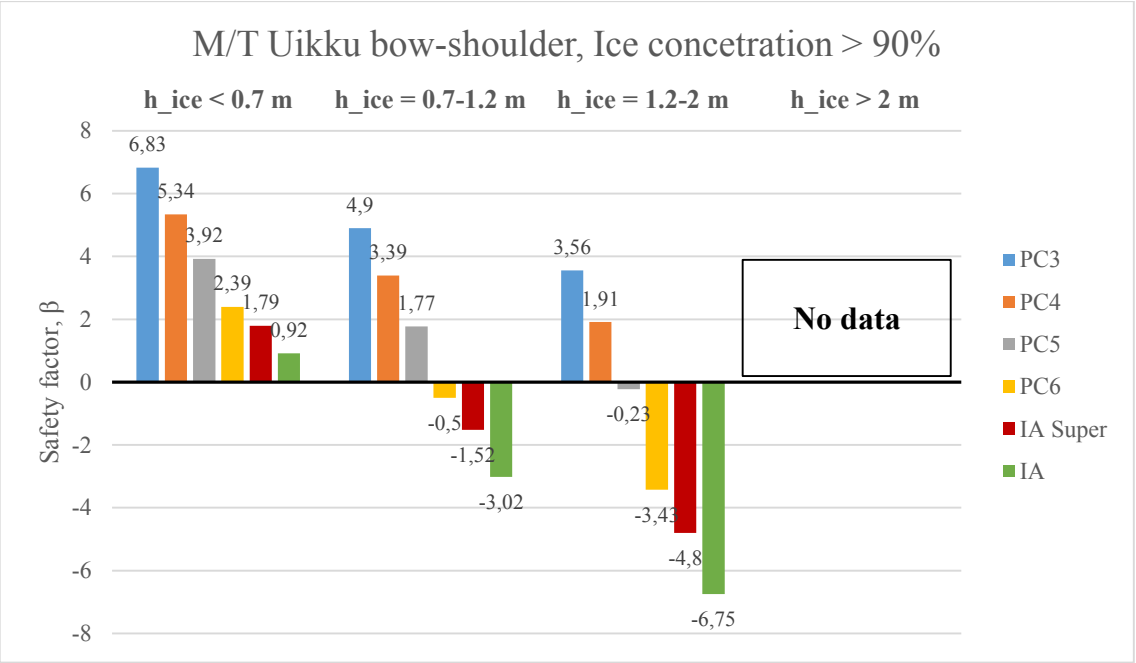

Figure 4.29 Safety indices of bow-shoulder framing in ice condition cases 9-12 (M/T Uikku)

For the bow- shoulder cases 1-8 show as seen before that an increase in ice thickness causes a drop in the safety indices. It seems that for those cases the lower ice concentration and higher ice thickness is most dangerous. For the most data rich ice conditions we can conclude the same as was concluded for the bow a decrease in safety as the thickness increases, which is possibly again related in M/T Uikku's case to being convoyed throughout the journey. As for S.A. Agulhas no such certain conclusion in the above 90% ice concentration cases could be reached.

And finally the safety indices of the stern of the ship in different ice conditions. Cases 1-4 are shown on Figure 4.30. Cases 5-8 are shown on Figure 4.31. And ice condition cases 9-12 are shown in Figure 4.32.

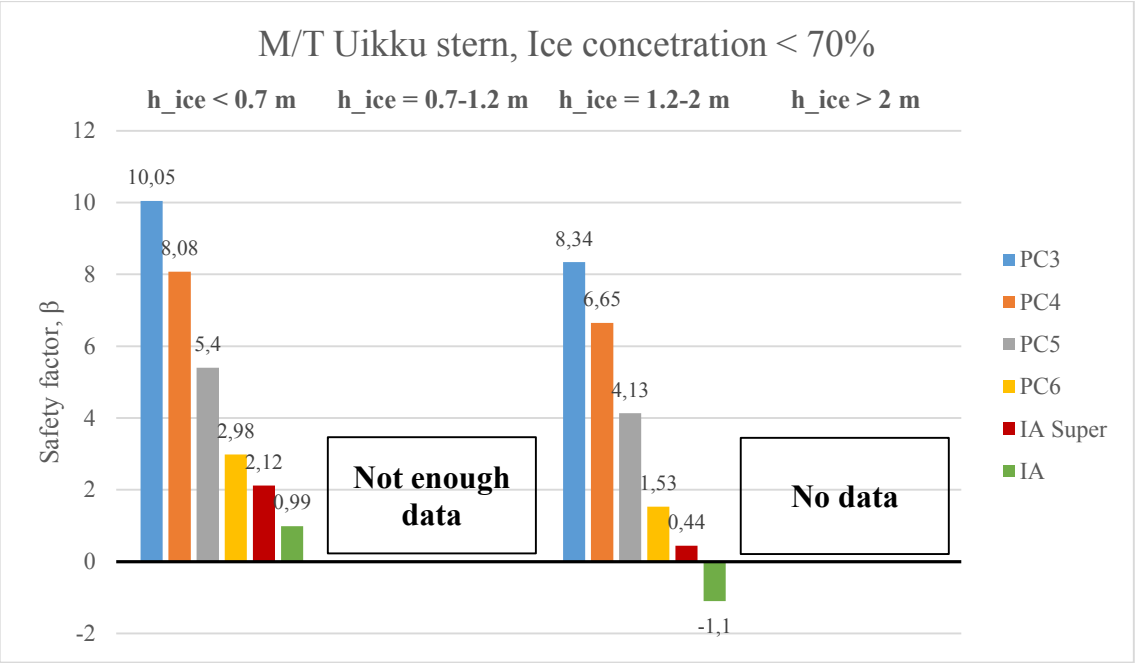

Figure 4.30 Safety indices of stern framing in ice condition cases 1-4 (M/T Uikku)

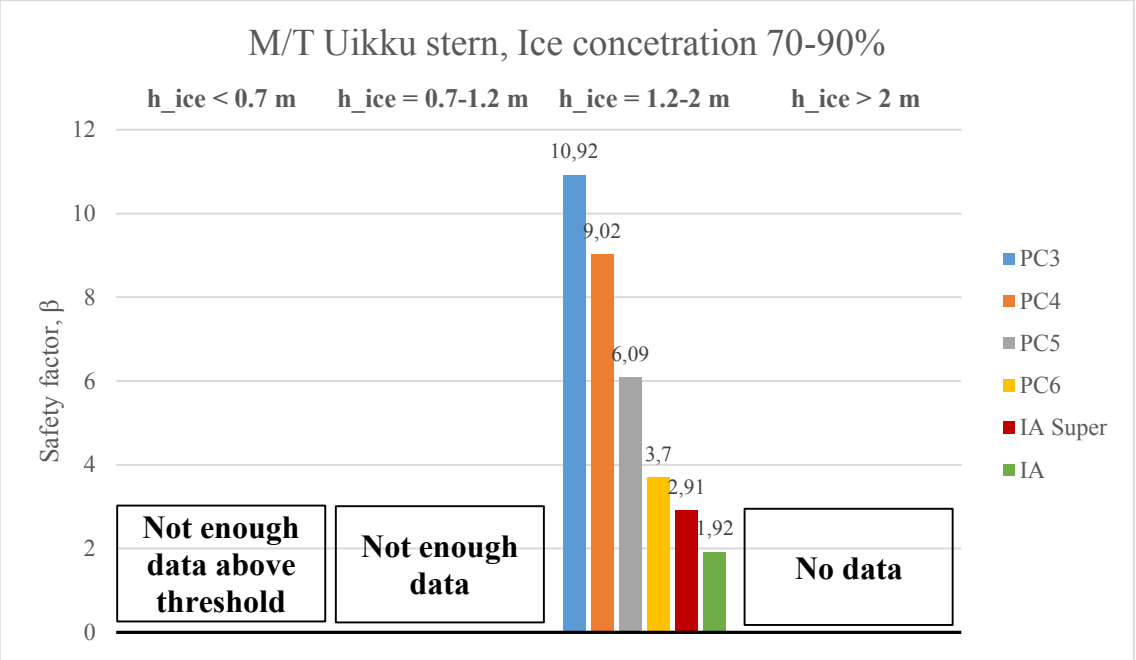

Figure 4.31. Safety indices of stern framing in ice condition cases 5-8 (M/T Uikku)

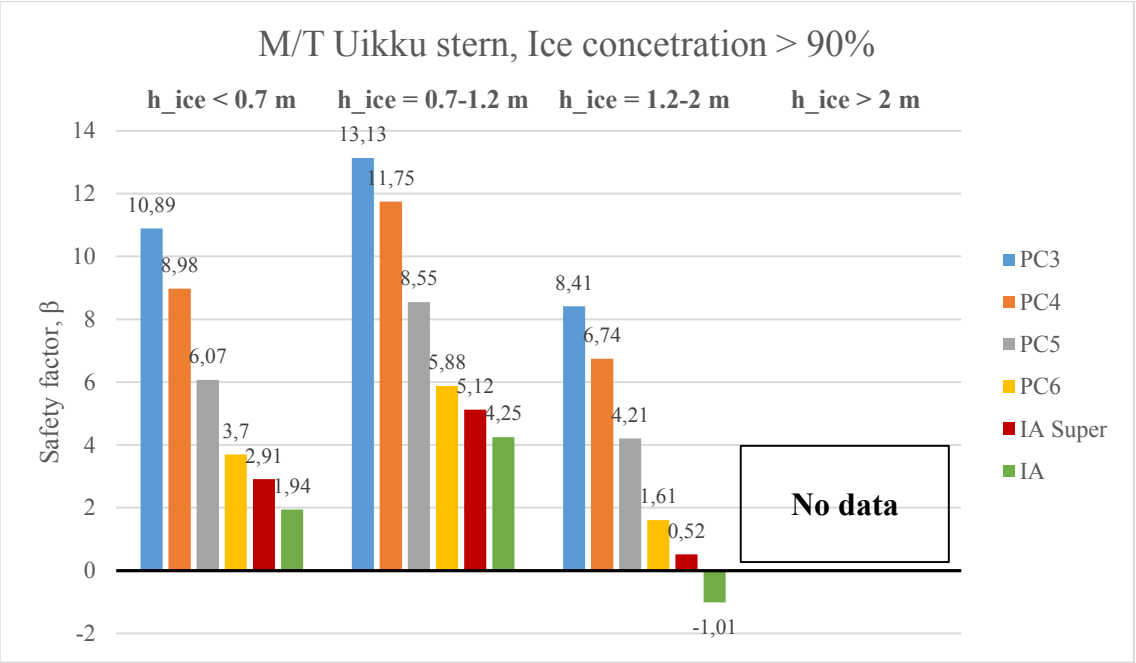

Figure 4.32 Safety indices of stern framing in ice condition cases 9-12 (M/T Uikku)

For cases 1-4 we can again see the ice thickness affecting the safety index negatively. It is hard to say anything about the ice conditions where ice concentration is 70-90%. However, ice condition cases where ice concentration is above 90% is showing behavior where there is no clear trend towards ice thickness growth decreasing safety indices. Here it is in reverse to the trend seen in S.A. Agulhas' data where ice thickness 0.7-1.2m showed the lowest safety indices in those conditions.

4.4. Comparison between risk and rule based structures

Here we compare the rule based structures calculated with the entire loading data in Chapter 4.2 to the risk-based structures, which would have a safety index of $\beta \geq 2$. A safety index of $\beta = 2$ gives a probability of failure of 0.02, which means in a ships lifetime of 25 years 2 ships out of 100 would experience loads above the limit state. We are looking for framing and plating dimensions for which the safety index is closest to and above the value of 2. The general value of the safety index β for structures is between 2 and 3 [12].

4.4.1. S.A. Agulhas II

First, plate thicknesses are calculated for bow and stern complying with safety index requirement of $\beta \geq 2$. Three different plate thicknesses are calculated corresponding to

three load heights analyzed in previous Section. As a result, three different frames are also going to be calculated that correspond to the calculated risk based plating and satisfy the safety index of $\beta \geq 2$. The safety indices and dimensions for rule and risk based plating and framing at the bow are shown in Table 4.21 and Table 4.22, respectively. The comparison between plastic section moduli of the risk and rule based frames for the bow are graphically shown in Figure 4.33 for the ice load height of $h_c = 100mm$. This is due to, the load height of 75mm being used in previous studies on risk based design of ship structures [12] [14]. Although, it must be said that those studies were based on ice loads measured in the Baltic Sea. Nevertheless, the smallest load height gives the most reasonable estimate for plate thicknesses.

Table 4.21 Rule and risk based plating for the bow (S.A. Agulhas II)

			Rule based plating						**Risk based plating**
			PC3	**PC4**	**PC5**	**PC6**	**IAS**	**IA**	
hc [mm]	100	β	3,88	2,68	1,74	-0,10	1,74	0,94	2,68
		Plate [mm]	30	25	22	18	22	20	25
	300	β	4,86	3,76	2,98	1,61	2,98	2,36	2,36
		Plate [mm]	30	25	22	18	22	20	20
	500	β	6,06	5,05	4,36	3,28	4,36	3,86	2,22
		Plate [mm]	30	25	22	18	22	20	15

Table 4.22 Rule and risk based framing for the bow (S.A. Agulhas II)

	Rule based framing						Risk-based framing		
	PC3	**PC4**	**PC5**	**PC6**	**IAS**	**IA**	**hc = 100 mm**	**hc = 300 mm**	**hc = 500 mm**
β	2,01	0,22	-2,92	-7,01	-8,08	-10,74	2,02	2,07	2,10
Pf	0,02	0,41	1,00	1,00	1,00	1,00	0,02	0,02	0,02
Frame [mm]	T-340x16 / 80x20	T-320x14 / 70x20	T-300x12 / 60x18	T-280x10 / 60x16	T-240x12 / 50x15	T-220x12 / 50x15	T-350x16 / 80x20	T-350x16 / 80x22	T-360x16 / 80x22
Z_p [cm^3]	1512	1178	870,5	652,3	611,3	527,7	1520	1531	1538
Plate [mm]	30	25	22	18	22	20	25	20	15

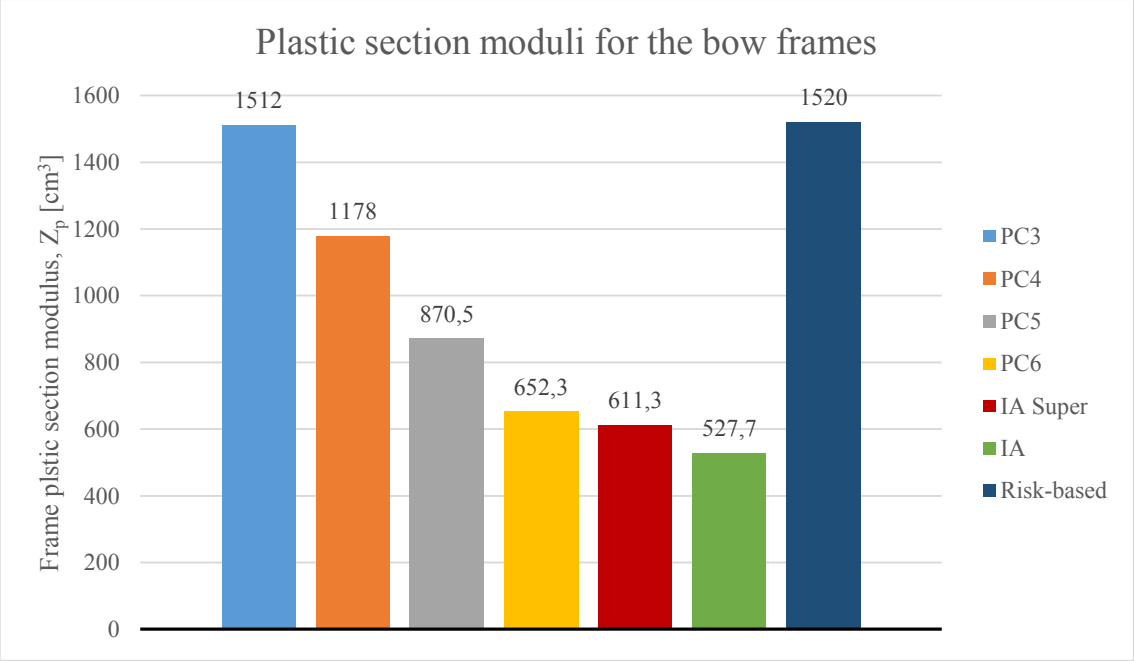

Figure 4.33 Plastic section moduli of the bow frames (S.A. Agulhas II, h_c = 100mm)

We can see on Figure 4.33 that the risk-based structure is slightly above the PC3 ice class. This means that the loads acting on the bow are significant. For instance, if the ship's hull was actually built according to PC5 ice class, since the ship is classified under PC5, the plastic section modulus would be about two times smaller than suggested by the probability based approach. However, the ship's hull is built according to DNV ICE-10,

which based on [34] is close to PC3 class. Therefore the structure would be sufficient to handle lifetime loads experienced in Antarctic waters.

The safety indices and dimensions for rule and risk based plating and framing at the stern are shown in Table 4.23 and Table 4.24 respectively. The comparison between plastic section moduli of the risk and rule based frames for the stern are graphically shown on Figure 4.34 for the ice load height of $h_c = 100mm$.

Table 4.23 Rule and risk based plating for the stern (S.A. Agulhas II)

			Rule based plating						**Risk based plating**
			PC3	**PC4**	**PC5**	**PC6**	**IAS**	**IA**	
hc [mm]	100	β	4,75	4,17	2,77	1,84	1,84	1,84	2,34
		Plate [mm]	22	20	16	14	14	14	15
	300	β	5,79	5,23	3,96	3,18	3,18	3,18	2,23
		Plate [mm]	22	20	16	14	14	14	12
	500	β	7,15	6,60	5,43	4,75	4,75	4,75	3,05
		Plate [mm]	22	20	16	14	14	14	10

Table 4.24 Rule and risk based framing for the stern (S.A. Agulhas II)

	Rule based framing						Risk-based framing		
	PC3	**PC4**	**PC5**	**PC6**	**IAS**	**IA**	**hc = 100 mm**	**hc = 300 mm**	**hc = 500 mm**
β	3,17	1,22	-3,69	-11,92	-12,73	-18,33	2,26	2,12	2,02
Pf	0,00	0,11	1,00	1,00	1,00	1,00	0,01	0,02	0,02
Frame [mm]	I-250x22	I-220x20	I-180x18	I-150x15	I-150x14	I-140x12	I-250x20	I-250x20	I-240x22
Z_p [cm^3]	753,1	539,8	326,6	196,7	189,0	147,2	638,8	622,5	611,9
Plate [mm]	22	20	16	14	14	14	15	12	10

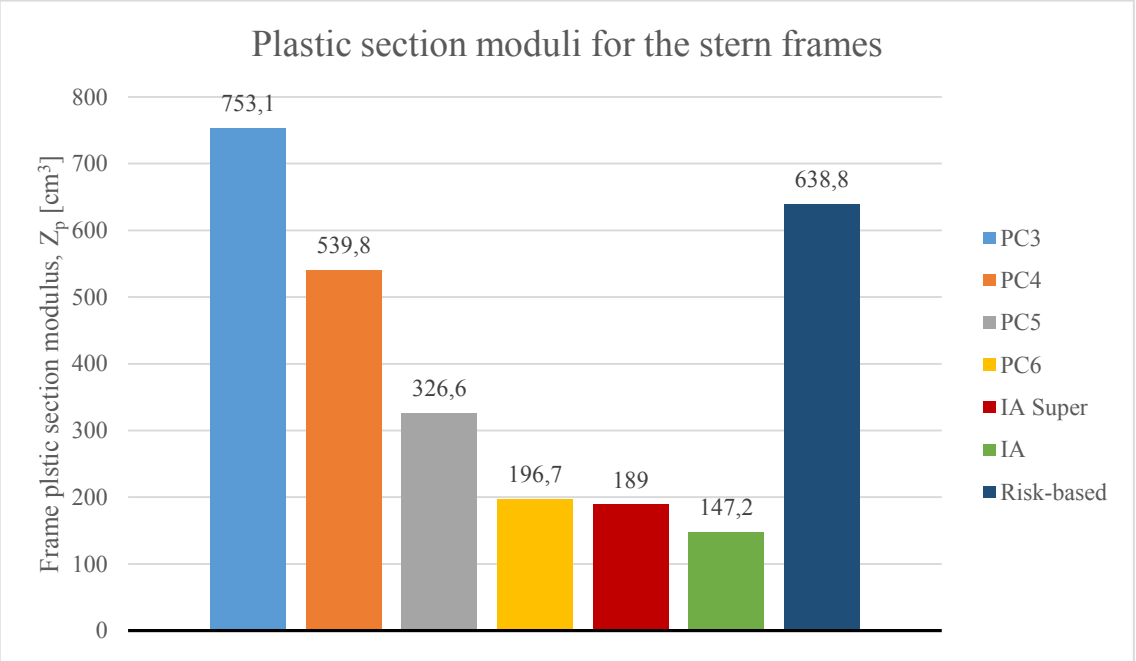

Figure 4.34 Plastic section moduli of the stern frames (S.A. Agulhas II, h_c = 100mm)

The risk-based structure in Figure 4.34 is between the PC3 and PC4 ice class structures for the stern. This shows that slightly less hostile conditions are present at the stern. However, if the ship would be built to PC5 ice class as it was classified the plastic section modulus would again be two times smaller than required by the measured long term loads.

4.4.2. M/T Uikku

The safety indices and dimensions for rule and risk based plating and framing at the bow are shown in Table 4.25 and Table 4.26 respectively. The comparison between plastic section moduli of the risk and rule based frames for the bow are graphically shown on Figure 4.35 for the ice load height of $h_c = 100mm$.

Table 4.25 Rule and risk based plating for the bow (M/T Uikku)

			Rule based plating						**Risk based plating**
			PC3	**PC4**	**PC5**	**PC6**	**IAS**	**IA**	
hc [mm]	100	β	6,39	5,28	4,53	3,98	3,98	3,98	2,22
		Plate [mm]	30	25	22	20	20	20	15
	300	β	7,50	6,41	5,68	5,15	5,15	5,15	2,33
		Plate [mm]	30	25	22	20	20	20	12
	500	β	N/A	8,04	7,25	6,75	6,75	6,75	2,46
		Plate [mm]	30	25	22	20	20	20	8

Table 4.26 Rule and risk based framing for the bow (M/T Uikku)

	Rule based framing						Risk-based framing		
	PC3	**PC4**	**PC5**	**PC6**	**IAS**	**IA**	**hc = 100 mm**	**hc = 300 mm**	**hc = 500 mm**
β	6,86	5,47	3,97	2,75	-0,20	-1,41	2,02	2,03	2,14
Pf	0,00	0,00	0,00	0,00	0,58	0,92	0,02	0,02	0,02
Frame [mm]	T-410x18 / 90x18	T-380x16 / 80x16	T-340x14 / 70x16	T-320x12 / 70x14	T-230x12 / 50x15	T-210x12 / 50x15	T-310x12 / 60x14	T-310x12 / 60x15	T-320x12 / 60x18
Z_p [cm^3]	2088	1557	1130	879,6	556,8	487,8	765,6	768,9	784,3
Plate [mm]	30	25	22	20	20	20	15	12	8

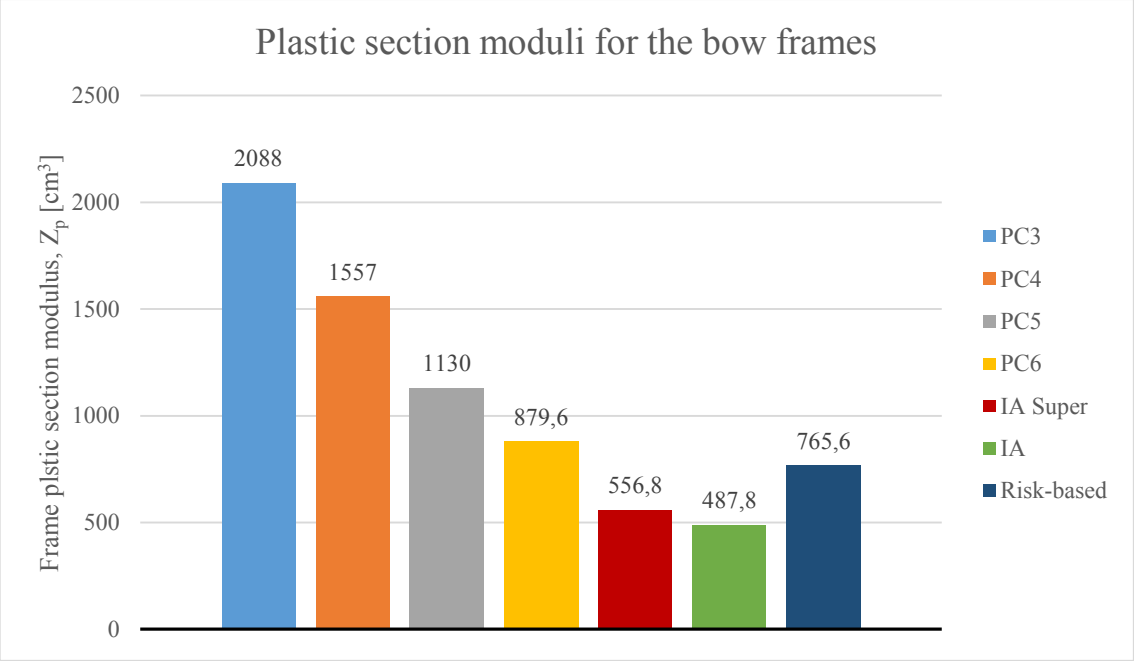

Figure 4.35 Plastic section moduli of the bow frames (M/T Uikku, h_c = 100mm)

From Figure 4.35 we can see that the measured ice-induced loads onboard M/T Uikku are about two times lower than on S.A. Agulhas II based on the required risk-based frame section modulus being $Z_p = 765,6\ cm^3$. As M/T Uikku was built to IA Super ice class we can see that the structure's plastic section modulus is slightly less than would be required based on the reliability analysis.

The safety indices and dimensions for rule and risk based plating and framing at the bow-shoulder are shown in Table 4.27 and Table 4.28 respectively. The comparison between plastic section moduli of the risk and rule based frames for the bow-shoulder are graphically shown on Figure 4.36 for the ice load height of $h_c = 100mm$.

Table 4.27 Rule and risk based plating for the bow-shoulder (M/T Uikku)

			Rule based plating						**Risk based plating**
			PC3	**PC4**	**PC5**	**PC6**	**IAS**	**IA**	
hc [mm]	100	β	3,27	2,47	1,82	-0,04	1,82	1,82	2,47
		Plate [mm]	25	22	20	16	20	20	22
	300	β	4,40	3,70	3,16	1,80	3,16	3,16	2,55
		Plate [mm]	25	22	20	16	20	20	18
	500	β	5,87	5,23	4,77	3,70	4,77	4,77	2,27
		Plate [mm]	25	22	20	16	20	20	12

Table 4.28 Rule and risk based framing for the bow-shoulder (M/T Uikku)

	Rule based framing						**Risk-based framing**		
	PC3	**PC4**	**PC5**	**PC6**	**IAS**	**IA**	**hc = 100 mm**	**hc = 300 mm**	**hc = 500 mm**
β	3,91	2,33	0,41	-2,47	-3,72	-5,52	2,05	2,06	2,01
Pf	0,00	0,01	0,34	0,99	1,00	1,00	0,02	0,02	0,02
Frame [mm]	T-420x18 / 90x22	T-380x16 / 80x20	T-360x14 / 70x16	T-340x12 / 60x14	T-280x14 / 60x15	T-260x14 / 60x14	T-360x16 / 80x22	T-350x18 / 90x20	T-370x18 / 90x22
Z_p [cm^3]	2460	1792	1325	972,1	874,2	762,9	1710	1715	1700
Plate [mm]	25	22	20	16	20	20	22	18	12

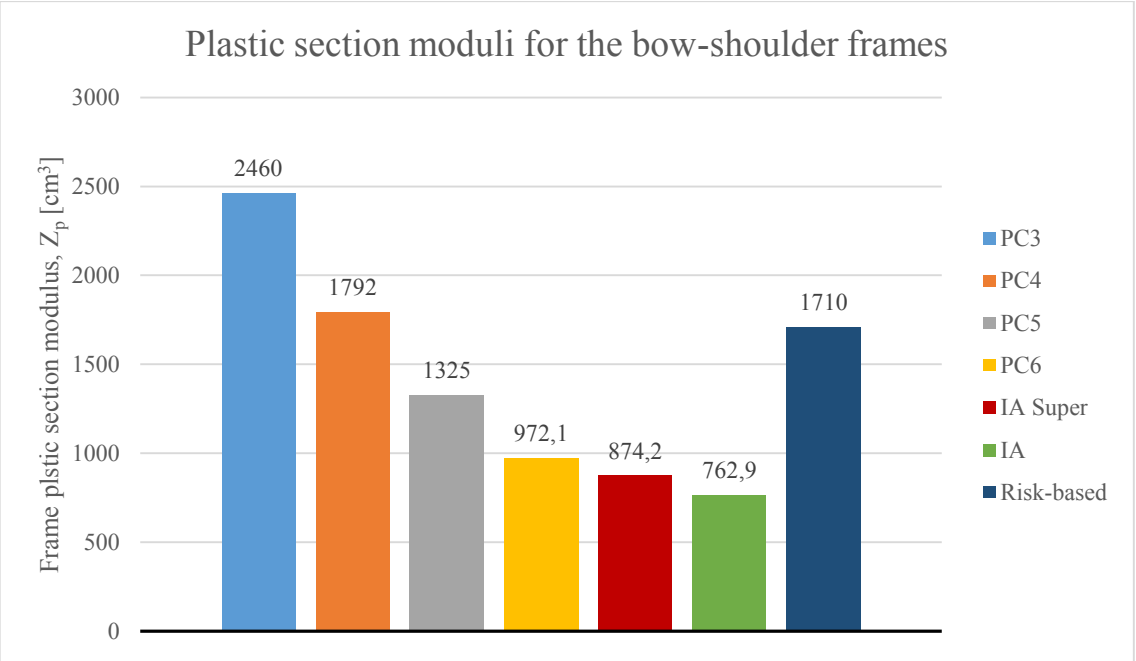

Figure 4.36 Plastic section moduli of the bow-shoulder frames (M/T Uikku, h_c = 100mm)

Figure 4.36 shows that the risk-based design is fairly close to the PC4 ice class design. Thus, the heaviest loads were experienced at the bow-shoulder, since the stern loads are usually always smaller than the bow and therefore the bow-shoulder also. It is expected that the highest loads are experienced at the bow-shoulder. Luckily there was enough data to confirm it without an evident bias in the measured loads.

The safety indices and dimensions for rule and risk based plating and framing at the stern are shown in Table 4.29 and Table 4.30 respectively. The comparison between plastic section moduli of the risk and rule based frames for the stern are graphically shown on Figure 4.37 for ice load height of h_c = *100mm*.

Table 4.29 Rule and risk based plating for the stern (M/T Uikku)

			Rule based plating						Risk based plating
			PC3	**PC4**	**PC5**	**PC6**	**IAS**	**IA**	
hc [mm]	100	β	10,49	9,73	7,48	7,07	7,07	6,18	2,26
		Plate [mm]	22	20	15	14	14	12	6
	300	β	11,83	11,22	9,17	8,65	8,65	7,57	3,03
		Plate [mm]	22	20	15	14	14	12	5
	500	β	13,21	12,84	11,40	11,02	11,02	10,11	2,94
		Plate [mm]	22	20	15	14	14	12	2

Table 4.30 Rule and risk based framing for the stern (M/T Uikku)

	Rule based framing						Risk-based framing		
	PC3	**PC4**	**PC5**	**PC6**	**IAS**	**IA**	**hc = 100 mm**	**hc = 300 mm**	**hc = 500 mm**
β	8,87	7,09	4,55	2,03	1,04	-0,35	2,13	2,28	2,17
Pf	0,00	0,00	0,00	0,02	0,15	0,64	0,02	0,01	0,02
Frame [mm]	I-200x25	I-210x20	I-170x18	I-140x15	I-130x14	I-120x14	I-150x16	I-160x15	I-170x18
Z_p [cm^3]	665,5	489,0	285,0	171,5	145,8	121,5	174,7	179,3	175,8
Plate [mm]	22	20	15	14	14	12	6	5	2

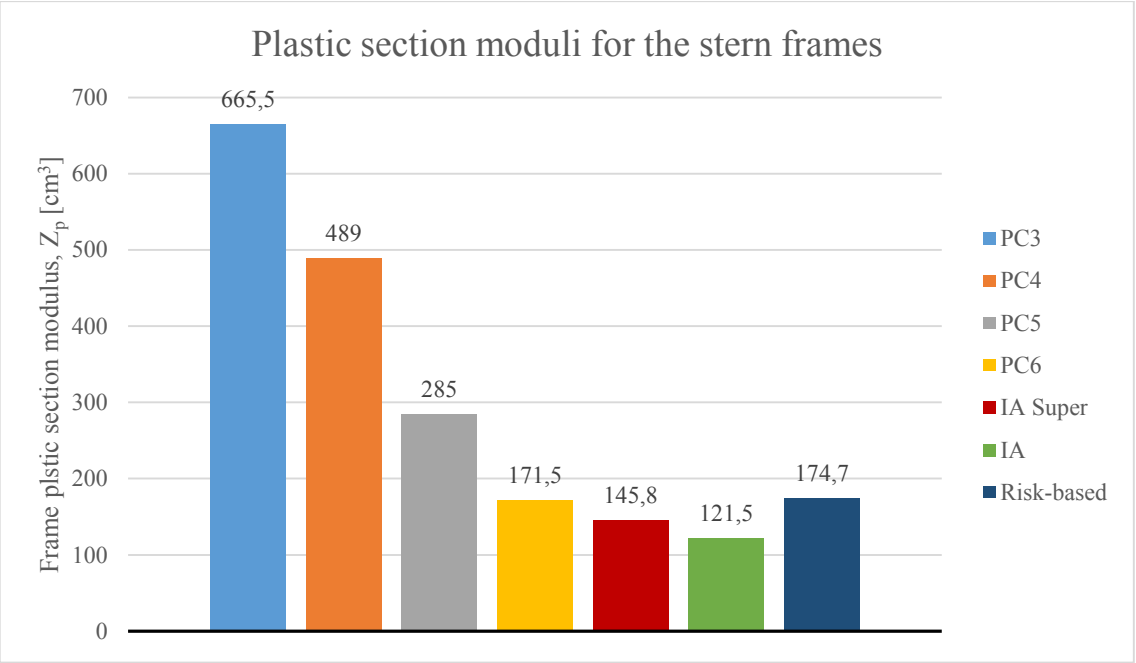

Figure 4.37 Plastic section moduli of the stern frames (M/T Uikku, h_c = 100mm)

Figure 4.37 shows again that the stern has the smallest measured loads. Although the stern of the ship requires significantly weaker design than the bow and bow-shoulder, it is still slightly above the design ice class of M/T Uikku, which is IA Super.

4.5. Comparison of rule based frame safety indices to RVs from POLARIS

In this chapter the rule based frames safety indices in different ice conditions are compared to the Risk Index Values (RVs) given in POLARIS [32]. Based on how the RVs were developed [32] they can be in a general form related to the safety index as follows:

$$\begin{cases} if \quad RV \geq 1 \quad then \quad \beta > 2 \\ if \quad RV = 0 \quad then \quad \beta = 2 \\ if \quad RV \leq -1 \quad then \quad \beta < 2 \end{cases} \tag{4.1}$$

This relation is based on the RV being assigned a zero score at the ice class limiting ice thickness [32]. Thus, as in general the safety index of β = 2 is used as the lower limit for safe design [12] we can assume that when RV=0 then β = 2 and if the RV value is another value below zero then β < 2 and vice versa. As, the RVs are developed for level ice

meaning 100% ice concentration, the closest values we can compare to the RVs are the safety indices where ice concentration is >90%.

Ice thicknesses corresponding to the ice types in Table 4.31 are taken based on the definitions shown on the left edge of Figure 4.38 [32], which are defined in detail in [30]. Thin First year (FY) ice corresponds to ice thickness < 0.7 m, the RVs for that ice thickness are taken form the 1st stage given in Table 4.31. The 1st stage basically corresponds to the lower half of the ice thicknesses defined for the whole category – detailed explanation in [30]. Medium First year (FY) ice corresponds to ice thickness 0.7-1.2 m, here we also chose the 1st stage, which has not been explicitly written in Table 4.31. In addition, medium first year (FY) ice 1st stage is not defined in the Sea Ice Nomenclature [30], but is instead defined by the POLARIS Technical Group in [32]. Thick first year (FY) ice corresponds to ice thickness 1.2-2 m. Second year ice corresponds to ice thicknesses above 2m. However, second year ice is actually defined as ice with a thickness of 2-3m in Figure 4.38. In this thesis we shall use it to define the cases where ice thickness is above 2 m. Considering that from visual observation the >2m ice thickness category has an average ice thickness of 2.6 m, the second year ice is well fit for defining the ice thicknesses above 2 m. Multi-year (MY) ice is also defined in Figure 4.38, however it is not in use in this thesis.

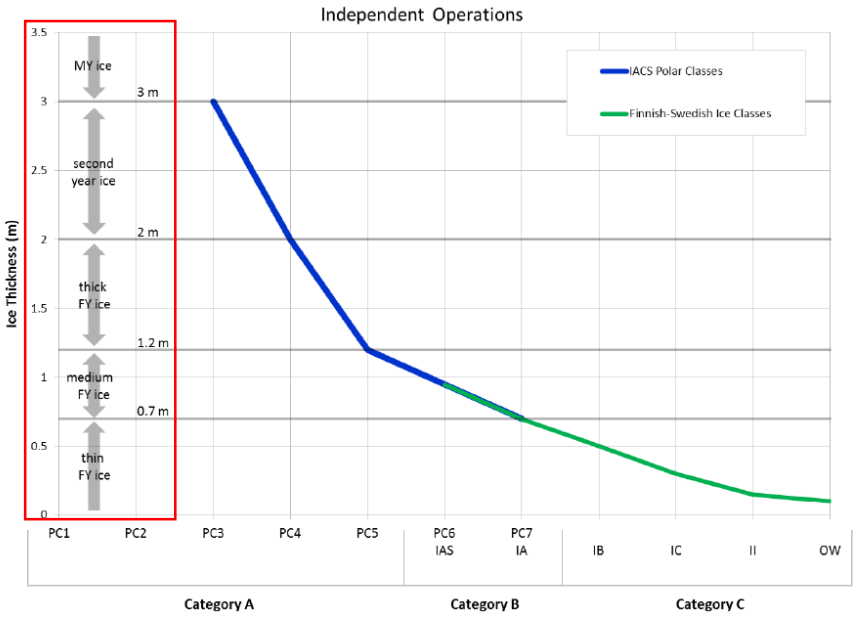

Figure 4.38 Ice thicknesses of different ice types (in the red box)

Table 4.31 Risk Index Values (RVs) [35]

Category	Ice Class	Ice Free	New Ice	Grey Ice	Grey White Ice	Thin First Year Ice, 1st Stage	Thin First Year ice, 2nd Stage	Medium First Year Ice	Medium First Year Ice 2nd	Thick First Year Ice	Second Year Ice	Light Multi Year Ice	Heavy Multi-Year Ice
A	PC1	3	3	**3**	3	2	2	2	2	2	2	1	1
	PC2	3	3	**3**	3	2	2	2	2	2	1	1	0
	PC3	3	3	**3**	3	2	2	2	2	2	1	0	-1
	PC4	3	3	**3**	3	2	2	2	2	1	0	-1	-2
	PC5	3	3	**3**	3	2	2	2	1	0	-1	-2	-2
B	PC6	3	2	2	2	2	1	1	0	-1	-2	-3	-3
	PC7	3	2	2	2	1	1	0	-1	-2	-3	-3	-3
C	IA Super	3	2	2	2	2	1	0	-1	-2	-3	-4	-4
	IA	3	2	2	2	1	0	-1	-2	-3	-4	-4	-4
	IB	3	2	2	1	0	-1	-2	-3	-3	-4	-5	-5
	IC	3	2	1	0	-1	-2	-2	-3	-4	-4	-5	-6
	Not ice strengthened	3	1	0	-1	-2	-2	-3	-3	-4	-5	-6	-6

4.5.1. S.A. Agulhas II

The comparison of safety indices of the bow and stern to the RVs at different ice thicknesses are shown in Table 4.32 and Table 4.33 respectively. The tables are color coded. Green means that the safety index fits the expression in Equation (4.1) and red that it doesn't. Therefore it is much easier to see how in general the safety indices calculated compare to the definitions given in Equation (4.1). We can see from Table 4.32 that with the increase of ice thickness the safety indices correlate better with the RVs. The same holds for the stern safety indices shown in Table 4.33.

Table 4.32 Bow frame safety indices comparison to RVs (S.A. Agulhas II, ice concentration >90%)

Ice Class	Thin first year ice (< 0,7 m)		Medium first year ice (0,7 – 1,2 m)		Thick first year ice (1,2-2m)		Second year ice (> 2m)	
	RV	**Safety index**	**RV**	**Safety index**	**RV**	**Safety index**	**RV**	**Safety index**
PC3	2	2,78	2	2,23	2	1,84	1	1,94
PC4	2	1,23	2	0,49	1	-0,02	0	-0,14
PC5	2	-1,47	2	-2,59	0	-3,28	-1	-3,02
PC6	2	-5,12	1	-6,62	-1	-7,48	-2	-7,11
IAS	2	-6,09	0	-7,69	-2	-8,58	-3	-8,18
IA	1	-8,5	-1	-10,32	-3	-11,3	-4	-10,83

Table 4.33 Stern frame safety indices comparison to RVs (S.A. Agulhas II, ice concentration >90%)

Ice Class	Thin first year ice (< 0,7 m)		Medium first year ice (0,7 – 1,2 m)		Thick first year ice (1,2-2m)		Second year ice (> 2m)	
	RV	**Safety index**	**RV**	**Safety index**	**RV**	**Safety index**	**RV**	**Safety index**
PC3	2	7,06	2	3,26	2	2,69	1	3,15
PC4	2	5,44	2	1,34	1	0,55	0	1,20
PC5	2	2,94	2	-3,49	0	-4,95	-1	-3,74
PC6	2	-0,61	1	-11,64	-1	-13,89	-2	-12,01
IAS	2	-1,01	0	-12,45	-2	-14,77	-3	-12,82
IA	1	-3,92	-1	-18,02	-3	-20,82	-4	-18,46

In general it seems the RVs do not correlate well with the safety indices calculated in this thesis. It seems that the RVs are meant for short term operational limitation estimation or planning single voyages, but not for life time operational limitations, as defined in POLARIS [32]. The safety indices on the other hand are calculated for the life time of the ship.

4.5.2. M/T Uikku

The comparison of safety indices of the bow, bow-shoulder and stern to the RVs at different ice thicknesses are shown in Table 4.34, Table 4.35 and Table 4.36 respectively. The same color coding is used in these tables as above. It is interesting to see that for the bow of M/T Uikku the correlation is significantly better than it was for S.A. Agulhas' bow. In contrast the correlation gets worse with the increase of ice thickness. Furthermore, both the bow-shoulder and stern have worse correlation between RVs and safety indices in the medium first year ice, than in other conditions. Nevertheless, M/T Uikku's safety indices show significantly better correlation with the RVs. This is interesting as the loads in ice conditions with ice concentration >90% did not have a good fit with the Gumbel I distribution, due to lack of ice loading data. Therefore, it seems that better correlation with RVs is achieved with worse Gumbel I fit. In addition, looking at the bow-shoulder return period graphs with ice concentration >90% in Appendix 2, we can see that the bow-shoulder showed the best fit to Gumbel 1, but has the worst correlation with the RVs, as seen in Table 4.35 .

Table 4.34 Bow frame safety indices comparison to RVs (M/T Uikku, ice concentration >90%)

Ice Class	Thin first year ice (< 0,7 m)		Medium first year ice (0,7 – 1,2 m)		Thick first year ice (1,2-2m)		Second year ice (> 2m)	
	RV	**Safety index**	**RV**	**Safety index**	**RV**	**Safety index**	**RV**	**Safety index**
PC3	2	8,82	2	7,37	2	6,96	1	N/A
PC4	2	7,14	2	5,96	1	5,55	0	N/A
PC5	2	5,62	2	4,47	0	4,03	-1	N/A
PC6	2	4,48	1	3,28	-1	2,78	-2	N/A
IAS	2	2,28	0	0,67	-2	-0,23	-3	N/A
IA	1	1,54	-1	-0,38	-3	-1,48	-4	N/A

Table 4.35 Bow-shoulder frame safety indices comparison to RVs (M/T Uikku, ice concentration >90%)

Ice Class	Thin first year ice (< 0,7 m)		Medium first year ice (0,7 – 1,2 m)		Thick first year ice (1,2-2m)		Second year ice (> 2m)	
	RV	**Safety index**	**RV**	**Safety index**	**RV**	**Safety index**	**RV**	**Safety index**
PC3	2	6,83	2	4,90	2	3,56	1	N/A
PC4	2	5,34	2	3,39	1	1,91	0	N/A
PC5	2	3,92	2	1,77	0	-0,23	-1	N/A
PC6	2	2,39	1	-0,50	-1	-3,43	-2	N/A
IAS	2	1,79	0	-1,52	-2	-4,80	-3	N/A
IA	1	0,92	-1	-3,02	-3	-6,75	-4	N/A

Table 4.36 Stern frame safety indices comparison to RVs (M/T Uikku, ice concentration >90%)

Ice Class	Thin first year ice (< 0,7 m)		Medium first year ice (0,7 – 1,2 m)		Thick first year ice (1,2-2m)		Second year ice (> 2m)	
	RV	**Safety index**	**RV**	**Safety index**	**RV**	**Safety index**	**RV**	**Safety index**
PC3	2	10,89	2	13,13	2	8,41	1	N/A
PC4	2	8,98	2	11,75	1	6,74	0	N/A
PC5	2	6,07	2	8,55	0	4,21	-1	N/A
PC6	2	3,70	1	5,88	-1	1,61	-2	N/A
IAS	2	2,91	0	5,12	-2	0,52	-3	N/A
IA	1	1,94	-1	4,25	-3	-1,01	-4	N/A

5. Discussion and conclusion

To the best of the author's knowledge this study is the first to correlate lifetime ice-induced loads with two parameters: ice thickness and ice concentration.

The safety of ship local structures was evaluated, using level 2 reliability analysis. Serviceability limit state equation developed by Hayward [18] was used to estimate the required line load to cause permanent deflections in plating. A simplified version of Varsta et al. [21] ultimate limit state equation was used to estimate the load required to cause three hinge plastic mechanism in the frame.

The ice-induced loads gathered during full-scale measurements onboard S.A Agulhas II and M/T Uikku were fitted with Gumbel I distribution and the long term return periods of the loads were evaluated. The distribution showed good fit to the data gathered by S.A. Agulhas II and M/T Uikku. When the loads were divided based on ice conditions, S.A. Agulhas II had significantly better fit in different ice condition cases than M/T Uikku solely because M/T Uikku had 6 times less measured data.

Based on the generalized form of the level 2 reliability analysis and Gumbel parameters of the long term ice induced loads the safety of the rule-based local structures was estimated with the iterative process developed by Kujala for safety index estimation [10]. Risk-based local structures were calculated based on the criterion that the safety index $\beta \geq 2$. The deterministically calculated rule-based structures were compared to the probabilistically calculated risk-based structures. The safety indices of rule-based structures were compared to the RVs developed in POLARIS [32]. RVs are based on level ice, thus the comparison between calculated loads was done where ice concentration is above 90%. Better correlation with RVs was seen for S.A. Agulhas II when ice thickness increased. M/T Uikku had all-around good correlation to the RVs, however the lack in loading data when divided into different ice conditions raises the question of how reliable are the results for M/T Uikku.

The safety analysis of the vessels showed in general that for the bow and stern the safety indices decrease with increasing ice thickness and ice concentration. However, in the highest ice concentration cases where ice concentration was >90% and the ice thickness was above 1.2m no obvious decrease in safety indices was observed. Moreover, an increase in safety indices could be observed, which is interesting. As, one would think

that at any ice thickness the increase of ice concentration would cause higher lifetime loads due to more load peaks experienced. Thus, a decrease in the safety indices should be observed. In addition, a sensitivity analysis was carried out for the load height h_c, which was explicitly used in risk-based plating calculations. The results showed a significant increase in safety factors of the plating with the increase of the load height. This is to be expected as a narrower load causes higher stresses, thus increasing the load on the plating and decreasing the safety indices.

For future consideration it would be interesting to see how the speed is correlated to the different ice conditions. As in some ice condition cases it seemed logical that the higher loads at lower ice concentrations with the same ice thickness were caused by increased speed due to more open water. Thus, the higher loads might be explained by hitting the same thickness ice blocks at higher speeds. In future studies where ice loads are divided into categories based on more than one parameter, more ice loading data should be gathered. Since, in some categories there might be too little data to fit a distribution to the gathered data.

The current study was a step forward in developing probabilistic rules for ice-going vessels. Furthermore, the more data is gathered the better we can estimate the required strength of the ships structures. In addition, the estimations become more reliable as more data is gathered. However, there is still a lack of data gathered in different ice conditions, thus this approach needs more full-scale measurements to be considered as a viable method for estimating the dimension of a structures.

The results gathered for S.A. Agulhas II show that the bow of the ship based on the rules is dimensioned very close to the risk based structure. For the stern a slight over dimensioning can be observed. M/T Uikku rule based results show a small under estimation in the dimensioning of the bow and stern region. However, the bow-shoulder region is under estimated by the rules more than two times compared to the risk based structure.

6. References

[1] P. Kujala, "On the Statistics of Ice Loads on Ship Hull in the Baltic (Doctoral Thesis)," Helsinki University of Tehcnology, Espoo, 1994.

[2] P. Kujala, M. Suominen and K. Riska, "Statistics of Ice Loads Measured on MT Uikku in the Baltic," in *Proceedings of the 20th International Conference on Port and Ocean Engineering under Arctic Conditions*, Luleaa, 2009.

[3] D. I. Kheisin and Y. N. Popov, "Ice Navigation Qualities of Ships," Cold Regions Research and Engineering Laboratory (CRREL), Hanover, New Hampshire, 1973.

[4] P. Kujala and J. Vuorio, "On the statistical nature of ice induced pressures measured on board I.B. Sisu," in *Proceedings of the 8th International Conference on Port and Ocean Engineering under Arctic Conditions*, Narssarssuaq, 1985.

[5] P. Kujala and J. Vuorio, "Research Report No 43 - Results and statistical analysis of ice load measurements on board icebreaker Sisu in winters 1979 to 1985," Winter Navigation Research Board, Espoo, 1986.

[6] M. Suominen and P. Kujala, "Analysis of short-term ice load measurements on board MS Kemira during the winters 1987 and 1988," Aalto University, School of Science and Technology, Department of Applied Mechanics, Espoo, 2010.

[7] E. Gumbel, Statistics of Extremes, New York: Columbia University Press, 1958.

[8] K. M. Ochi, Applied probability and stochastic processes in engineering and physical sciences, New York: John Wiley & Sons, 1990.

[9] P. Kujala, "Results of Long-term Ice Load Measurements Onboard M/S Kemira During the Winters 1985-1989," in *10th International Conference on Port and Ocean Engineering under Arcitc Conditions*, Luleaa, 1989.

[10] P. Kujala, "Probability based safety of ice-strenghtened ship hull in the Baltic Sea (Licentiate Thesis)," Helsiniki University of Technology, Espoo, 1989.

[11] M. Suominen, P. Kujala and M. Kotilainen, "The Encountered Extreme Events and Predicted Maximum Ice-induced Loads on the Ship Hull in the Southern Ocean," in *Proceedings of the ASME 2015 34th International Conference on Ocean, Offshore and Arctic Engineering*, St. John's, Newfoundland, Canada, 2015.

[12] P. Kujala, "Reliability of ice-strengthened shell structures of ships navigating in the Baltic Sea," *Journal of Structural Mechanics,* vol. 41, no. 2, pp. 108-118, 2008.

[13] P. Kujala, "Safety of Ice-Strenghtened Ship Hulls in the Baltic Sea," RINA Transactions, London, 1991.

[14] J. Kaldasaun, "Risk-based Approach for Structural Design of Ice-strenghtened Vessels Navigating in the Baltic Sea," Espoo, 2010.

[15] A. H.-S. Ang and W. H. Tang, Probability Concepts in Engineering Planning and Design Volume II, New York: John Wiley & Sons, 1984.

[16] P. Kujala, *Introduction to Risk Managment (Lecture notes),* Espoo: Not published (In Finnish), 2009.

[17] M. Hannus, *The Reliability of Structures,* Helsinki: Technical Research Center of Finland, 1973.

[18] R. Hayward, "Plastic Response of Ships side shell plating subjected to loads of finite height (Master's thesis)," Memorial University of Newfoundland, St. John's, 2001.

[19] N. Jones, "Review of the plastic behaviour of beams and plates," *International Shipbuilding Progress,* vol. 19, no. 218, pp. 313-327, 1972.

[20] K. Lepik, J. Peetsalu, S. Viljakainen and V. Voog, "Allowable plate deflections according to DNV," 2010.

[21] P. Varsta, I. Droumov and M. Hakala, "On Plastic Design of an Ice-Strengthened Frame," Winter Navgiagtion Research Board, Espoo, 1978.

[22] K. Kotisalo and P. Kujala, "Analysis of Ice Load Measurements Onboard MT Uikku," Helsinki University of Technology, Espoo, 1999.

[23] M. Suominen, J. Romanoff, H. Remes and P. Kujala, "The Determination of the Ice-induced Loads on the Ship Hull from Shear Strain Measurements," in

Proceedings of the 5th International Conference on Marine Structures, Southampton, 2014.

[24] M. Souminen, M. Kotilainen and P. Kujala, "The Encountered Extreme Events and Predicted Maximum Ice-induced Loads on the Ship Hull in the Southern Ocean," in *Proceedings of the ASME 2015 34th International Conference on Ocean, Offshore and Arctic Engineering*, Newfoundland, 2015.

[25] International Association of Classification Societies, Requirements Concerning Polar Class, 2011.

[26] Transport Safety Agency, Finnish-Swedish Ice Class Rules 2010, Helsinki, 2010.

[27] Z. Kala, J. Melcher and L. Puklicky, "Material and geometrical characteristics of structural steels based on statistical analysis of metallurgical products," *Journal of Civil Engineering and Managment,* vol. 15, no. 3, pp. 299-307, 2009.

[28] J. Valkonen, "Determination of ice load from hull ice damages," Espoo, 2006.

[29] *MEPC 68/21/Add.1,* International Code for Ships Operating in Polar Waters (Polar Code), 2015.

[30] *WMO No.259,* WMO Sea Ice Nomenclature, volumes I, II and III, 2014.

[31] P. Kujala, J. Kämäräinen and M. Suominen, "Analysis of a suitable ice class of ship hull for Antarctic operations," in *5th World Maritime Technology Conference November 3-7 2015*, Rhode Island Convention & Omni Hotel Providence, Rhode Islan, USA, 2015.

[32] *MSC 94/INF.13,* Technical Backgorund to POLARIS, 2014.

[33] *Arctic Ice Regime Shipping System - Pictorial Guide TP 14044,* Transport Canada.

[34] H. Nyseth and K. Bertelsen, "ICE CLASSES in Brief," DNV GL, 2014. [Online]. Available: http://www.codanmarine.com/repository/com/Files/Seminar/Ice Navigation/Ice classes in brief.pdf. [Accessed 30 5 2016].

[35] *MSC 94/3/7,* POLARIS - proposed system for determining operational limitation in ice Submitted byt he International Association of Classification Societies (IACS), 2014.

Appendix 1

The long term return periods of ice loads for the bow of S.A. Agulhas II in different ice conditions.

Case 1 – Ice concentration < 70% and ice thickness < 0.7 m

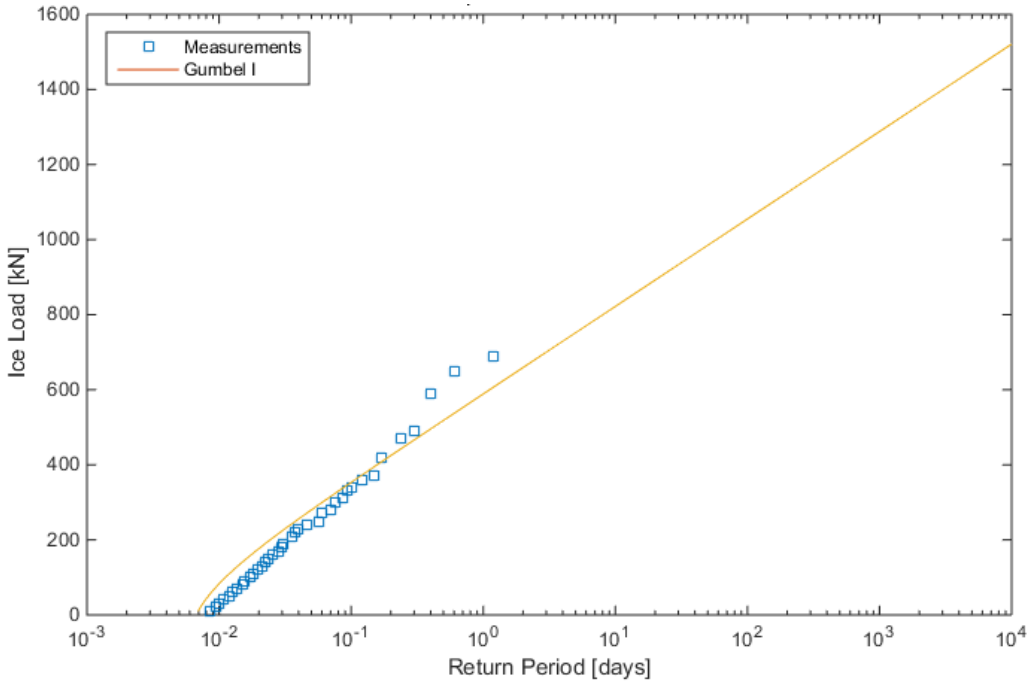

Case 2 – Ice concentration < 70% and ice thickness 0.7-1.2 m

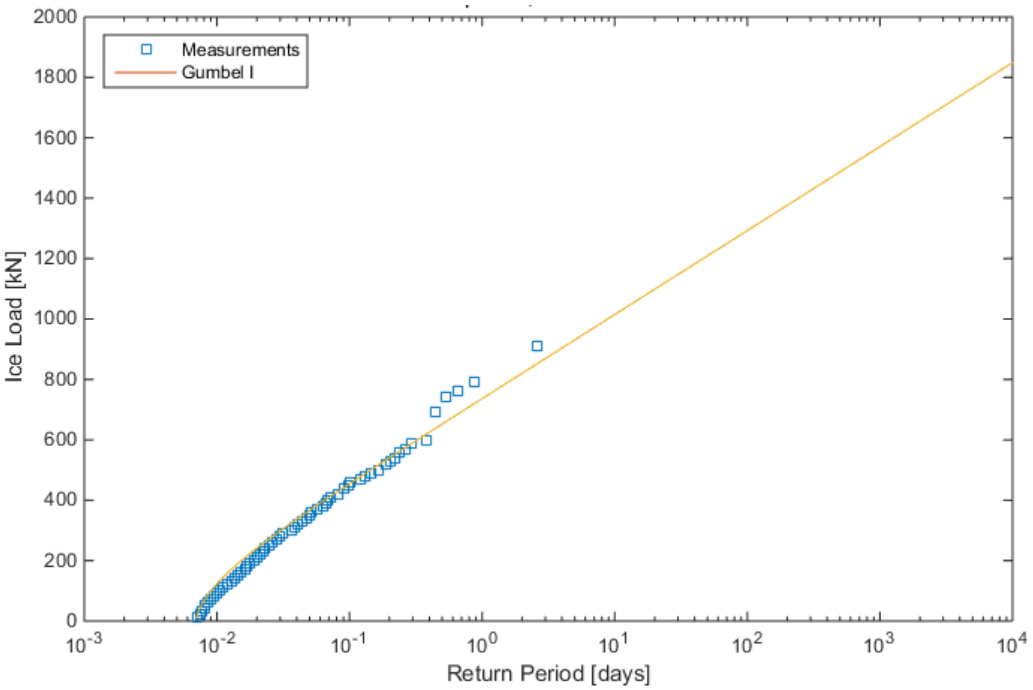

Case 3 – Ice concentration < 70% and ice thickness 1.2-2 m

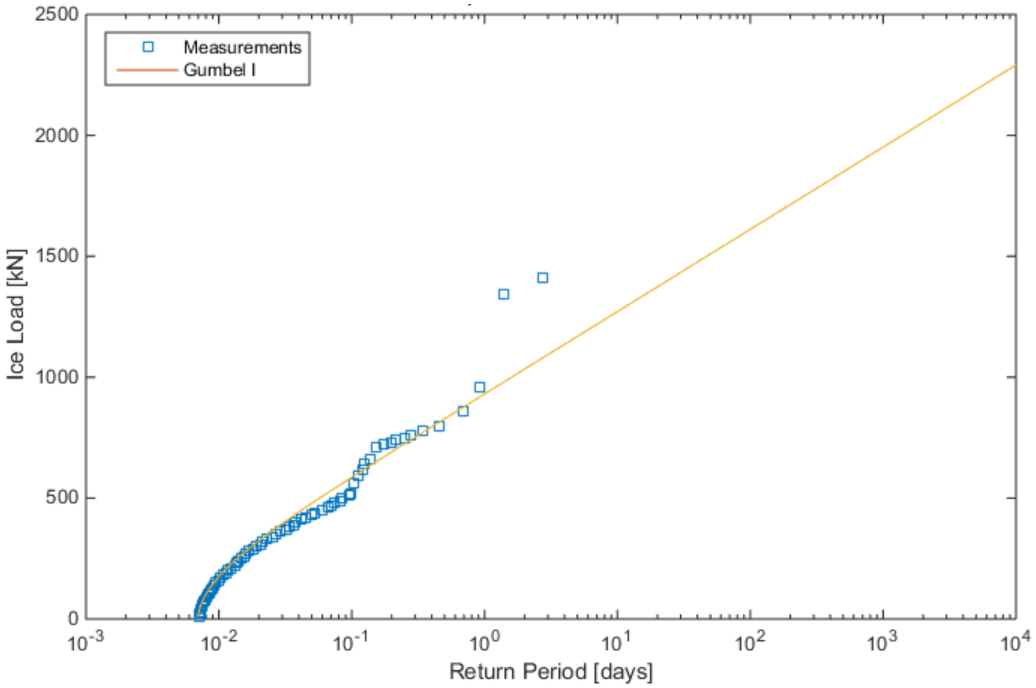

Case 4 – Ice concentration < 70% and ice thickness > 2 m

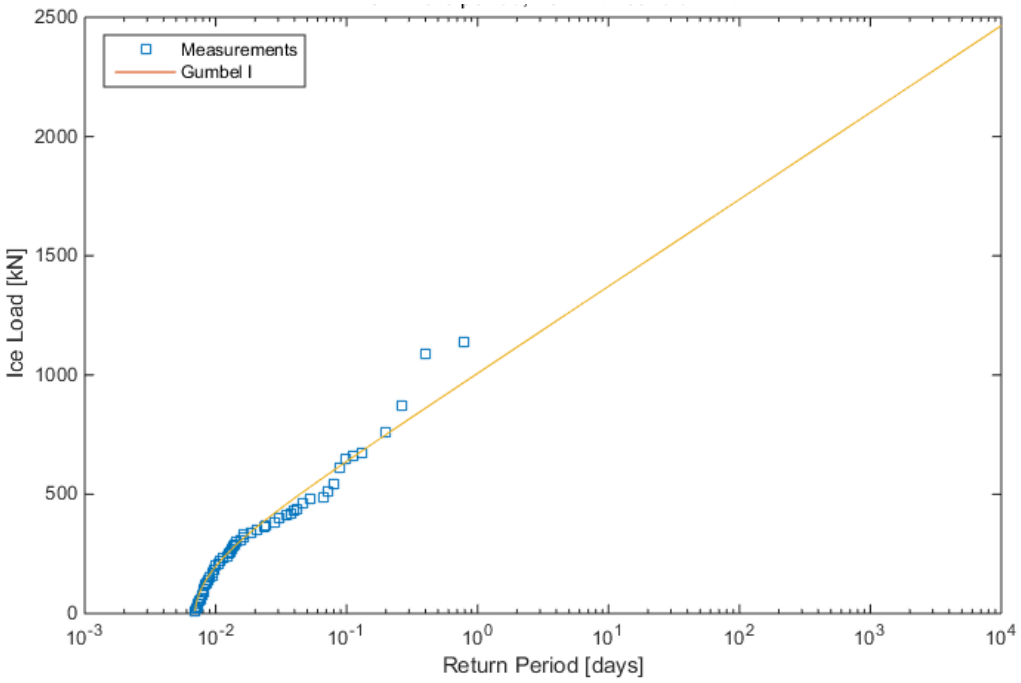

Case 5 – Ice concentration 70-90% and ice thickness < 0.7 m

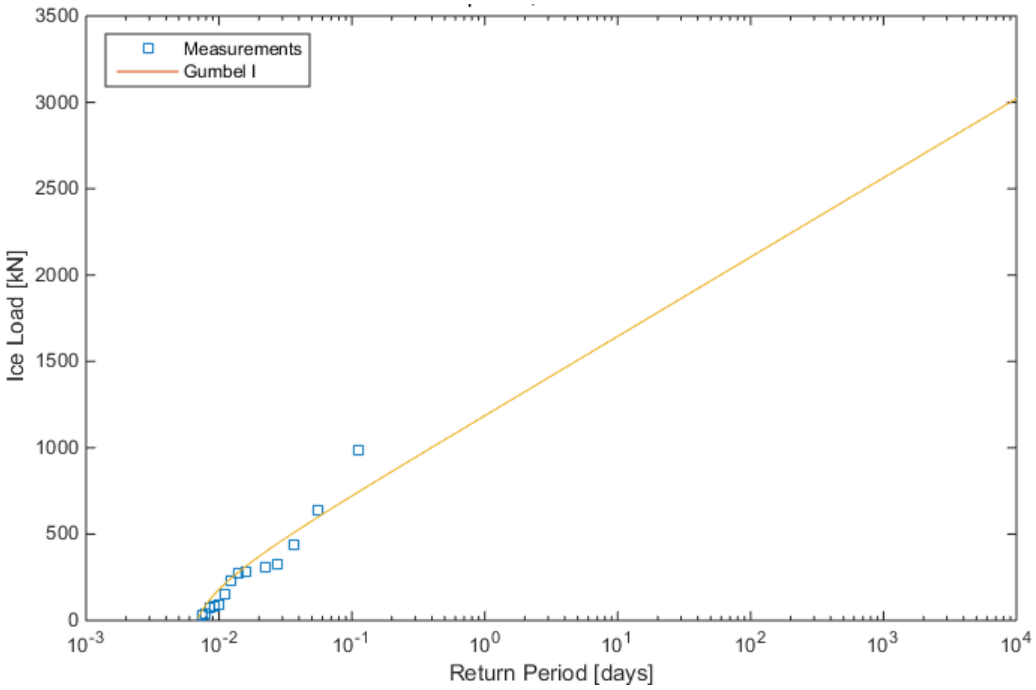

Case 6 – Ice concentration 70-90% and ice thickness 0.7-1.2 m

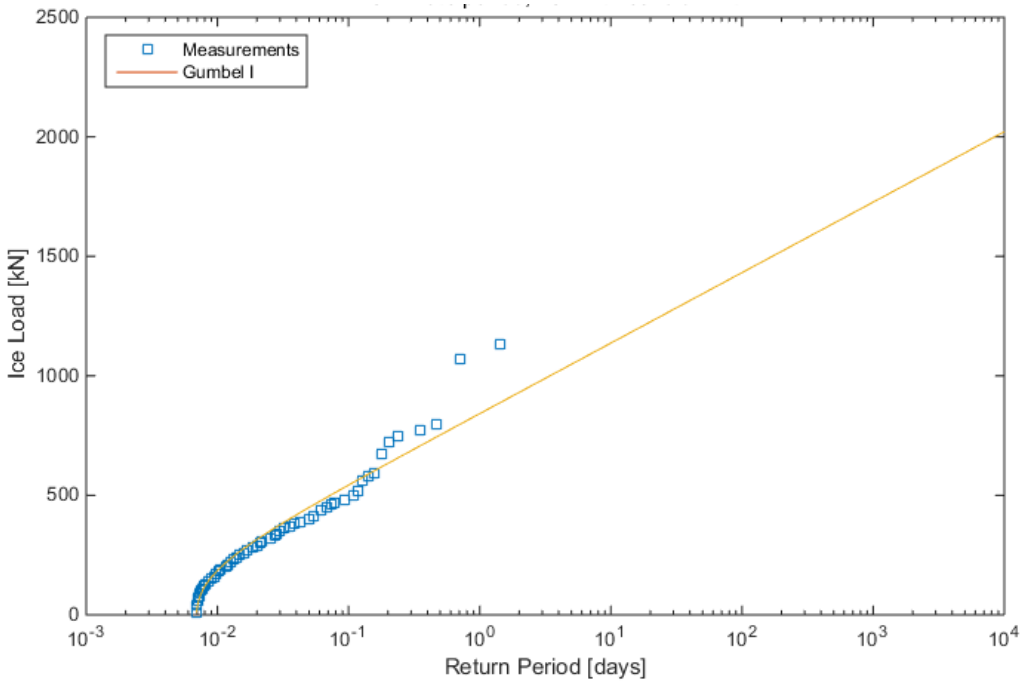

Case 7 – Ice concentration 70-90% and ice thickness 1.2-2 m

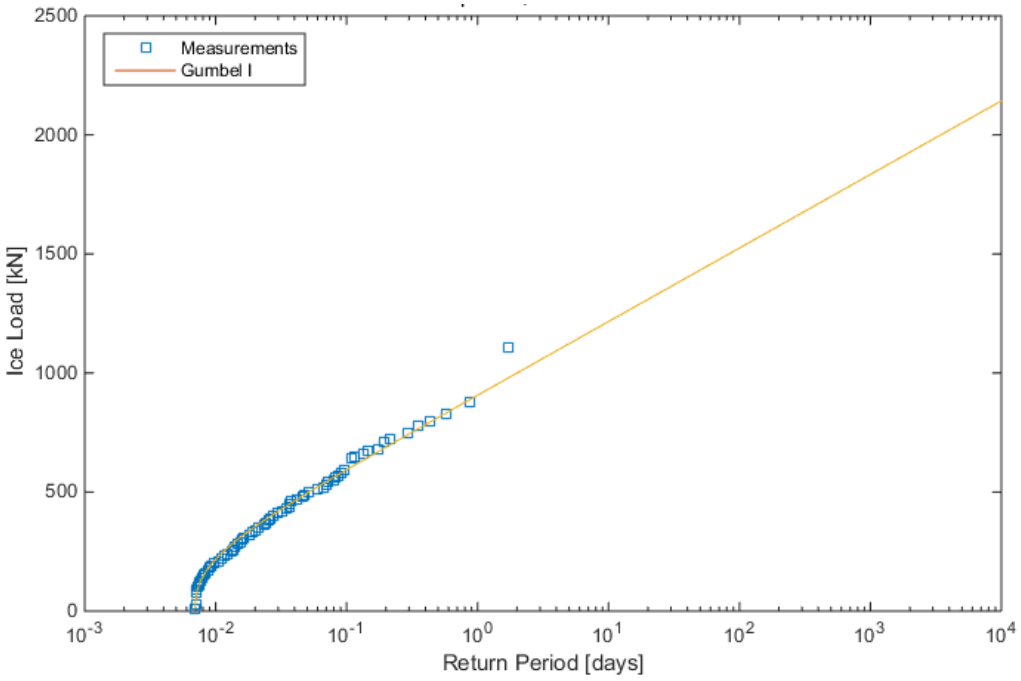

Case 8 – Ice concentration 70-90% and ice thickness > 2 m

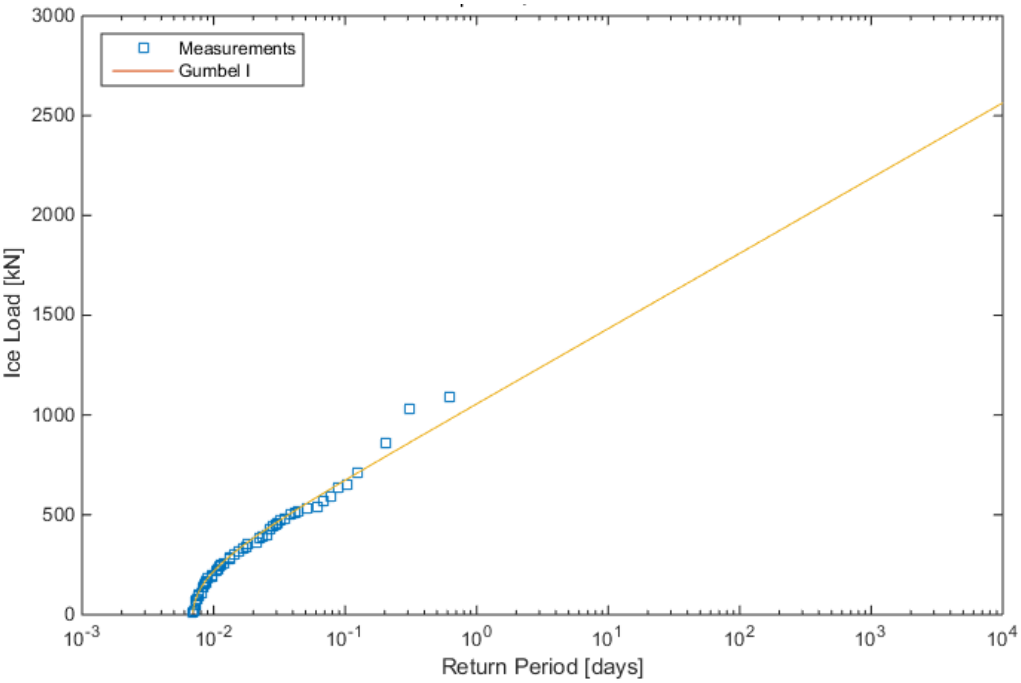

Case 9 – Ice concentration > 90% and ice thickness < 0.7 m

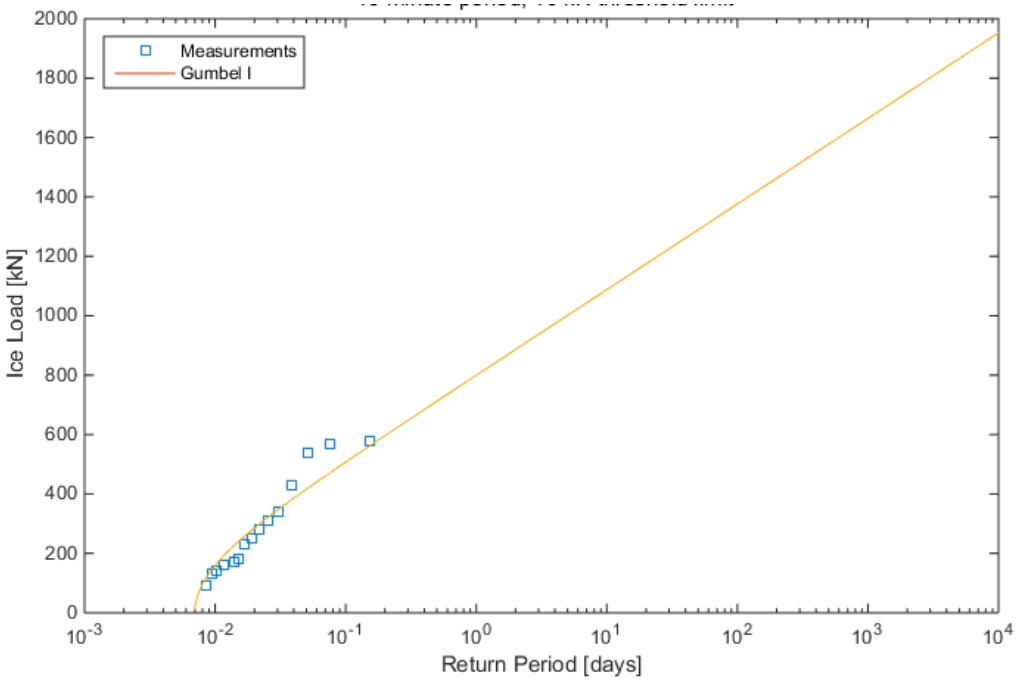

Case 10 – Ice concentration > 90% and ice thickness 0.7-1.2 m

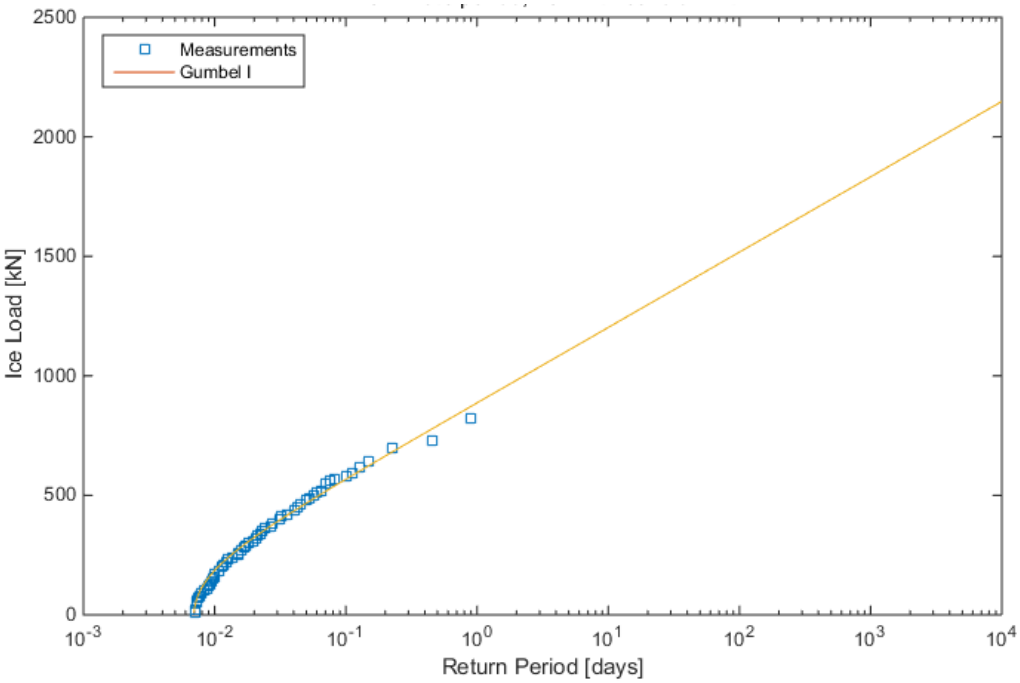

Case 11 – Ice concentration > 90% and ice thickness 1.2-2 m

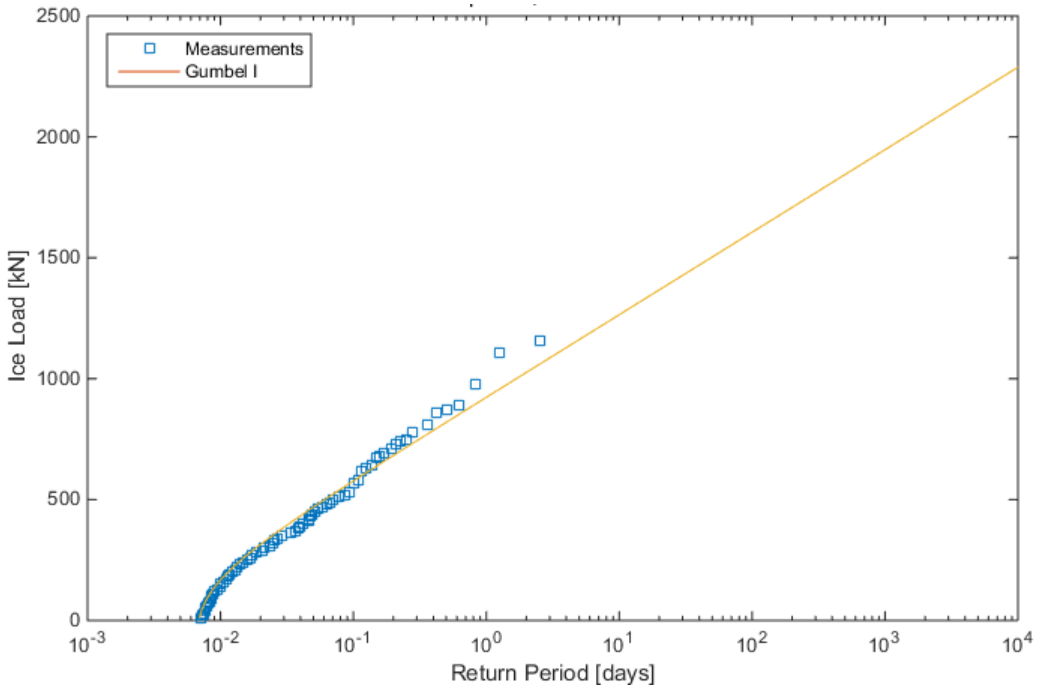

Case 12 – Ice concentration > 90% and ice thickness > 2 m

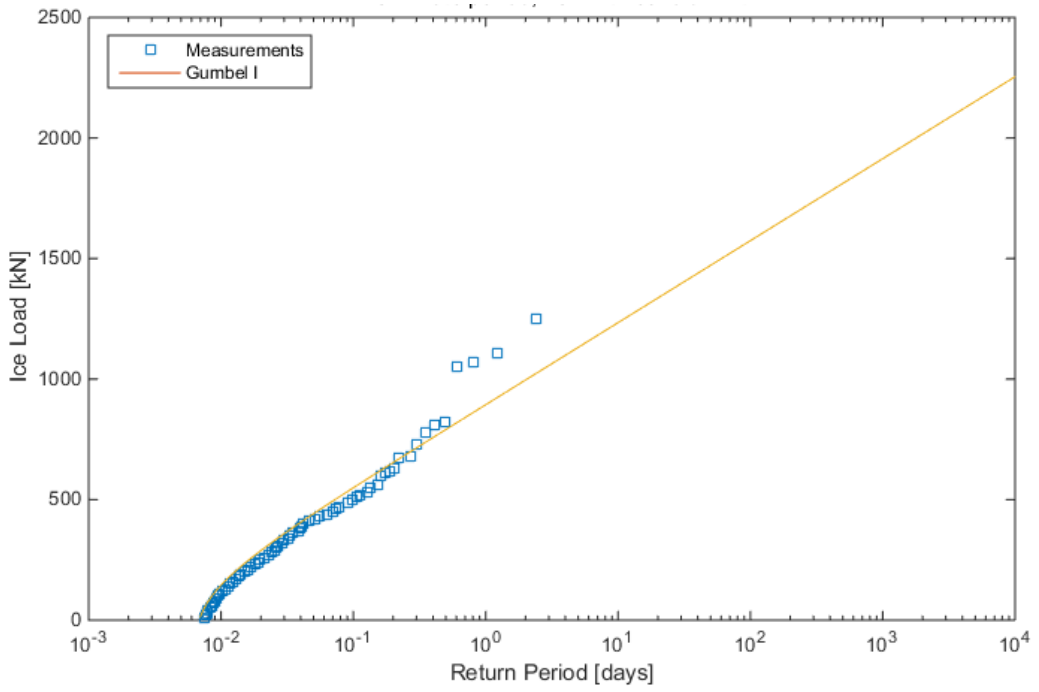

The long term return periods of ice loads for the stern of S.A. Agulhas II in different ice conditions.

Case 1 – Ice concentration < 70% and ice thickness < 0.7 m

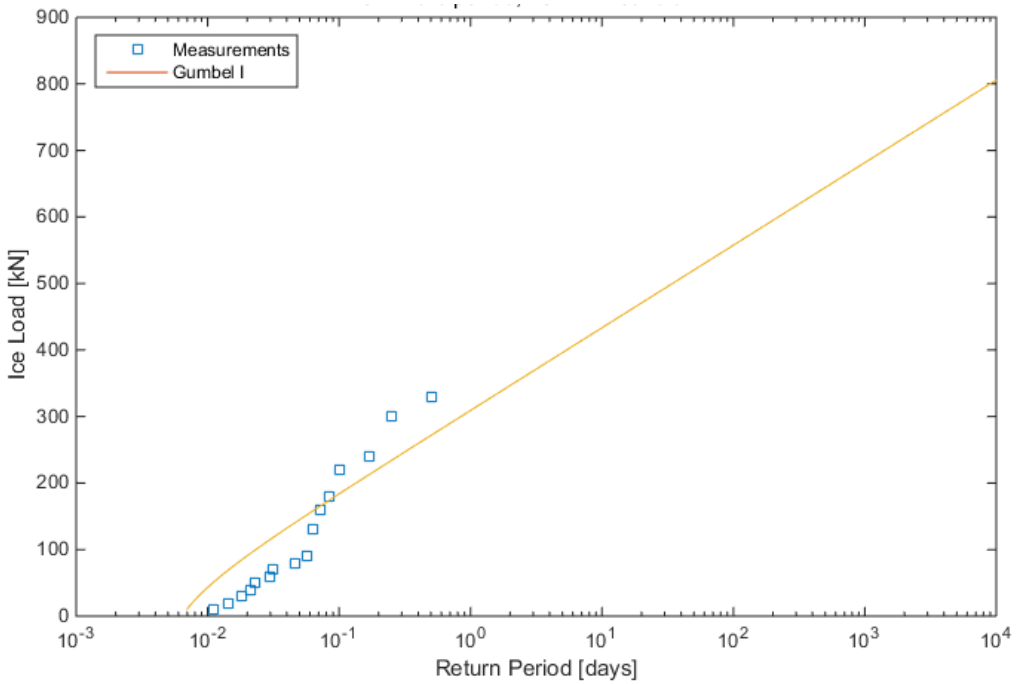

Case 2 – Ice concentration < 70% and ice thickness 0.7-1.2 m

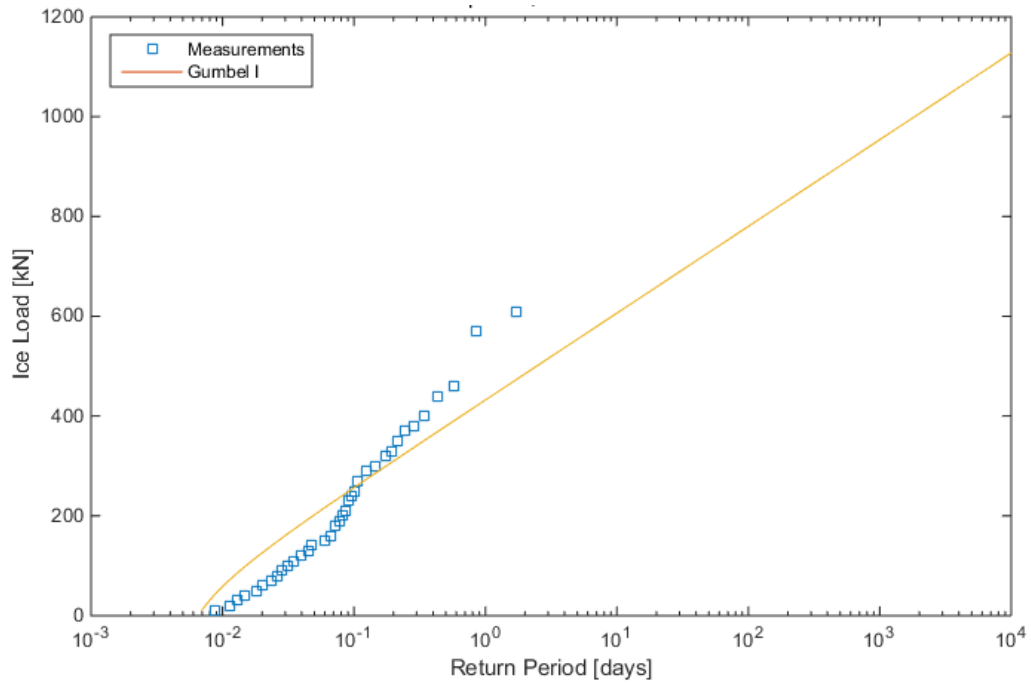

Case 3 – Ice concentration < 70% and ice thickness 1.2-2 m

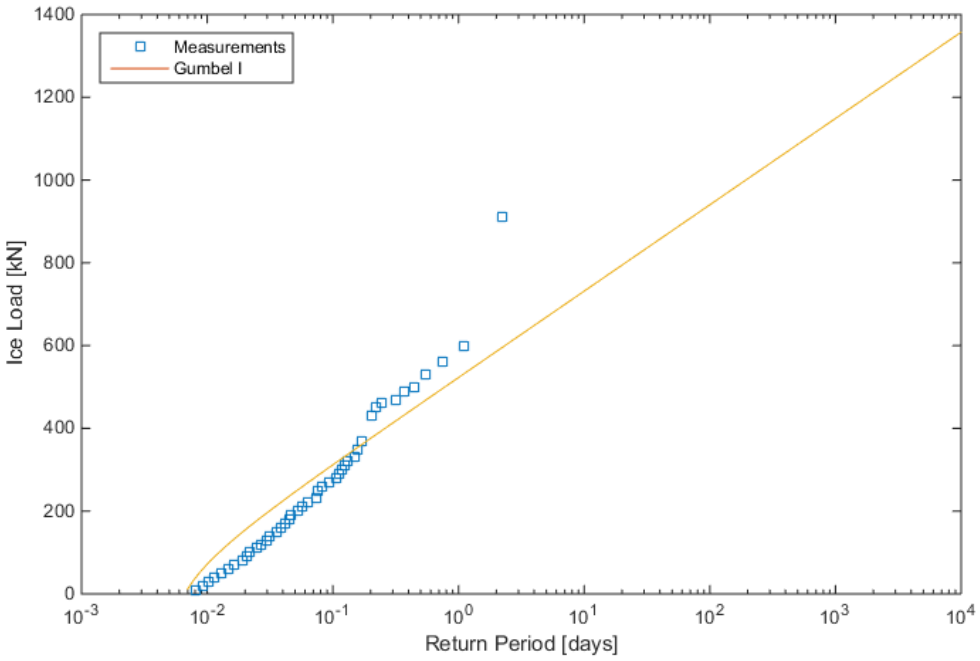

Case 4 – Ice concentration < 70% and ice thickness > 2 m

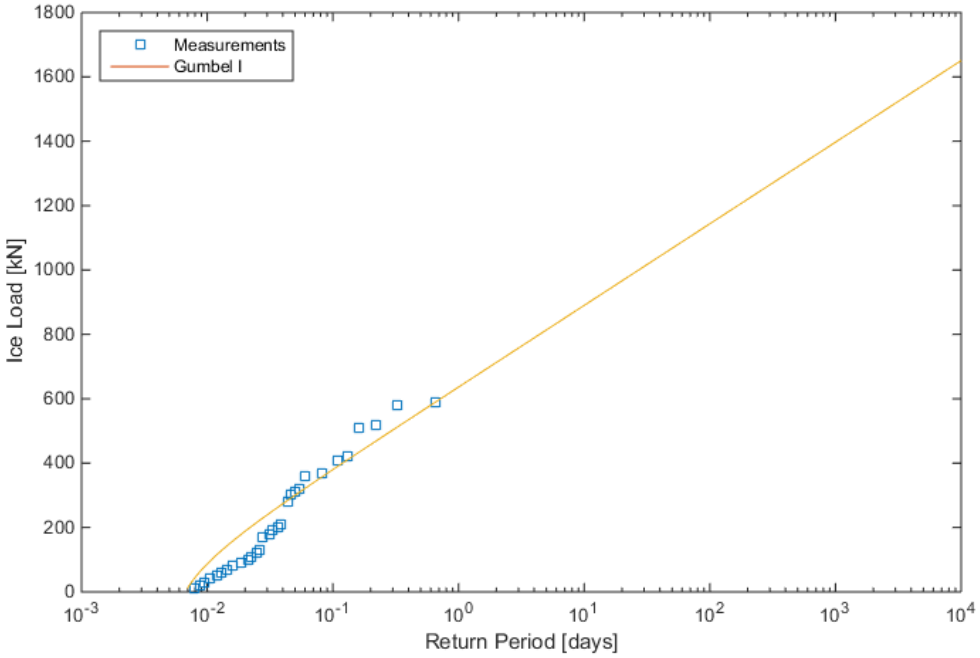

Case 5 – Ice concentration 70-90% and ice thickness < 0.7 m

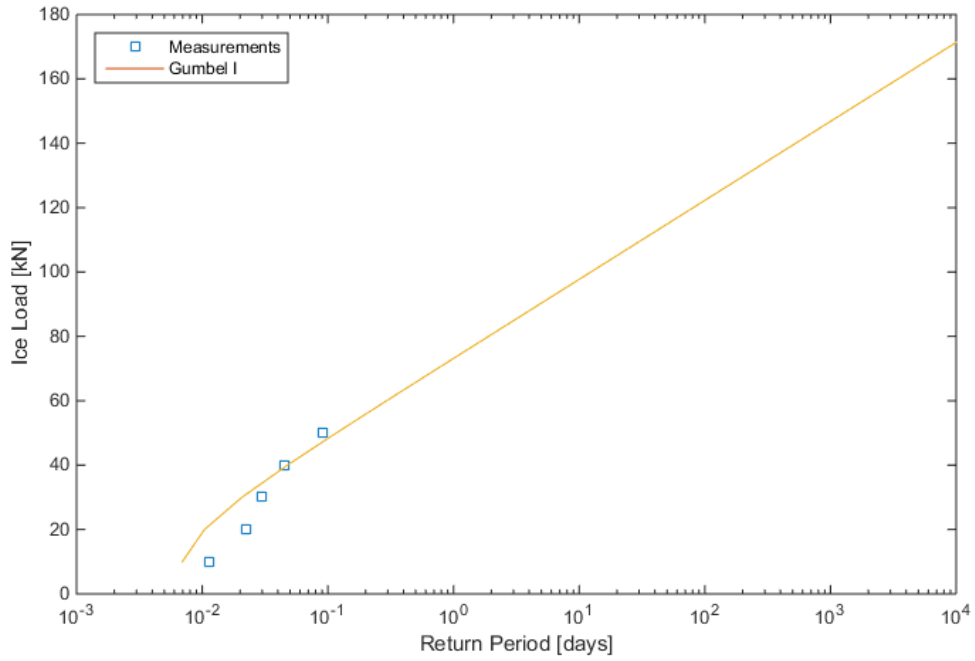

Case 6 – Ice concentration 70-90% and ice thickness 0.7-1.2 m

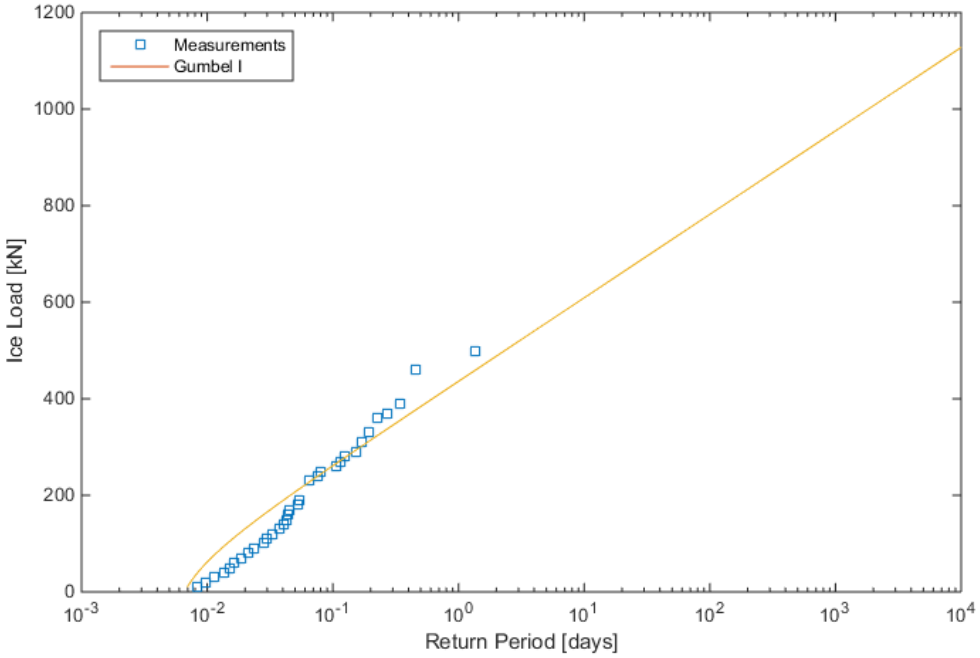

Case 7 – Ice concentration 70-90% and ice thickness 1.2-2 m

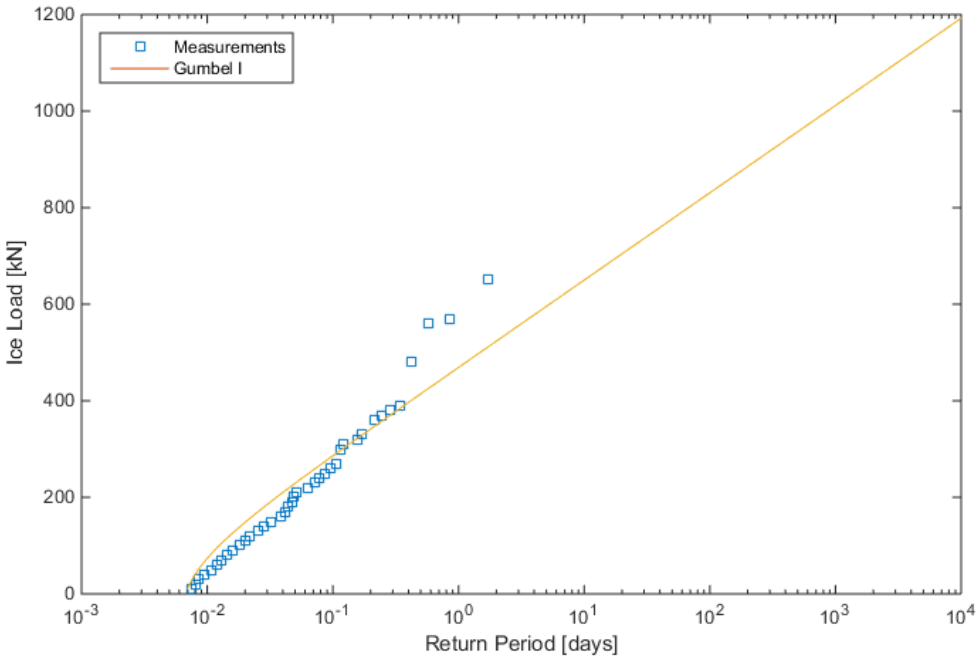

Case 8 – Ice concentration 70-90% and ice thickness > 2 m

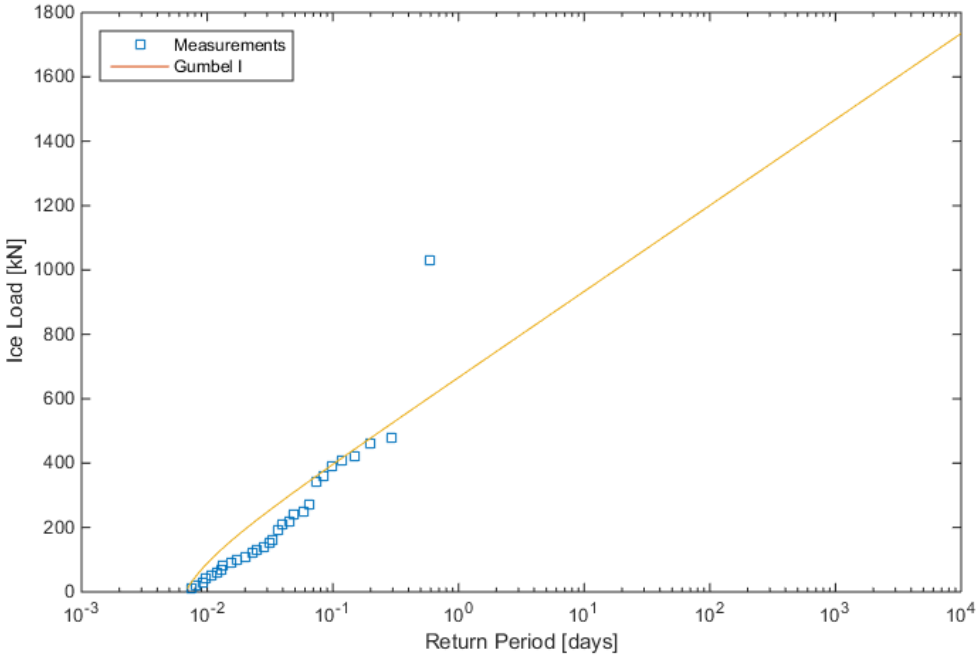

Case 9 – Ice concentration > 90% and ice thickness < 0.7 m

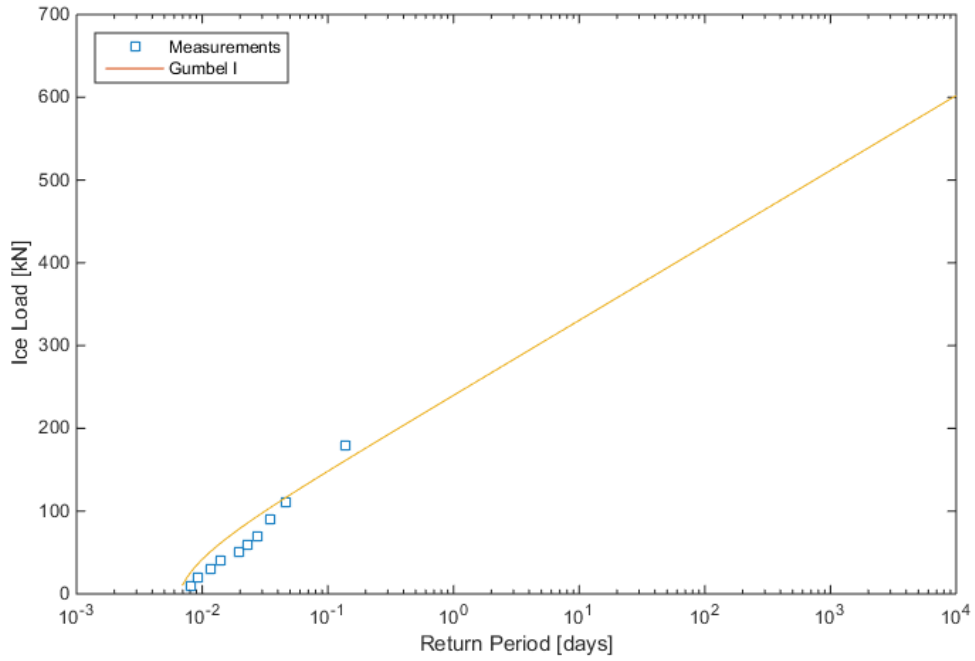

Case 10 – Ice concentration > 90% and ice thickness 0.7-1.2 m

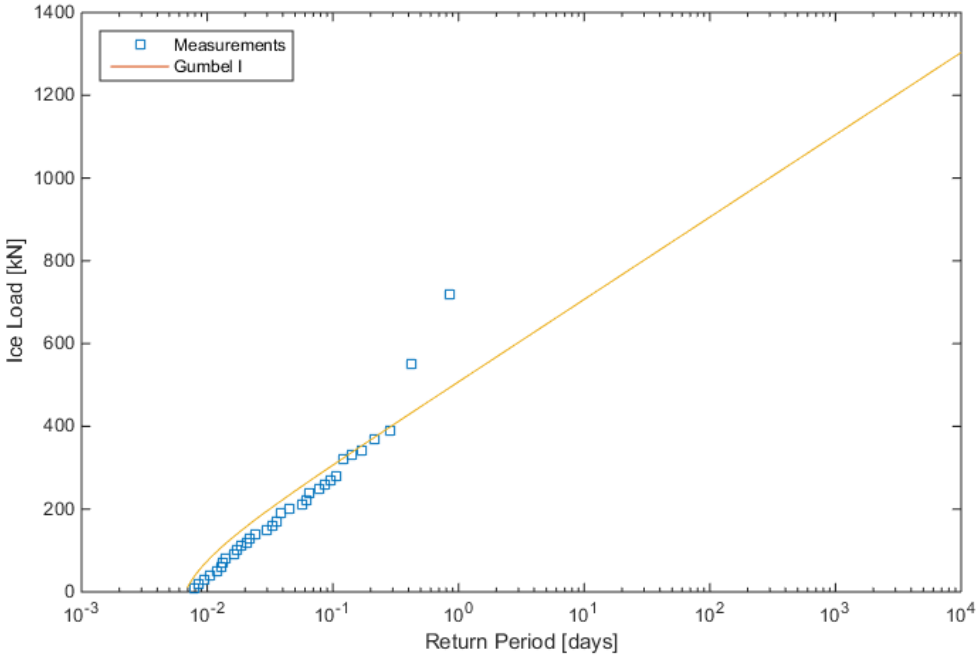

Case 11 – Ice concentration > 90% and ice thickness 1.2-2 m

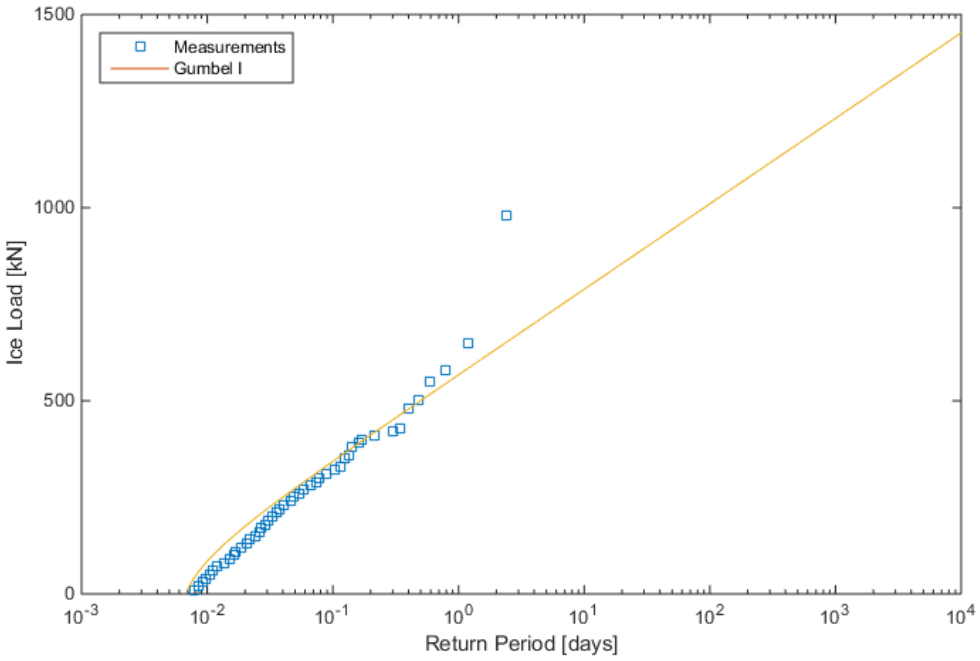

Case 12 – Ice concentration > 90% and ice thickness > 2 m

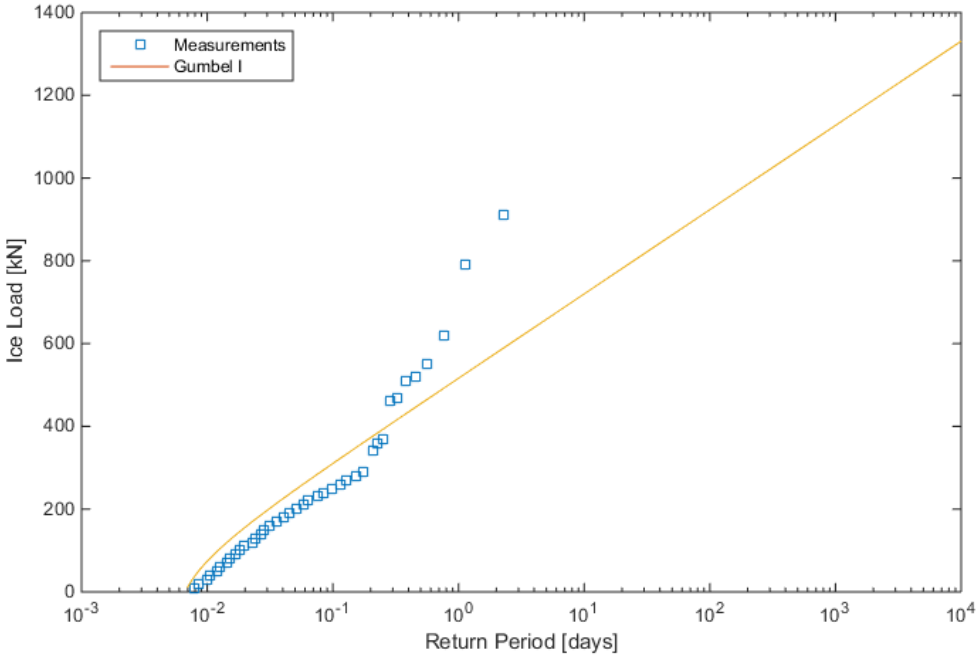

Appendix 2

The long term return periods of ice loads for the bow of M/T Uikku in different ice conditions.

Case 1 – Ice concentration < 70% and ice thickness < 0.7 m

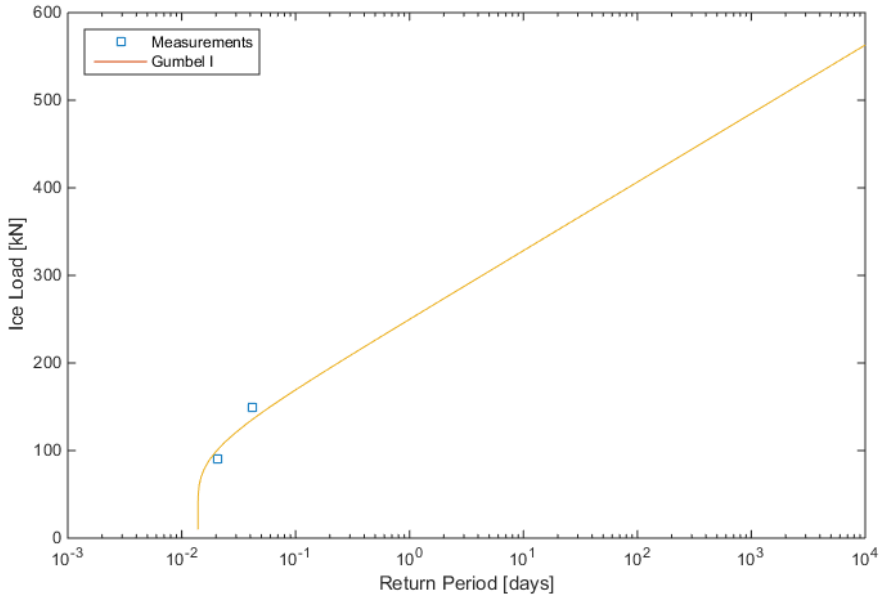

Case 2 – Ice concentration < 70% and ice thickness 0.7-1.2 m

Not enough data in these conditions.

Case 3 – Ice concentration < 70% and ice thickness 1.2-2 m

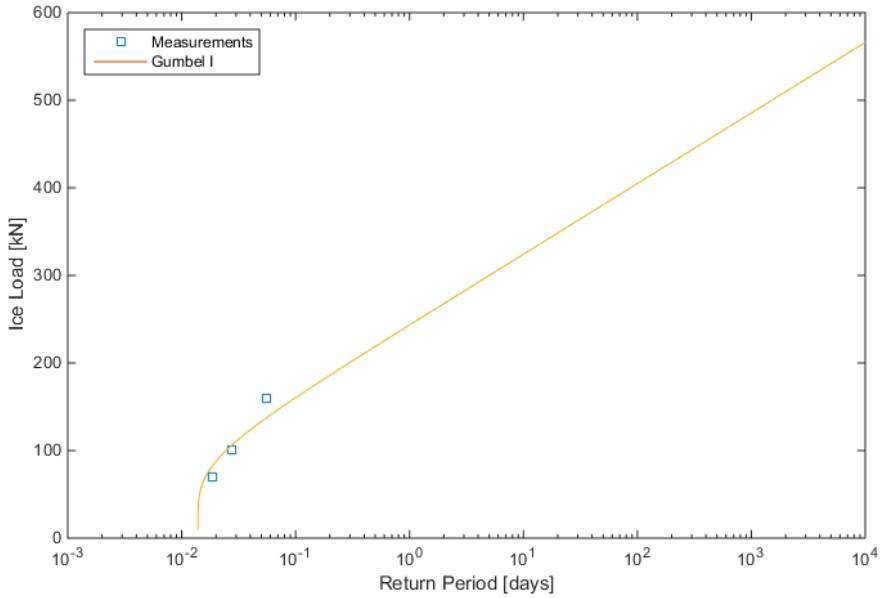

Case 4 – Ice concentration < 70% and ice thickness > 2 m

No data in conditions where ice thickness is above 2 m.

Case 5 – Ice concentration 70-90% and ice thickness < 0.7 m

Not enough data above the threshold value in these conditions.

Case 6 – Ice concentration 70-90% and ice thickness 0.7-1.2 m

Not enough data in these conditions.

Case 7 – Ice concentration 70-90% and ice thickness 1.2-2 m

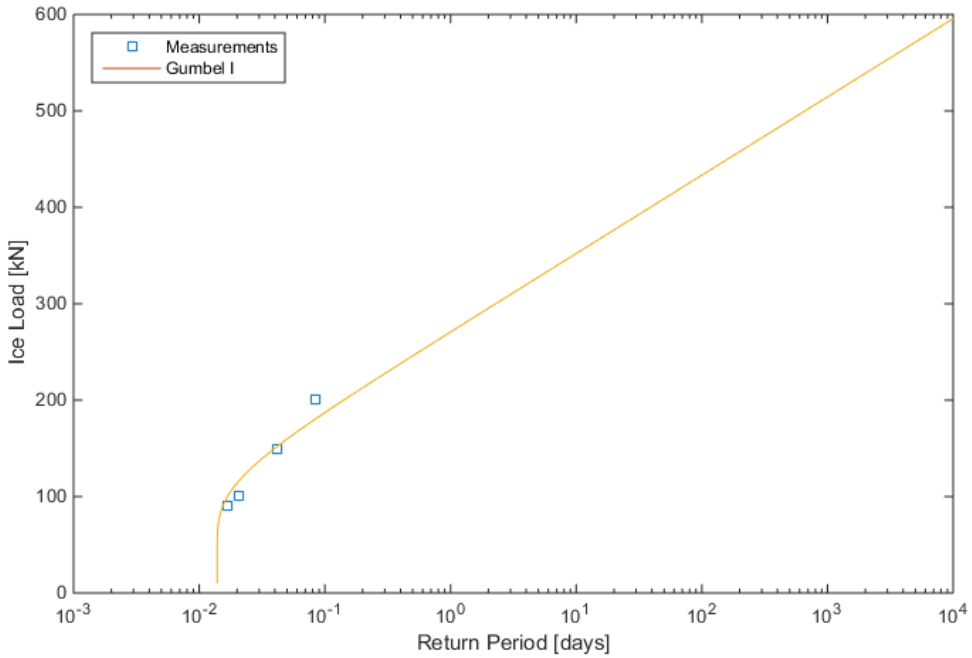

Case 8 – Ice concentration 70-90% and ice thickness > 2 m

No data in conditions where ice thickness is above 2 m.

Case 9 – Ice concentration > 90% and ice thickness < 0.7 m

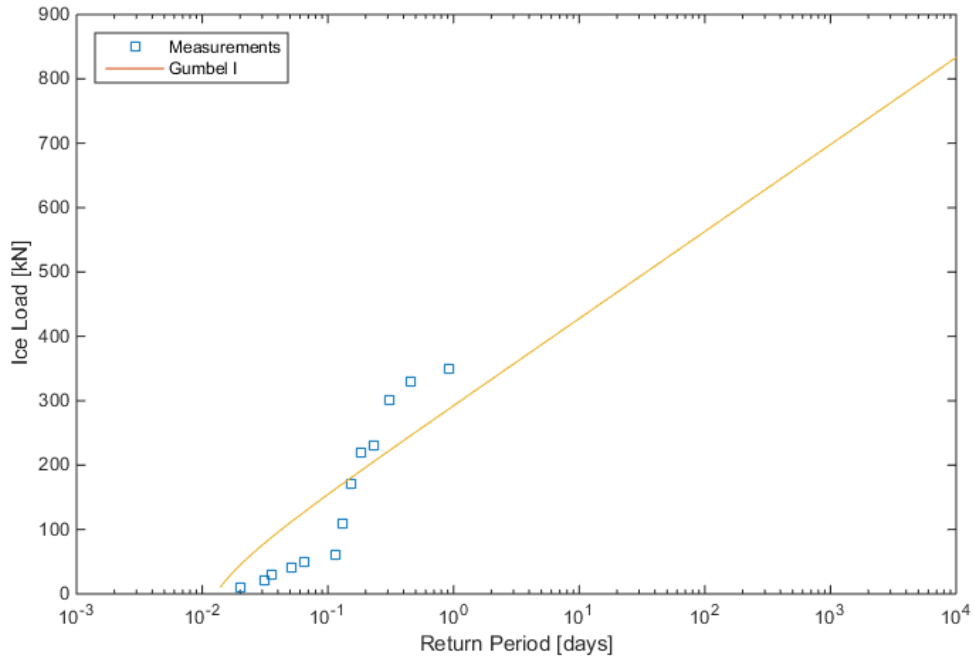

Case 10 – Ice concentration > 90% and ice thickness 0.7-1.2 m

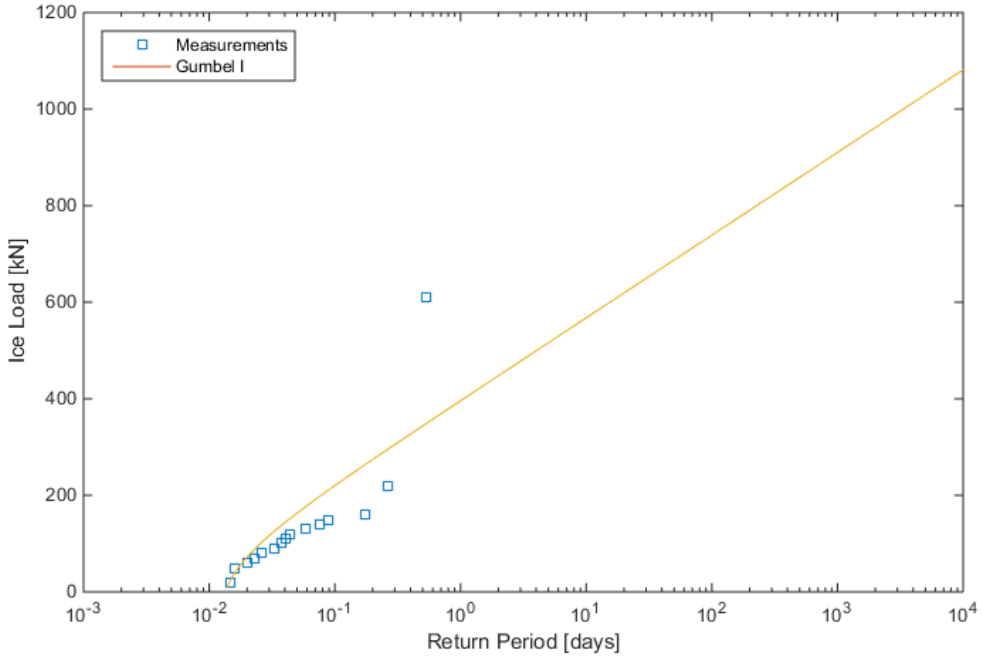

Case 11 – Ice concentration > 90% and ice thickness 1.2-2 m

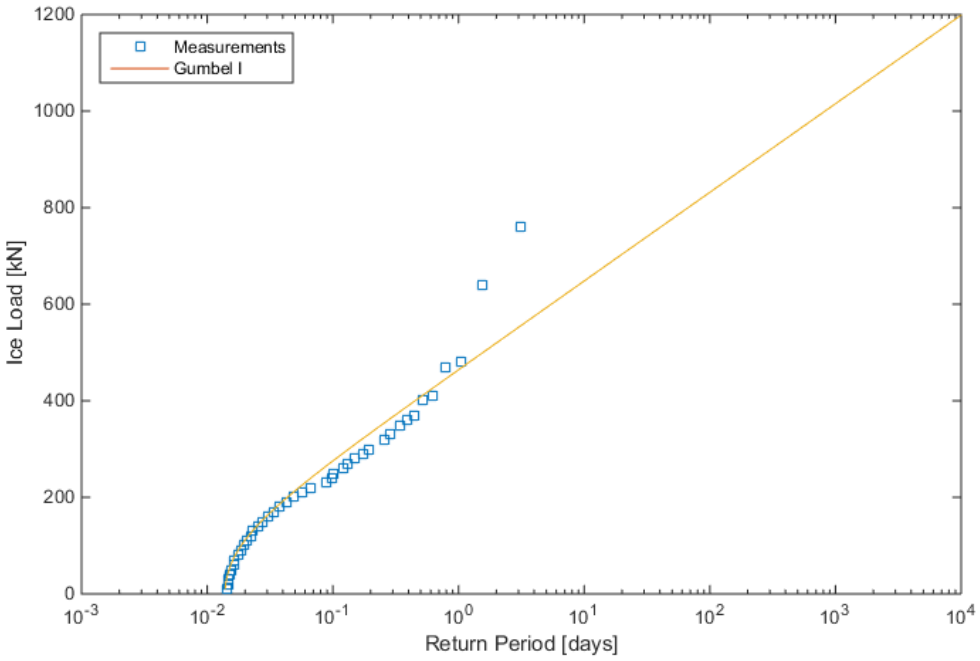

Case 12 – Ice concentration > 90% and ice thickness > 2 m

No data in conditions where ice thickness is above 2 m.

The long term return periods of ice loads for the bow-shoulder of M/T Uikku in different ice conditions.

Case 1 – Ice concentration < 70% and ice thickness < 0.7 m

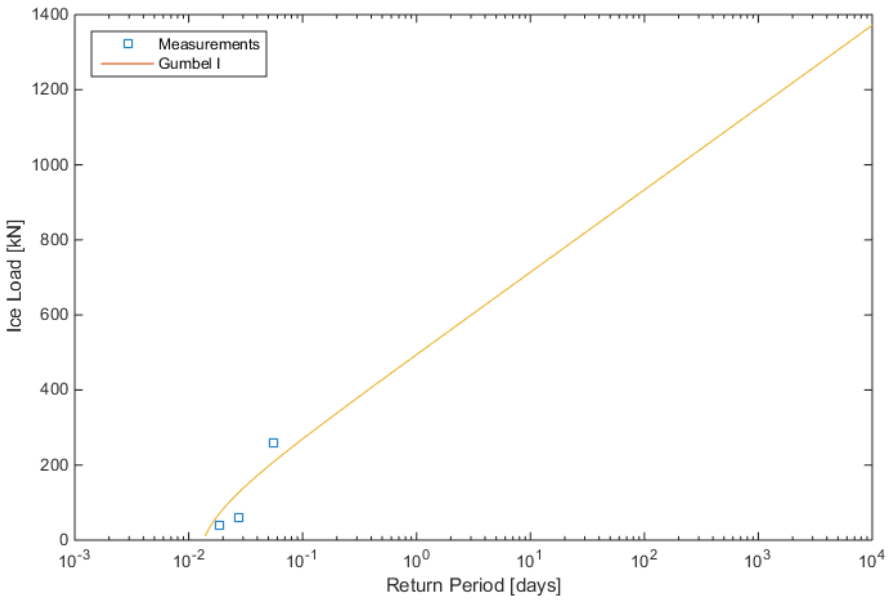

Case 2 – Ice concentration < 70% and ice thickness 0.7-1.2 m

Not enough data in these conditions.

Case 3 – Ice concentration < 70% and ice thickness 1.2-2 m

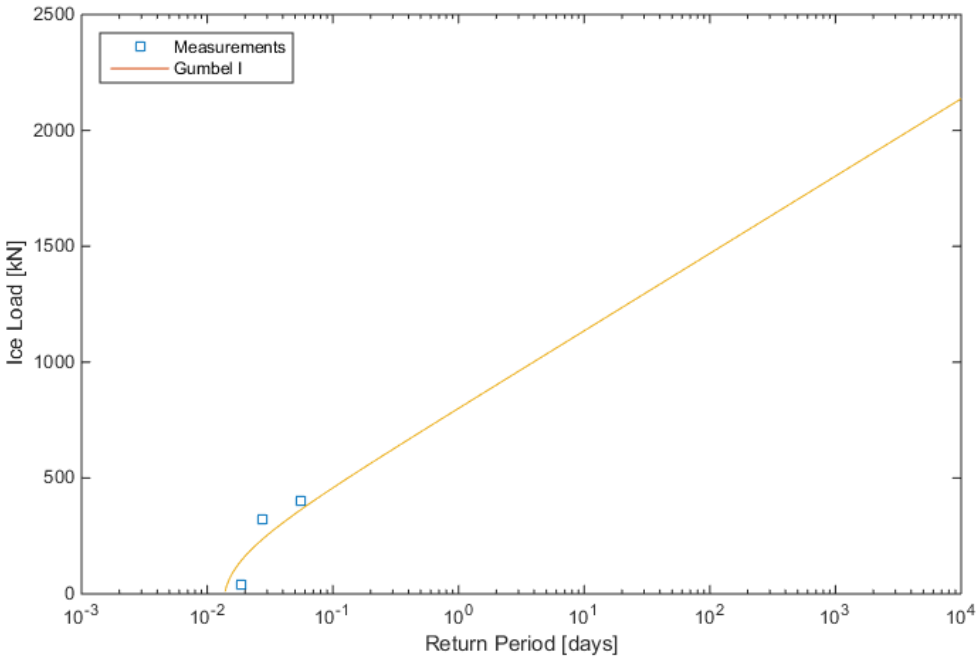

Case 4 – Ice concentration < 70% and ice thickness > 2 m

No data in conditions where ice thickness is above 2 m.

Case 5 – Ice concentration 70-90% and ice thickness < 0.7 m

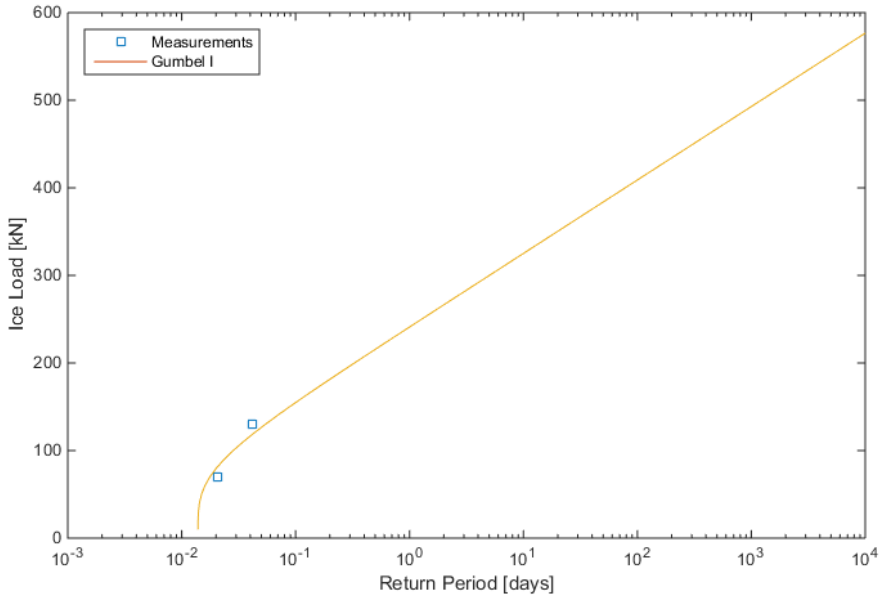

Case 6 – Ice concentration 70-90% and ice thickness 0.7-1.2 m

Not enough data in these conditions.

Case 7 – Ice concentration 70-90% and ice thickness 1.2-2 m

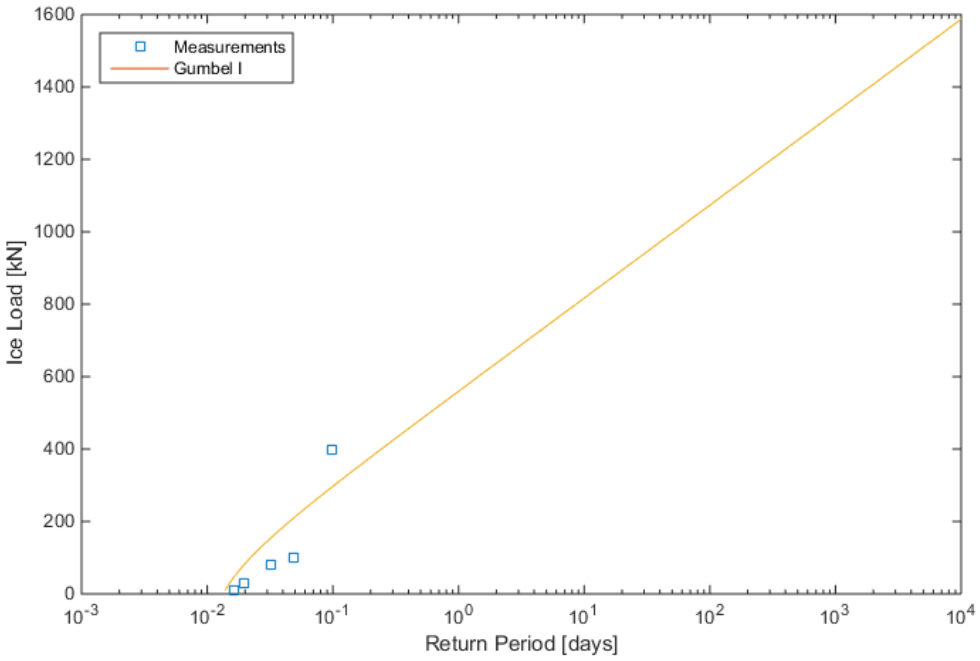

Case 8 – Ice concentration 70-90% and ice thickness > 2 m

No data in conditions where ice thickness is above 2 m.

Case 9 – Ice concentration > 90% and ice thickness < 0.7 m

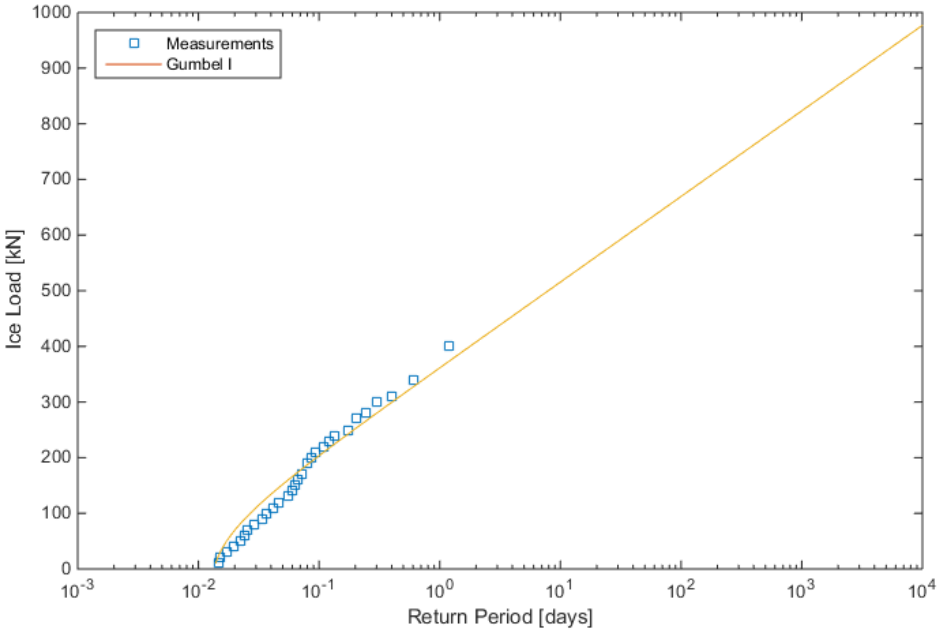

Case 10 – Ice concentration > 90% and ice thickness 0.7-1.2 m

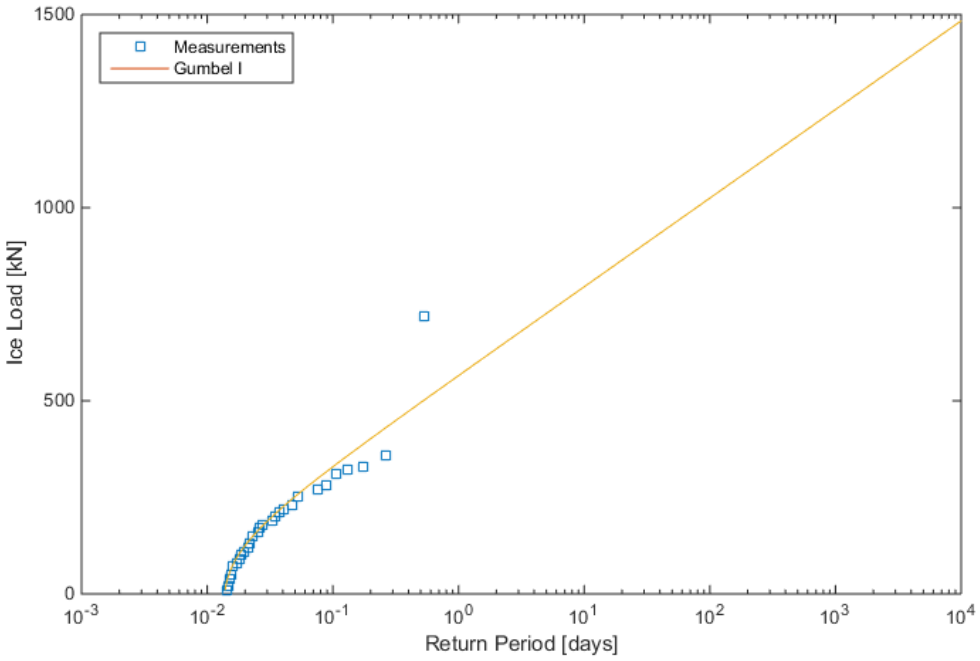

Case 11 – Ice concentration > 90% and ice thickness 1.2-2 m

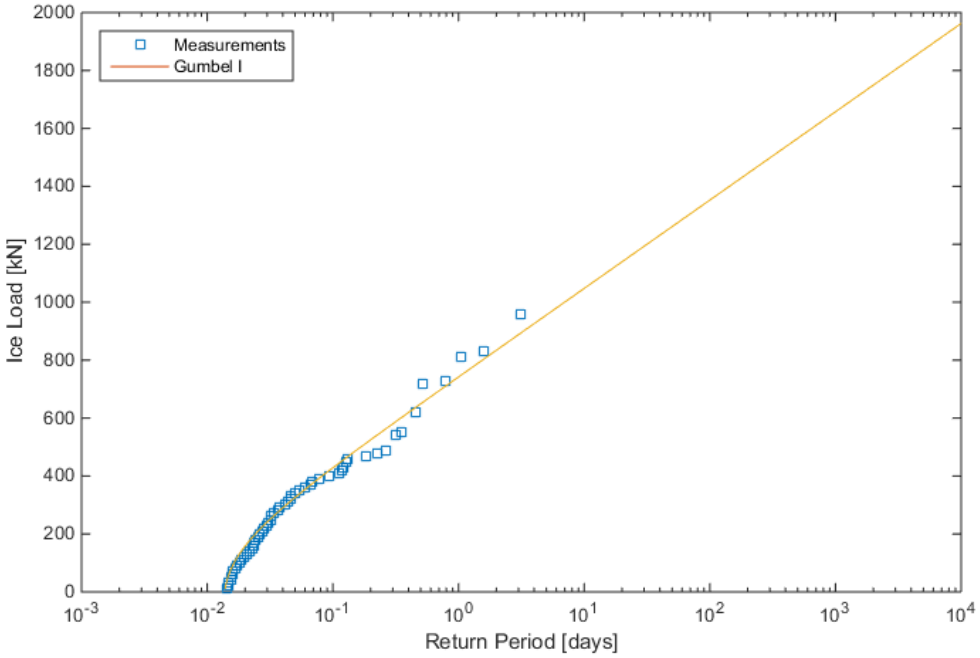

Case 12 – Ice concentration > 90% and ice thickness > 2 m

No data in conditions where ice thickness is above 2 m.

The long term return periods for the stern of M/T Uikku in different ice conditions.

Case 1 – Ice concentration < 70% and ice thickness < 0.7 m

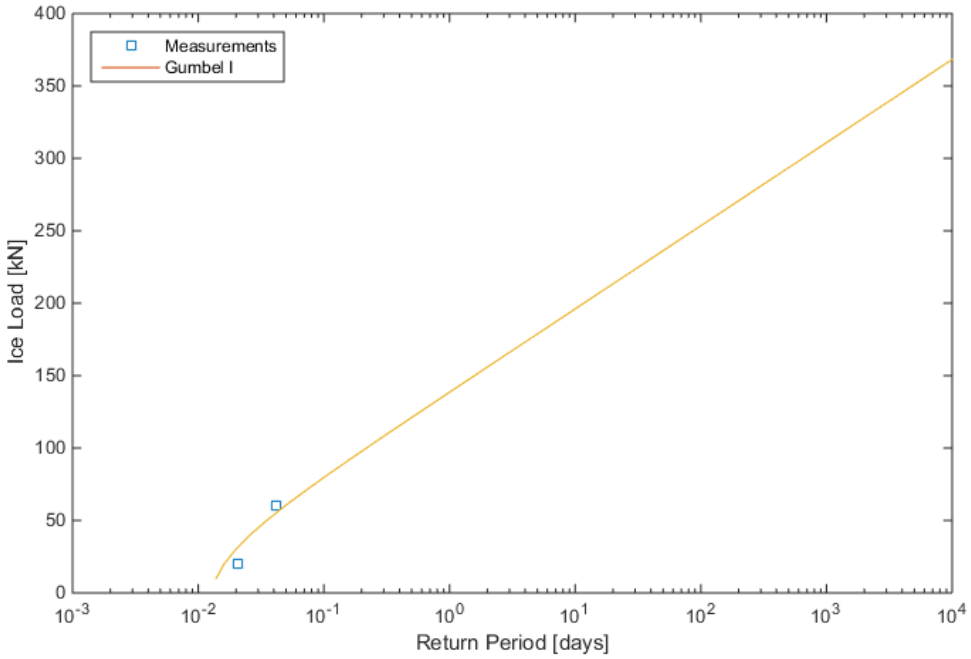

Case 2 – Ice concentration < 70% and ice thickness 0.7-1.2 m

Not enough data in these conditions.

Case 3 – Ice concentration < 70% and ice thickness 1.2-2 m

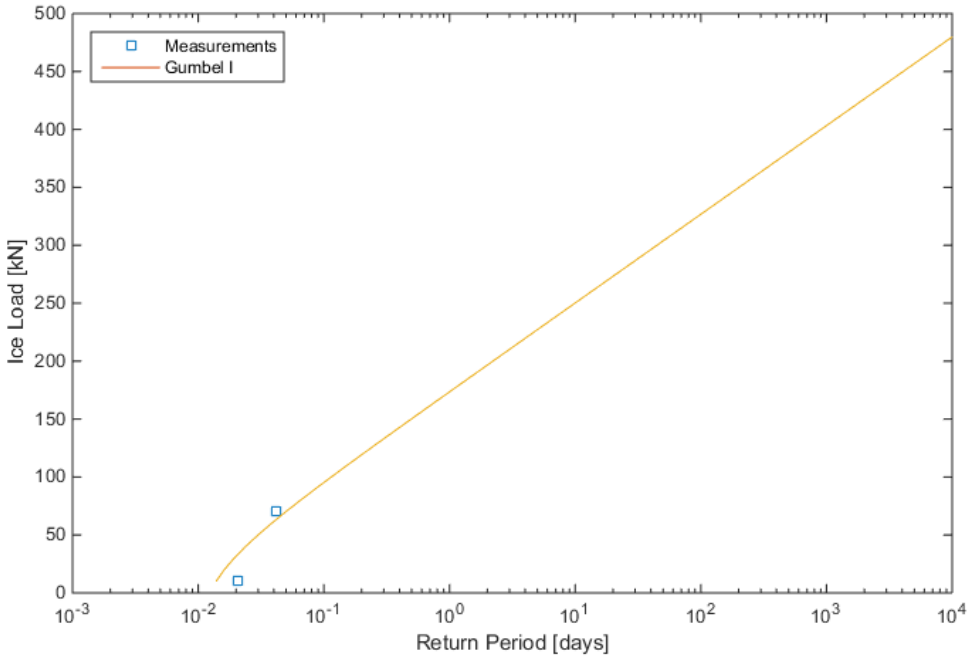

Case 4 – Ice concentration < 70% and ice thickness > 2 m

No data in conditions where ice thickness is above 2 m.

Case 5 – Ice concentration 70-90% and ice thickness < 0.7 m

Not enough data above the threshold value in these conditions.

Case 6 – Ice concentration 70-90% and ice thickness 0.7-1.2 m

Not enough data in these conditions.

Case 7 – Ice concentration 70-90% and ice thickness 1.2-2 m

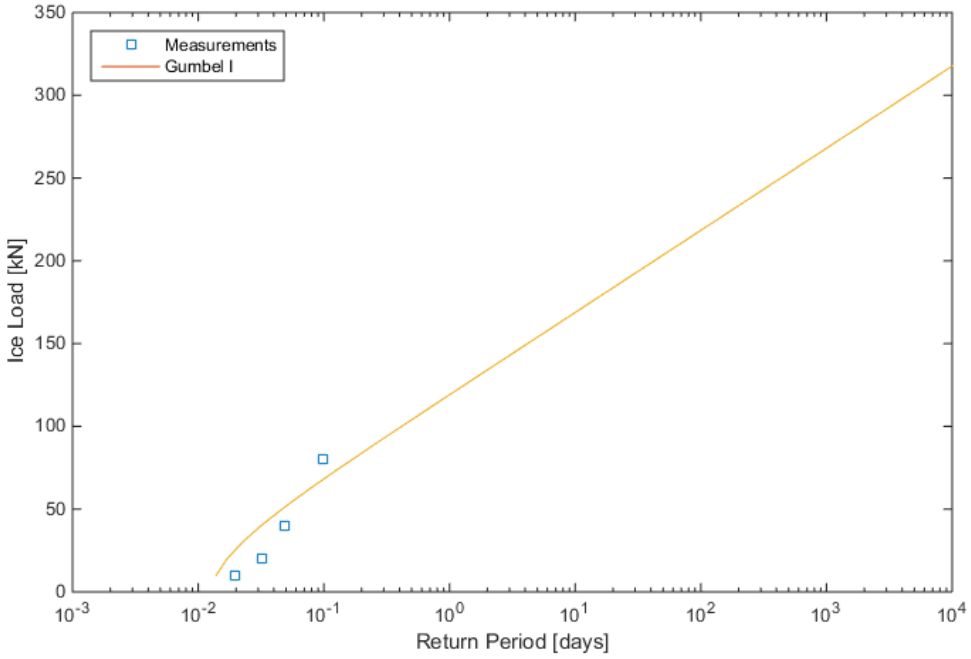

Case 8 – Ice concentration 70-90% and ice thickness > 2 m

No data in conditions where ice thickness is above 2 m.

Case 9 – Ice concentration > 90% and ice thickness < 0.7 m

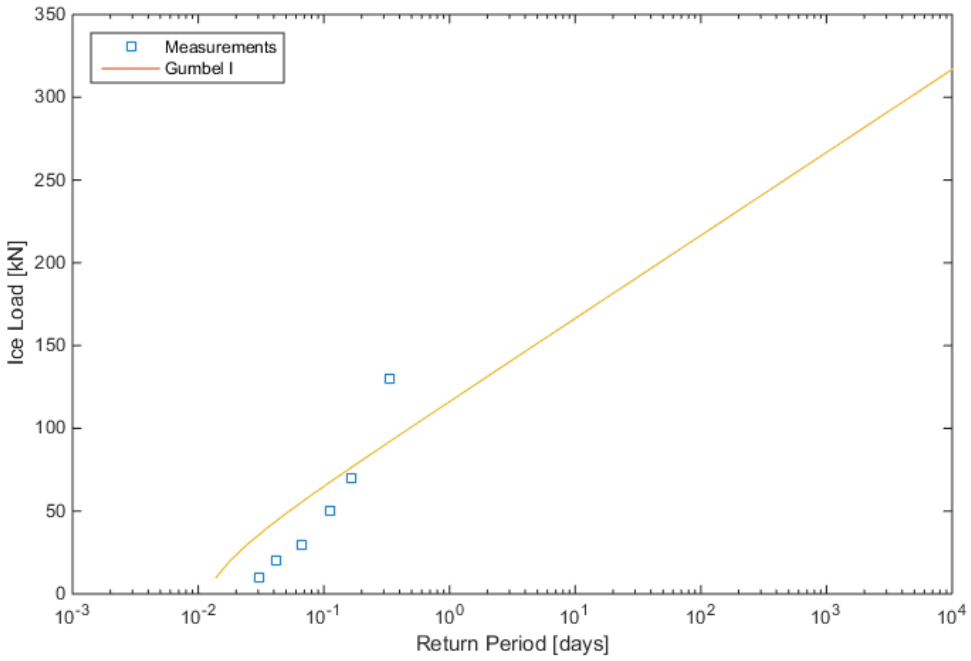

Case 10 – Ice concentration > 90% and ice thickness 0.7-1.2 m

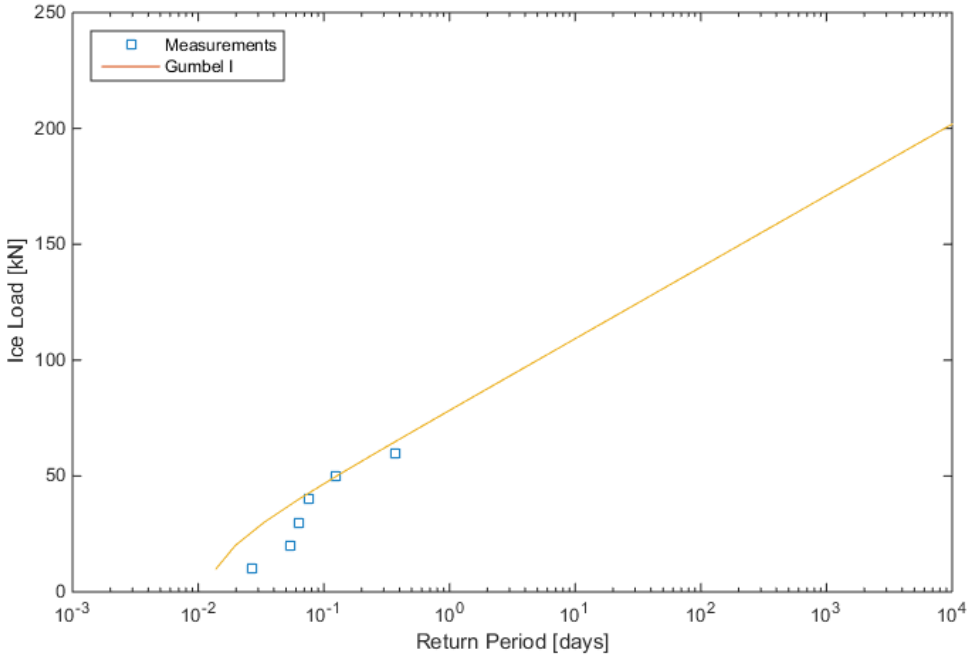

Case 11 – Ice concentration > 90% and ice thickness 1.2-2 m

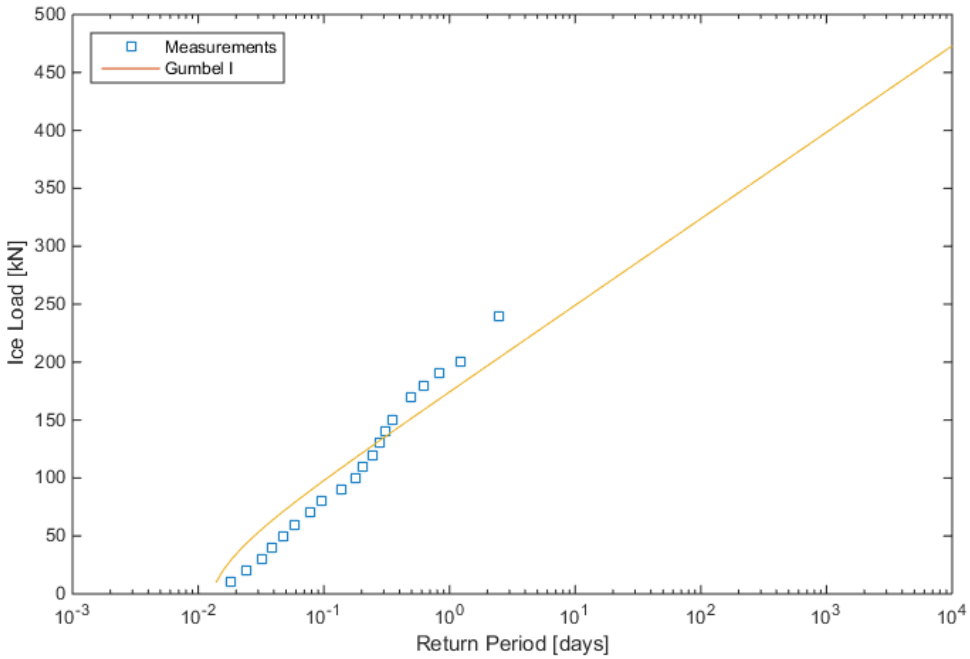

Case 12 – Ice concentration > 90% and ice thickness > 2 m

No data in conditions where ice thickness is above 2 m.